Optimization based nonlinear feedback control for pedestrian evacuation from a network of corridors

Apoorva Shende

Dissertation submitted to the Faculty of the
Virginia Polytechnic Institute and State University
in the partial fulfillment of the requirements for the degree of

Doctor of Philosophy
in
Engineering Mechanics

Prof. M. P. Singh, Chair

Prof. P. Kachroo, Co-Chair

Prof. R. C. Batra, Member

Prof. M. Cramer, Member

Prof. S. Ragab, Member

Dec, 16^{th}, 2008
Blacksburg, Virginia

Keywords: Control, Optimization, Conservation of mass, Network, Evacuation

ABSTRACT

An organized evacuation of pedestrians entrapped in a building in emergencies such as those caused by fire, bomb blast, or intentional or unintentional release of toxins in the environment is of utmost importance. The focus of this study is on the development of a formal control methodology for an orderly and jam-free evacuation of pedestrians entrapped in a network of corridors in buildings in such emergency situations. To develop an effective solution, the pedestrian evacuation from a network of corridors is divided into two basic problems of flow routing and flow control. In this study the solutions of these two basic problems are developed.

The proposed solution for the flow routing problem is based on the concept of shortest paths on a graph wherein the shortest paths are determined by the dynamic programming approach. The proposed approach can be used to determine the static shortest paths that are commonly displayed as evacuation routes in the buildings. The approach can also be used to determine the real-time evacuation routes if the real-time changes in the passage conditions are monitored. Such monitoring will usually consist of quantitative assessments of the congestion enroute and of the corridor availabilities along the evacuation paths. Based on these assessments one could compute either the shortest-distance-to-exit paths using the actual corridor lengths or shortest-time-to-exit paths using the congestion based corridor traverse time estimates. The application of the proposed shortest path routing scheme is demonstrated on a realistic problem of evacuation of pedestrians from a large network of corridors in a building consisting of multiple floors and multiple exits.

Next the problems of pedestrian flow in a long corridor as well as in a network of corridors are considered. Analytical formulations are developed to define the flow conditions in the two cases. The time evolution of pedestrian flow in a corridor is defined by ordinary differential equation with the average pedestrian density in the

corridor as the state variable. To accommodate the possible spatial variations in the pedestrian densities, a long corridor can be divided into several subsections with the flow in each subsection defined by an ordinary differential equation. With this, the flow evolution in a long corridor or a network of corridors is defined by a system of differential equations. The pedestrian in-flow consisting of rear input discharge as well room input discharges are considered in the formulation. For a long corridor flow control, analytical models for three flow conditions representing the end, middle and beginning phases of an evacuation in an exit corridor are developed. This is followed by the development of an analytical framework for the flow control in a network of corridors. The state variables representing the flow conditions and the control variables to regulate the pedestrian flow are introduced. For both the corridor and the network models, first the control variable values are defined to simulate the uncontrolled situation. These values are typically those that can be expected in a panic situation. Simulation of such uncontrolled scenarios for different models clearly indicates serious interruptions in evacuation caused by the jamming of corridors at different locations. To avoid the jam problem associated with the uncontrolled flow, the feedback control schemes are developed. An optimization-based approach is proposed for designing the feedback control. The control scheme is designed to ensure that the flow states continuously track a certain optimal state and that a certain objective function of the control variables is optimized. From the implementation point of view, an important aspect of the proposed control methodology is that the control actions always remain within the desired bounds. Numerical simulations for the uncontrolled and controlled flow scenarios are performed for an evacuation from a complex network of corridors representing a realistic evacuation problem. A comparison of the numerical results of the controlled and the uncontrolled flow scenarios clearly demonstrates the superiority of the controlled case in terms of smooth evolution of the flow parameters with continuous outflow of pedestrians from the network at some optimum level.

Acknowledgements

I would like express my deepest gratitude to my adviser's, Dr. Mahendra P. Singh and Dr. Pushkin Kachroo for their invaluable support and guidance throughout the course of my graduate studies at Virginia Tech.

Special thanks go to my committee members, Dr. Romesh C. Batra, Dr. Mark Cramer and Dr. Saad A. Ragab for their helpful comments and suggestions. I would like to take this opportunity to thank all the faculty members in ESM and other departments at Virginia Tech with whom I have had very productive interactions.

I am also grateful to all my friends and colleagues here in Blacksburg, Virginia for all their support. I would like to especially thank my lab-mates Saurabh Bisht and Harsh Nandan for all their support as also for all the fruitful and rewarding discussions I have had with them. I would like to thank Sabiha Wadoo and Sadeq Al-Nasur for helping me in the initial stages of this work. Special thanks go to Rakesh Pathak, Saurabh Bisht, Nitin Shukla, Kiran Konde,Soumya Bhattacharya and Phanikrishna Thota who have been my room-mates at various points during my Graduate studies at Virginia Tech. Graduate life would'nt have been as much fun without you all.

I am deeply indebted to my parents Dr. Seeta Shende and Dr. Ram Shende for their constant support and encouragement for the pursuit of knowledge.

This research is supported by National Science Foundation through grant no. CMS-0428196 with Dr. S. C. Liu as the Program Director. This support is gratefully acknowledged. Any opinion, findings, and conclusions or recommendations expressed in this study are those of the writers and do not necessarily reflect the views of the

National Science Foundation.

Contents

List of Figures

List of Tables

Chapter 1

Introduction

Evacuation from a disaster hit area is a problem of utmost importance in the present day scenario given the heightened danger of a terrorist attack or a natural and equally perilous situation like fire, earthquake, hurricane etc. During an intentional or unintentional industrial disaster such as the release of harmful chemicals form a chemical plant or radiation release from a nuclear power plant, or a natural disaster such as wide spread flooding due to hurricane or heavy rains, an affected area could be very large. The main focus of evacuation in such cases is an efficient management of traffic out of such areas using the road network. A parallel pedestrian evacuation problem also arises when there is intentional or unintentional conflagration or release of toxins inside a large building with several occupants. The main focus of this research is on the active management of such pedestrian traffic to evacuate pedestrians safely out of entrapped areas as fast as is possible.

To facilitate such evacuations from buildings, codes and regulations such as the life safety code handbook by National fire protection association (NFPA) (Cote and Harrington, 1987), have been formulated. These codes and regulations prescribe minimum dimensions for corridor widths as well as placement and size of exits depending upon the number of building occupants. For evacuation from buildings designed using such codes, usually fixed evacuation maps are posted at conspicuous locations. The occupants are expected to familiarize themselves with these maps and proceed with the evacuation by themselves with only some guidance provided by some designated persons in an emergency situation. The evacuees usually have no idea if they are to

move fast or slow in order to avoid jamming other than their own intuition which is highly varied in case of a panic situation. Also under a situation like fire or release of toxins, the escape routes might become unsuitable for egress due to fire or toxicity. In such cases, letting the evacuees just follow the static maps can result in dangerous situations of their getting into links that are not usable for evacuation. It is thus necessary to assess the condition of the evacuation routes in terms of the damage that has occurred as well as how densely the pedestrians are occupying the links. Based on the most current information about the state, the evacuation control algorithm can then compute the control inputs that would impact the flow speeds and their directions along with the flow discharges.

This study is concerned with the problem of controlling the pedestrian evacuation flow in a network of corridors. Corridors and stairs are primary conduits for pedestrian flow in any building structure. In a normal situation, pedestrians in a network move around in a rather random and undirected fashion depending upon their needs to perform their activities. In an emergency evacuation scenario, however, all pedestrian in a building have the common goal of evacuating a building through available exits as soon as possible. Such pedestrian evacuation flows will thus have highly directional characteristics. These directions are usually given through display of evacuation routes placed at conspicuous and critical locations in the buildings. In spite of these directives, however, there is a tendency in people to follow the crowd which could lead to congestions in corridors and stairwells and ensuing chaos especially in emergency situations causing flow routing problems. Such congestions will obviously lead to a slowdown of the evacuation process. In extreme cases the congestion could rise to the level of jamming where at least temporarily there is a stoppage of flow. Such a jamming would not only slow down the evacuation process considerably but can also result in possible chaos and panic. Chaos and panic in high pedestrian congestion can possible lead to catastrophic events like stampedes. These problems can be avoided by proper routing of pedestrian flow as well as timely regulation of flow control parameters. In this study we address both the flow routing and the flow control aspects of the problem.

The flow routing concerns directing the pedestrians to the appropriate exit through a network of corridors from a given location on the network. As time to egress needs to be minimized it is natural to route the pedestrians to the nearest exit from their

current location. However as the speed of the pedestrians in the links depends on how congested the links are the time-wise closest exit might not necessarily be distance-wise closest exit. In the determination of shortest-time-to-exit paths, thus, it is necessary to consider the pedestrian densities in different segments of a network. In order to affect appropriate routing of pedestrians we propose to use the dynamic programming methodology to find the shortest paths from every given location on a network of corridors to the nearest exit. The proposed methodology can be used to identify the fixed shortest path routes for conventional posting at critical locations. This can also be used to define a real-time routing scheme that considers evolving pedestrian congestion in the network links and unavailability of any part of a route due to unexpected path blockage or damage.

The flow control aspect of the problem deals with regulating the controllable flow variables such that congestion is avoided. We can even regulate the flow control variables such that certain optimal flow conditions are realized. For this we control the pedestrian velocities in the corridors, the room discharges into the corridors and the discharges from the corridor intersections into the corridors. We consider the flow control problem at the corridor level and the network level. The flow control in a corridor is important especially for the corridors adjacent to an exit. As all the pedestrians in the layout would use one of the exit corridors for egress, the level of congestion in the exit corridors could be high. High congestion in the exit corridors would inhibit the flow, which in turn would reduce the overall rate of evacuation. Thus the objective of a flow control scheme in an exit corridor is to ensure that the level of congestion is maintained below a certain critical value.

The objective of a flow control scheme in a network is to ensure that the congestion levels in all the corridors and corridor intersections are kept below an appropriate level. This is achieved by controlling the pedestrian velocities in the corridors along with the room discharges and the input discharges into the corridors from corridor intersections. The control variables can be regulated even to achieve certain optimal flow conditions. The problem of flow control in a network is a more complex than the flow control in a corridor, but there are similarities in the solution approaches.

In this study the three modules that can be used for pedestrian evacuation are developed. The first module provides the shortest path solution of the flow routing

problem from every location in the building to the nearest exit and is given in Chapter 2. The second module provides the solution of the flow regulation in a corridor to ensure an uninterrupted smooth flow of people. This employs a feedback control method and can be used together with the first module to manage the congestion in the exit corridors efficiently. The third module solves the network flow control problem in an optimal manner again to achieve an uninterrupted smooth flow of people in the entire network evacuating through an exit. This solution again can be used in conjunction with the first module which defines a directed single exit flow control layout using the shortest path methodology.

1.1 Literature Survey on Evacuation

To our knowledge there is no previous study that is directly related to the problem of control of pedestrian evacuation in an emergency situation. There are, however, some studies that have some peripheral connection with the problem of pedestrian movement and walking behavior. In the following paragraph we attempt to describe some of the studies and their motivations.

Hoogendoorn and Bovy (2004) have developed a theory concerning flow of pedestrians through a facility on the basis of the decisions they make as they move. The rational basis for this decision making is to maximize a certain utility or minimize a certain cost by choosing the optimal path. The authors claim that this is done sub-consciously and cite various examples supporting their claim. A walking behavior needs to be assumed for this implicit optimization which takes into account the interactions between the pedestrians. This walking behavior on which the tactical decision is based is presented by Hoogendoorn (2001) . However this work concerns movement in a normal situation where in there is no urgency to exit a built up facility. Also the authors develop models at the microscopic level *i.e.* they describe the movement of the individual pedestrian and not that of a collection or crowd of pedestrians. However, since we approach the study of pedestrian flow in a macroscopic manner, this study is not of direct relevance to our work. Hill (1982) has defined "'directness"' in route selection by pedestrians as a combination of factors like length, number of turns, comfort etc. He further analyzes pedestrian movement in the facilities and claims that directness is an important aspect

in the way the pedestrians choose their paths. This work attempts to model voluntary pedestrian movement and not pedestrian movement in an evacuation scenario. Other simulation based works on voluntary pedestrian route choice selection can be found in (Bovy and Stern, 1990 ; Gipps, 1986). These works discuss rationale behind the route selection procedure at the individual pedestrian level and are not concerned about macroscopic behavior of the pedestrian flow. Helbing et al. (2000) have used simulation based models of pedestrians and analyzed panic situations. They have categorized human behavior in panic as individualistic and herding. Individualistic behavior corresponds to the knowledge based decisions made by the individuals concerning their environment where as herding behavior constitutes following the crowd strategy. For these two situations they describe the dynamics of the individual pedestrian motion and do simulations in a 2-D environment. They conclude that for achieving minimum evacuation time a mix of individualistic and herding behavior is needed.

Cellular automata has also been used as a tool for simulation of pedestrian movement(Burstedde et al., 2001 ; Kirchner et al., 2004 ; Kirchner et al., 2003 ; Kirchner and Schadschneider, 2002 and Schadschneider, 2002). These models typically consider a floor plan and divide it into a regular grid. A box in the grid is typically a position holder for pedestrians. Based on how the adjacent boxes surrounding a pedestrian are occupied rules are asserted that determine the next configuration of the pedestrian location with respect to the grid. While these models give a very detailed simulation of the evolving situation of pedestrian movement they are rule based and also computationally very intensive. Hence they cannot typically be used to design controls for crowd motion. A continuum theory for the pedestrian movement has been proposed by Hughes (2002). In this theory the author makes use of a potential function which is a indication of the goal that the pedestrians have. Thus the potential dictates the flow of pedestrians. However his emphasis is more on modeling the flow of large crowd like the Hajj pilgrimage rather than crowd control in an evacuation situation.

Various strategies for design and routing of pedestrian and traffic evacuation networks are available. Bakuli and Smith (1996) have addressed the problem of sizing of the circulation elements like corridors and stairwells in a building using queuing theory. He also discusses the effects of varying the circulation element widths on the throughputs. However the implications of this work are only on sizing the circulation

elements and not on the actual network flow assignment. Chalmet et al. (1982) discuss a triple optimization problem wherein three objectives are simultaneously met. These three objectives are: 1) minimization of the average evacuation time per pedestrian, 2) maximization of the number of evacuees getting out of the building and 3) minimizing the time of evacuation of all the evacuees. However the optimization problem is solved by flow assignment to various links in the network and the density dependence of the flows is disregarded. Such methodologies are static as they ignore density variations with time and are primarily static or time-based flow assignment optimization approaches. Cova and Johnson (2003) develop a lane based vehicular traffic routing model for an evacuation scenario. The road capacity exceeds the road demand during an evacuation scenario. The main bottle necks during evacuation occur at the intersections. The authors develop a lane based routing strategy for evacuation. The main objective of doing this is to create a free flowing intersection which will avoid jams and reduce delays. To solve the lane-based routing problem, they use the mixed integer programming in network flow optimization procedure with density independent flow assignment to links in the control approach.

Control of vehicular traffic by sensing the state of the system is addressed formally in the dynamic traffic assignment literature (Kachroo and Kumar, 2000 ; Kachroo and Ozaby, 1998 ; Kachroo and Ozaby, 2004 ; Kachroo, 1997 and Kachroo and Ozbay, 1999). The state sensed is the density of the vehicles in a section of the road and the control commands are the split factors at a traffic node and the ramp input rate. In Kachroo and Ozbay, 1999 the authors have discretized the conservation of mass partial differential equation into ordinary differential equations and come up with a strategy to equalize travel times on alternate road links between an origin and a destination. The resulting ordinary differential equations are non-linear and the authors have used the feedback linearization approach to attain an asymptotic equalization of travel times. This methodology of feedback linearization for nonlinear control is of significant relevance to our work in this study.

1.2 Dissertation Organization

The three basic modules, describing the solutions of three basic problems needed to achieve smooth and uninterrupted flow of pedestrian in a network of corridors are described in the following three chapters.

In Chapter 2 we present the application of the dynamic programming to find the shortest paths for evacuation routing of the pedestrians from all points in a network of corridors to the nearest exit. In an emergency evacuation situation, the shortest path assignment can be done either statically or in real time. Static route assignment assumes that there is no damage in the building layout and the travel times along the corridors of the layout are not affected by congestion. However, the real-time route assignments can also be made if we explicitly know about the damage to the layout and the density dependent travel times along individual corridors using a well coordinated sensor network. Using this real time data, the shortest paths (i.e. the paths with a minimum time requirement) can be recomputed and conveyed to the pedestrians. The applications of the static and dynamic shortest path assignments are demonstrated on an example problem of the pentagon layout with multiple floors and multiple exits. The dynamic path assignments consider various damage scenarios along the evacuation routes.

In Chapter 3 we take the first step towards pedestrian flow control. The focus of the study in this chapter is primarily to address the control of pedestrian flow in the exit corridors in the end, middle and beginning phases of evacuation. To account for the possibility of having different pedestrian densities along the corridor, the corridor is divided in to several sections. The time evolution of the state variable of the pedestrian density in each section is then defined in a macroscopic sense by an ordinary differential equation, derived using the principle of conservation of pedestrian mass. (Here in this study, we will use the term pedestrian mass to represent the number of pedestrian. In fact, at places in this dissertation, the pedestrian mass and number of pedestrian will be interchangeably used.) These equations consider the pedestrian input to corridor from the rear end as well as the input discharge from the rooms in to the corridor sections. The section free flow velocities as well as the inputs to the corridor are considered as the control variables which can be regulated. The three evacuation phases (namely beginning, middle and end) are characterized by the availability of the

pedestrians to sustain the rear end input and the room discharges. In the end phase of the evacuation, the pedestrians will only be left in the corridor and no one is likely to be available to sustain the room discharges and the rear end input discharges. In the middle phase scenario, we assume that only the pedestrians contributing to the rear end input discharge will be available and the pedestrians from the rooms on the exit edges would have already exited the network. In the beginning phase, however, there will be pedestrians available to sustain both the rear end input discharge and the room discharges. For each one of these scenarios we propose what one could expect in a panic driven uncontrolled situation. In order to alleviate the congestion and jamming that develops in these uncontrolled situations we develop optimization-based feed-back control methodologies for these three flow scenarios. We also propose methods for adjusting the gains in the beginning and the middle flow cases in case the constraints are infeasible with the initially chosen gains.

Chapter 4 combines the shortest path methodology of Chapter 2 and the flow control approach of Chapter 3 to develop flow control methodology for a network of corridors. Using the fact that a multi-exit layout can be decomposed into multiple single exit directed flow control layouts using the shortest path methodology of Chapter 2, this chapter develops a flow control approach that can be applied to each one of these single exit directed layouts. The directed network is treated as a directed graph. The corridors are the edges of this graph and the corridor intersections are the nodes of this graph. Using the conservation of pedestrian mass principle, a system of equations is developed that governs the flow in the network at a macroscopic level. The state variables in this approach are the average edge densities and the number of pedestrians at the nodes. The control variables are the edge free flow velocities, the nodal input discharges and the edge room discharges. An optimization- based feed-back control approach is proposed that simultaneously seeks to track the states to certain desired values as well as satisfy the bound constraints along with optimizing a certain objective function. As multiple goals are addressed simultaneously, this is a highly efficient control methodology for the problem. In this chapter, we also propose a method of adjusting the gains in case they are too high to meet the control bound constraints. Along with this we also propose a method to fine tune the network level control at the local level to make the densities in the corridor more uniform and hence the network flow model more reliable. In the end

we present the simulation results of the flow control implemented on a directed shortest path layout for a realistic problem of pedestrian evacuation from the Pentagon.

Chapter 5 summarizes the work chapter wise and presents the main findings and conclusions of this study. Also discussed are some related topics for future study in this area.

Chapter 2

Evacuation along the shortest path

2.1 Introduction

A large building will usually have several floors with several interconnected corridors and several exits from one floor to another and to the exterior of the building. Efficient evacuation of pedestrians from such a building in an emergency is a difficult problem to solve. For emergency evacuation from such buildings, usually static evacuation routes are posted at selected locations in the buildings. These routes usually direct pedestrians to the nearest exits out of the building. Identification of the shortest paths in a simple building layout with one or two corridors is usually not a difficult problem. However, in a complex building such as large government building, for example the Pentagon, there can be a multitude of possible shortest or quickest routes one can take from a point in the building to an exit. Identification of such routes is not a trivial task for big layouts, and a systematic and automatic procedure is needed to define the shortest paths. It should be noted that for relatively high density crowds the flow velocity of the crowd is dependent on the density of the pedestrians. It is important to realize that in such cases the time to traverse an edge is not only dependent on the edge length but also on the pedestrian density along the length of the edge. This will result in some length wise shortest paths not turning out to be the time wise shortest or the quickest paths. To determine the quickest path in such situation one would need the information about the time it takes to traverse different segments of the path. The possibility of having different pedestrian flow speeds in different segments can be

accommodated by making measurements of the pedestrian densities along the paths using sensors. The pedestrian flow speed can then be calculated using empirical models such as Greenshield's model commonly used in traffic flow analysis. The flow velocity and segment length then determines the time it would take to traverse the segment. The shortest and the quickest paths, will however, be the same if the pedestrians can freely move along the path that is, the corridors are wide enough to accommodate any congestion without affecting the pedestrian flow speed.

Another point to consider in determining the shortest or the quickest paths is that not all nodes, links and exits might be available for evacuating pedestrians in an emergency situation. This is due to the fact that there could be excessive damage or smoke accumulation along some links or nodes. The initial availability of nodes and links for evacuation could also possibly change with time; that is, the links that were open once may not be available because some evolving hazardous conditions that could result in their blockage. In such cases, valuable time may be lost in using a blocked passage if the pre-decided path is followed. It will be highly desirable if such evolving conditions can be monitored and the resulting information used to determine the shortest route as the evacuation proceeds. These shortest paths will have to be computed and conveyed to the evacuees in real time.

In this chapter we use the dynamic programming approach to find the shortest or quickest routes from all different locations of a building. The dynamic programming is a well established approach, and its theory is available in several texts such as (Bertsekas, a) and (Bertsekas, b). In the following sections we define the framework of this approach for evacuation from single and multiple exits, and from multiple interconnected floors. In the end we also present the shortest route identification results obtained for a realistic example of evacuation from Pentagon under different route availability scenarios.

2.2 Problem Framework

The main objective of the evacuation problem defined herein is to determine the best routes that the pedestrians should take to exit from a network of interconnected corridors on a floor or several interconnected floors. Due to the minimum time requirement of the evacuation process we assume that the quickest route is the best route. The

quickest route is also the shortest route if the flow velocity is independent of the density.

To formulate and solve the pedestrian evacuation problem from a building, we model the building layout consisting of rooms, corridors, corridor intersections, stairwells etc as a connected planar graph $G(V, E)$ where $V = \{1, 2, ...i, ...n\}$ represents the set of n vertices and $E = \{E_{i,j} : i, j \in V\}$ represents the set of edges of the plane graph $G(V, E)$. The edges $E_{i,j} \in E$ corresponds to circulation elements like the corridors and the stairwells. At this point we recognize the fact that to find the quickest route we need a time estimate to traverse an edge $E_{i,j} \in E$. This time estimate has to be derived from an estimate of the velocity which in case of density dependent flows depends on the density. To account for the space variance of the density along the edge we divide the edge into sections. Also these sections are useful in deciding the routing directions on the edges that are not on the shortest path. This will be discussed later in Sec. 2.5.

Corresponding to each edge is an edge weight. This edge weight could be the time estimate to traverse the edge in a density dependent flow or the length of the edge in case of density independent flow (which is directly proportional to the time estimate). Similarly section weight corresponds to a section. The section weights are the time estimates to traverse the sections in case of the density dependent flows or the length of the sections in case of density independent flows. As the sections are lined up along the edge, the edge weights are the sum of section weights. The vertices in V correspond to either the rooms, intersection of corridors, stairwell entrances or exits. Often, we will also call them as the nodes of the network.

The solution of the shortest path identification consists of two steps. In the first step, we find the shortest paths from all the nodes to the exits. This part also assigns the pedestrian flow directions to the edges that lie on the shortest path. This process may, however, not assign directions to edges that do not belong to a shortest path. Herein we call such edges as unresolved edges. In the second part, we define the routing directions on the sections of these unresolved edges.

The methodology adopted in this chapter to determine the shortest path assumes that the edge weight $w(i, j)$ for different edges are known at the time of computing the shortest path. For the real time implementation the weights can, however, change at discrete instants of time based on the crowding and damage conditions in various edges

or corridors for re-calculation of the shortest path. This allows us to dynamically re-configure the paths when the conditions along different paths change as the evacuation proceeds. By the shortest path we mean the path with the minimum sum of the edge weights along the path.

As stated earlier we consider three problems with increasing levels of complexity in this work. In the first problem we just assume that there is a single exit and all the shortest paths have to be directed to it. Then we add a level of complexity by considering the existence of multiple exits. Finally we consider the multi-floor case where each floor could have multiple stair exits. However the basis of the solution to these problems is the solution of the single exit problem. This is done using the dynamic programming methodology as described in Sec. 2.3, subsection 2.3.1.

2.3 Shortest Paths to A Single Exit

In case of a single exit on a floor, the problem of determining the optimal routing consists of solving the shortest path problem. That is, on a undirected graph $G(V, E)$ with $V \equiv \{1, 2.., i, .n-1, n\}$, with node n being the exit node, we need to determine a directed path $P_s(i)$ from $\forall i \in V$ to $n \in V$ such that the sum of the edge weights along that path is the least of all the alternative paths. For this problem to have a solution all the cycles in the graph should have a non-negative length. This is so because if any cycle had a negative length then it would be possible to go round this cycle and keep reducing the cost to $-\infty$. This requirement is trivially satisfied in our case as all the edge weights are positive. To determine the shortest or the quickest paths we use the dynamic programming algorithm as follows.

2.3.1 Dynamic programming (DP) algorithm

Dynamic programming is a mathematical programming methodology applicable to optimization problems that are sequential in nature. By sequential it is meant that the problem is iteratively solved in steps called stages. Every stage comprises of states that have meaning that is specific to the problem being solved. In the shortest path problem the states correspond to the nodes of the graph. The stage cost depends on the state from which the transition is to be made and the decision variable which defines the

decision we make at the state. The decision variable at a stage defines how the system would evolve in the current stage. In case of the shortest path problem, the decision variable at a node represents the node to which the pedestrian can go in the next stage. At each stage there are several states from which the transition is to be determined to states in the subsequent stage that will have a minimum cost to go from the state in the current stage. The stage cost is additive in nature and hence the net cost incurred is the sum of all the stage costs. The objective of dynamic programming is to minimize the net cost incurred. The decisions or the policy or the control parameters in dynamic programming is based on the state information at the current stage. The central idea of dynamic programming is represented by the Bellman's optimality principle: "*An optimal policy has the property that whatever the initial state and the initial decision are, the remaining decisions must constitute an optimal policy with regard to the state resulting from the first decision.*"'

Thus dynamic programming consists of finding a cost function of states which is the net cost to go from a state obtained by using an optimal policy beginning at that state. The shortest path problem can be viewed as a problem of finding this cost function and optimal policy at every state (*i.e.* the node). In the context of the shortest path problem the policy decision determines the transition node in the next stage to which one should move from the current node. The net cost in this case corresponds to the shortest distance or the least time estimate to the exit. Since for a n node problem at most $n-1$ transitions are required to reach the exit node from any node, we can consider the shortest path problem to be an n stage sequential optimization problem. Dynamic programming is inherently a method for solving sequential optimization problems. There could be nodes from which the shortest path to the exit may consist of less than $n-1$ transitions. In such cases, to implement this approach with exactly $n-1$ transitions, we need to allow self transitions i.e. transitions to the same state with a stage cost of 0.

We illustrate this using a simple example in Figure 2.1, how the shortest path problem can be formulated and solved as a dynamic programming problem. In Figure 2.1(a) is shown a four-node graph with Node 4 being the exit node to which the shortest paths are to be determined. The edge weights for each edge are also shown on the graph. To determine the shortest paths, a 4-stage procedure is set up, as illustrated

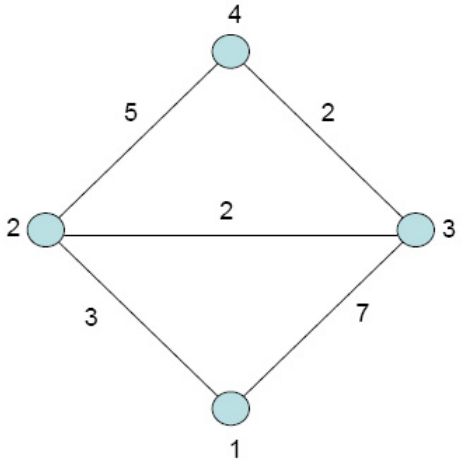

(a) A 4 node graph

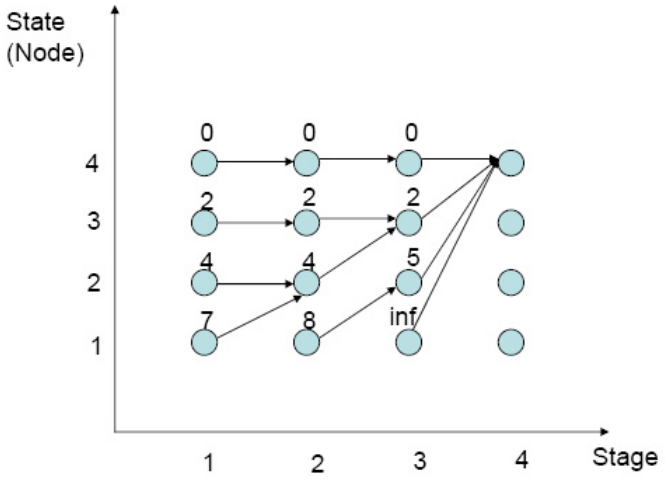

(b) Stage wise state transitions for shortest path.

Figure 2.1: Dynamic programming approach to shortest path problem.

in Figure 2.1(b). In Figure 2.1(b) the x-axis is the stage axis and the y-axis is the node axis or the state axis. All the points illustrated in the figure by small circles illustrate the stage-node points. All the transitions from stage 3 to stage 4 have to end up in node 4 as node 4 is the exit node. As seen in Figure 2.1(b) there are 4 states in each stage $1, 2, 3$ which correspond to the 4 nodes present in the graph in Figure 2.1(a). Let $i \in V$ be a state variable or a node at the the k^{th} stage. We need to find a transition node from all the nodes at every stage $k = 1, 2, 3, ...n-2$. This transition node has to be such that the net cost to go from the node at the current stage has to be minimum. The stage cost of transition from node i in stage k to node j in stage $k+1$ is given by the edge weight $w(i, j)$.

As stated earlier the transitions from all the nodes in stage 3 are to node 4 in stage 4. Denote by $J_k(i)$ the net cost to go to the exit from node i at the stage k. Thus all the costs to go in stage 3 from nodes $i \in V$ are given by $J_3(i) = w(i, 4)$. $w(i, 4)$ is the edge weight of the edge $E_{i,4}$ which is the edge connecting node i to node 4. In Figure 2.1(b) the costs to go from a node in a stage are written above the circles corresponding to the stage-node points. Thus in stage 3 we can see that the cost to go from node 4 i.e. the self transition cost is $J_3(4) = 0$, the cost to go from node 3 to the exit is $J_3(3) = w(3, 4) = 2$ and the cost to go from node 2 to the exit is $J_3(2) = 5$. As node 1 is not directly connected to node 4 we assume that the nodes are connected by a hypothetical edge of edge weight $w(1, 4) = \infty$. Thus the cost to go from node 1 at stage 3 is $J_3(1) = w(1, 4) = \infty$.These costs are updated by going backward in stages all the way till stage 1. The cost to go from stage 1 to the exit for node i, $J_1(i)$, is the shortest path distance from node i to the exit. The cost updating algorithm of dynamic programming given by equation (2.1) is presented next.

As in the above example for the n node problem we have to set up a $n-1$ stage procedure for updating the costs. The transitions from all the nodes i in stage $n-1$ are to node n in stage n. Thus as in the above example we set $J_{n-1}(i) = w(i, n)$, with $w(i, n) = \infty$ if nodes i and n are not connected. Then we use the following dynamic programming cost update iteration which goes all the way backwards from stage $n-1$ to stage 1:

$$J_k(i) = \min_{j=1,...,n} [w(i, j) + J_{k+1}(j)] \quad k = 1, 2....(n-2), \tag{2.1}$$

with $J_1(i)$ being the shortest path distance from node i. Henceforth we denote by

$J(i) = J_1(i)$ the shortest path values from node i. In each successive stage the cost to the exit either decreases or remains the same. This is illustrated in the example problem in Figure 2.1(b). For node 1, $J_3(1) = \infty$, $J_2(1) = 8$ and $J_1(1) = 7$. Similarly for nodes 2 and 3 we see that the costs to go either remain the same or decrease.

The next obvious question to be asked is what is the sequence of nodes from a node $i \in V$ to the exit node along the shortest path? This is the issue of tracing the shortest path $P_s(i)$ which is a sequence of nodes from node i to the exit. To trace the shortest path we need to find the transition node from every node in the graph. This is easily done using the following equation:

$$j = \underset{k \in \{1,2..i-1\} \cup \{i+1,..n\}}{argmin} [w(i,k) + J(k)]. \tag{2.2}$$

Equation (2.2) reflects the fact that the shortest path from a given node comprises of 2 steps:

1. transition to a subsequent node.

2. following the shortest path from that subsequent node.

Hence we choose the subsequent node in such a way that amongst all the transitions possible this one has a minimum sum of edge weight and subsequent shortest path distance. This is what is conveyed by equation (2.2). Once the transition node has been determined at every node we can trace the shortest path by sequentially transitioning from a given node till the exit.

Thus we can summarize the dynamic programming algorithm by the following 2 procedural steps:

1. Finding a value function $J(i), i : i \in V$ which is the minimum cost to go or the shortest path from the node i to node t.

2. Finding the shortest path $P_s(i,t)$ using $J(i)$.

2.4 Shortest Paths to Multiple Exits

The above dynamic programming approach to solve the shortest path problem for a single exit can be easily adapted to the case of multiple exits. In the multiple exit case,

we solve the single exit shortest path problem for each exit separately. This provides the shortest path values to every exit from every node for a given building layout. Next for each node we compare the shortest path values to each exit. The least of the values to different exits identifies the exit and the corresponding path to use from this node. Thus if $J^{(k)}(i)$ is the value of the shortest path distance from the i^{th} node to the exit k then we need to choose the exit $e(i)$ for node i such that

$$e(i) = argmin_k J^{(k)}(i)\,. \tag{2.3}$$

If a node to different exist has the same least values then, we have a redundancy in the system; that is, any of these multiple routes can be chosen from that particular node.

2.5 Route Directions On Unresolved Edges

In the single and multiple exits problem, all edges that lie on the shortest path trees are assigned a direction. This implies that all the pedestrians on these edges move in the direction of the edge. Some of the edges, however, may not fall on the shortest path tree due to the structure of the building layout graph $G(V, E)$. This would mean that they do not have an assigned direction in the initial phase when the shortest paths from the nodes are found. We call these edges unresolved edges. An additional step needs to be performed beyond the initial shortest path solution. This step would involve assigning direction to the sections on the unresolved edges.

In order to assign routing direction to the unresolved edges we utilize the sections in which the edge is divided. The section numbers are local to the edge. In the convention adopted here, they increase from the lower numbered node to the higher numbered node at the ends of the corridor. Let us denote the k^{th} section on the edge, $E_{i,j}$ connecting nodes i,j to be s_{ij}^k. Thus the 1^{st} section in the corridor will be adjacent to the lower numbered node and the last section will be adjacent to the higher numbered node of the edge. Let the section weight of the k^{th} section on the edge $E_{i,j}$ be denoted by $w^k(i, j)$. The section weight may depend upon the density in the section ρ_{ij}^k. As the sections are lined up along the edge we have a simple additive relation between edge

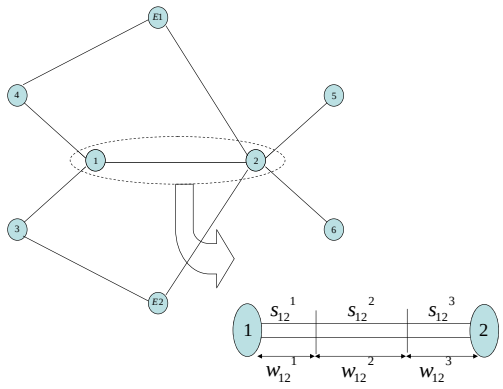

Figure 2.2: Schematic of the graph.

weights and section weights. This is given by:

$$w(i,j) = \sum_{k=1}^{nsec} w^k(i,j). \tag{2.4}$$

A schematic of a layout is shown in Figure 2.2. Link $E_{1,2}$ joining nodes (1,2) is divided into three sections and their numbering scheme is shown. Let i be a lower numbered node and let j be the higher numbered node. We can define the end points of the sections as nodes numbered along the edge $E_{i,j}$. Let n_{ij}^k denote the k^{th} node on edge $E_{i,j}$. For the k^{th} section the node closer to i is n_{ij}^k and the node closer to j is denoted by n_{ij}^{k+1}. In every section k the routing can either be from $i \rightarrow j$ direction or from $j \rightarrow i$ direction. Of the two choices we need to choose the one in which all the pedestrians in the section have to travel a minimum sum of the edge weights to the exits, that is, the estimated time to exit should be a minimum. Thus, if we are to choose the routing direction from $i \rightarrow j$ then we need to ensure that the minimum time estimate to the closest exit via node j for the section is less than the minimum time estimate to the closest exit via node i. In computing the minimum time estimate through either of the end nodes of the edge we need to make sure that we traverse across the section to go all the way to the opposite node of the edge. Consider a section k on such an edge connecting the nodes i and j. We account for the section weight of the section k to decide on the routing direction. Assume that $i < j$. Thus the shortest distance from

the section k on edge $E_{i,j}$ to an exit is given by:

$$J_{ij}^{k} = min(J(i) + \sum_{l=1}^{k} w^{l}(i,j), J(j) + \sum_{l=k}^{n} w^{l}(i,j)). \tag{2.5}$$

If the 1^{st} term in the *min* operator is the minimum then the pedestrians in the section are routed towards i else they are routed towards j. Thus if we start from i and proceed towards j assigning directions to the sections then we have to find the 1^{st} section that is directed towards j as all the subsequent sections will automatically be directed towards j.

2.6 Evacuation from Multiple Floors

The above approach can also be used to deal with the evacuation from the floors connected at multiple points by stairwells. Since the floors are joined at distinct points, the shortest path problems for each floor are uncoupled. By assigning a cost to the floor exit corresponding to the onward time estimate along that stairwell to the building exit we can solve the shortest path problem for every floor separately on a separate processor and use the results to define the global routing policy for the entire building. This requires that we move from the bottom floor up to define the evacuation paths. The solution approach can thus be split into two steps:

1. In the first step we calculate for each floor exit the cost which corresponds to the onward time estimate from that exit to the building exit corresponding to that stairwell.

2. In the second step we solve the shortest path problem for each floor using these exit costs. We can use different processors to calculate the shortest paths for each floor by exploiting the decoupled nature of the problem.

2.7 Implementation

The implementation of the algorithm described above was programmed in Matlab. It consists of the following steps:

1. In case of a multistory problem, separate the floors and assign a cost to each floor exit which corresponds to the onward time estimate from the floor exit to the corresponding building exit at the 1^{st} floor. This requires solving the shortest path problem for all floors below the current floor. This is done by implementing the following successive steps.

2. Defining the floor layout in terms of nodal co-ordinates and nodal connectivity using edges.

3. Constructing the weights matrix using the nodal co-ordinates and nodal connectivity and appropriately permuting the rows and columns so that the rows and columns corresponding the the exit are at the end. This procedure needs to be repeated for each exit independently.

4. For an n node problem repeat the value iterations described by equation (2.1) n times. The value vector $J_0(i)$ that we get after doing this is the shortest path value at every node. Repeat the procedure for every exit to get the shortest path value corresponding to it at every floor.

5. Using the shortest path values at every node corresponding to an exit find the transition node/s at every node in the shortest path. This can be done using equation (2.2). We could find multiple nodes using this equation. In practice we allow the shortest path values to differ by a certain negligible tolerance in order to assign the transition node.

6. Comparing the shortest path distance values at every node corresponding to every exit, choose the exit corresponding to the least value at every node. This is reflected in equation (2.3). Assign the transition nodes above corresponding to this exit to the node under consideration. We allow a certain negligible tolerance in practice by which the shortest path values corresponding to various exits could differ from the least value for the exits to be assigned to the node.

7. Find the unresolved edges corresponding to every node. Consider only those unresolved edges which go on to the higher numbered node so as to prevent assigning the same direction twice to each edge. For the sections on these unresolved edges assign a direction using equation (2.5).

8. Plot the layout with the shortest paths defined on it. In practice the information on the exits and the transition node will have to be conveyed to the pedestrians using appropriate route indicating devices.

2.8 Example Problem

As an example problem, the Pentagon building in Northern Virginia, was considered. Pentagon is one of the largest office buildings in the world, housing the US department of defense. This building represents a realistic situation from the evacuation point of view. The building is a critical high security building with complex layout and hence very important from the evacuation point of view.

Figure 2.3 shows the layout of a floor with various corridors. This was obtained from `http://www.hqda.army.mil/aoguide/Pentagon_Map.htm`.The layout is not symmetric and hence the assignment of the shortest paths to the exits is not trivial. It consists of 5 concentric pentagonal rings of corridors. Along with these there are 10 straight corridors that span from the inner most ring to the outer most ring. It can be seen that the portion of ring B between corridors 9 and 2 is missing. There are three stairwell exits on the outer most ring. One is at the end of corridor 3, another is adjacent to the corridor between corridors 8 and 9 and another is adjacent to the corridor between corridors 6 and 7. As can be seen from the figure these exits are unsymmetrically placed.

Due to the complex nature of the building layout it is necessary that various evacuation paths are clearly defined for an emergency evacuation. This is precisely what can be done by the shortest path methods to ensure that the time estimate to the exit from every section in the layout is a minimum. Also certain links could be rendered unusable for evacuation in an emergency situation. Thus we might need to recompute the shortest path layout in real time assuming that these links are missing. This information will have to be conveyed to the evacuees in terms of the direction they are supposed to take while evacuating so that they are on the shortest path. Recomputing the shortest path in real time can be easily and efficiently done using the proposed value iteration method of the dynamic programming algorithm. For the pentagon example we will deal with the static case in which the edge weights remain constant over time.

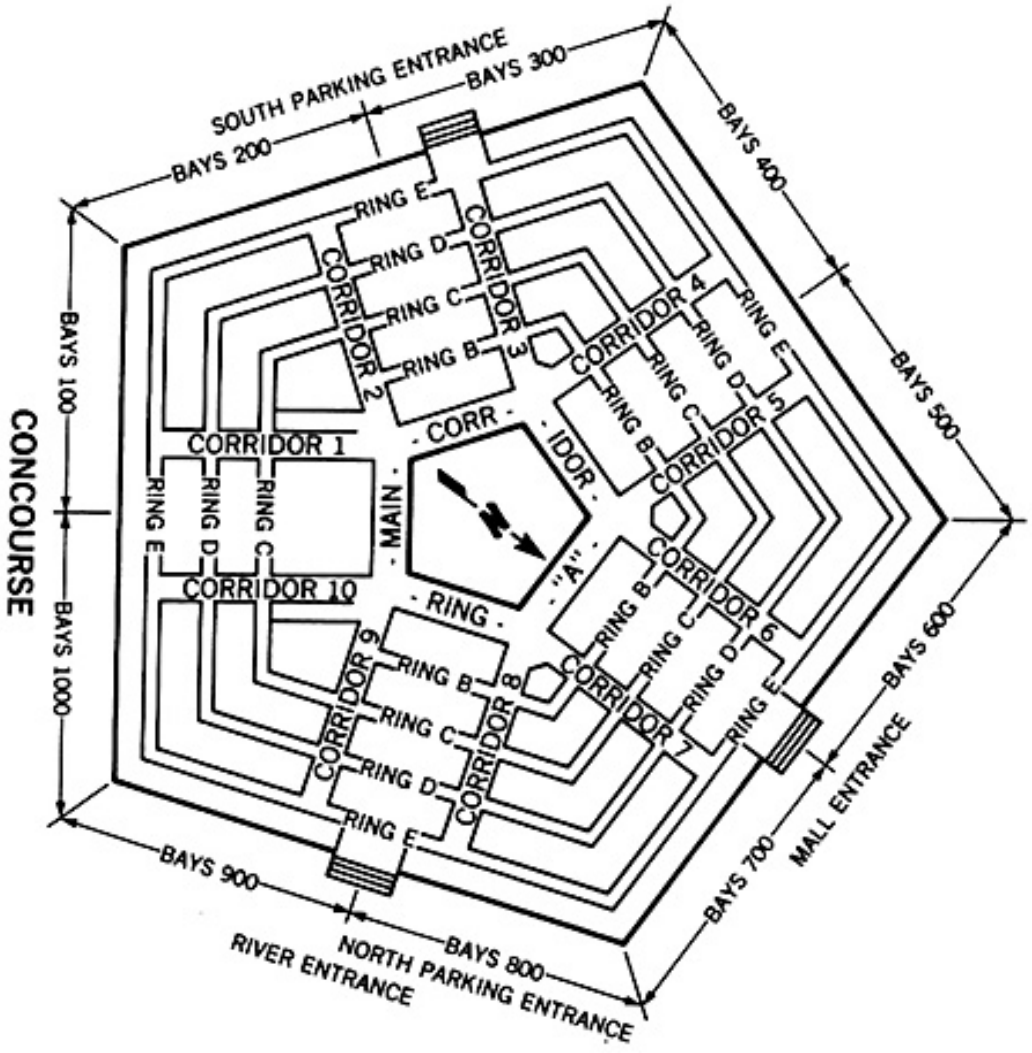

Figure 2.3: Pentagon Floor Layout.

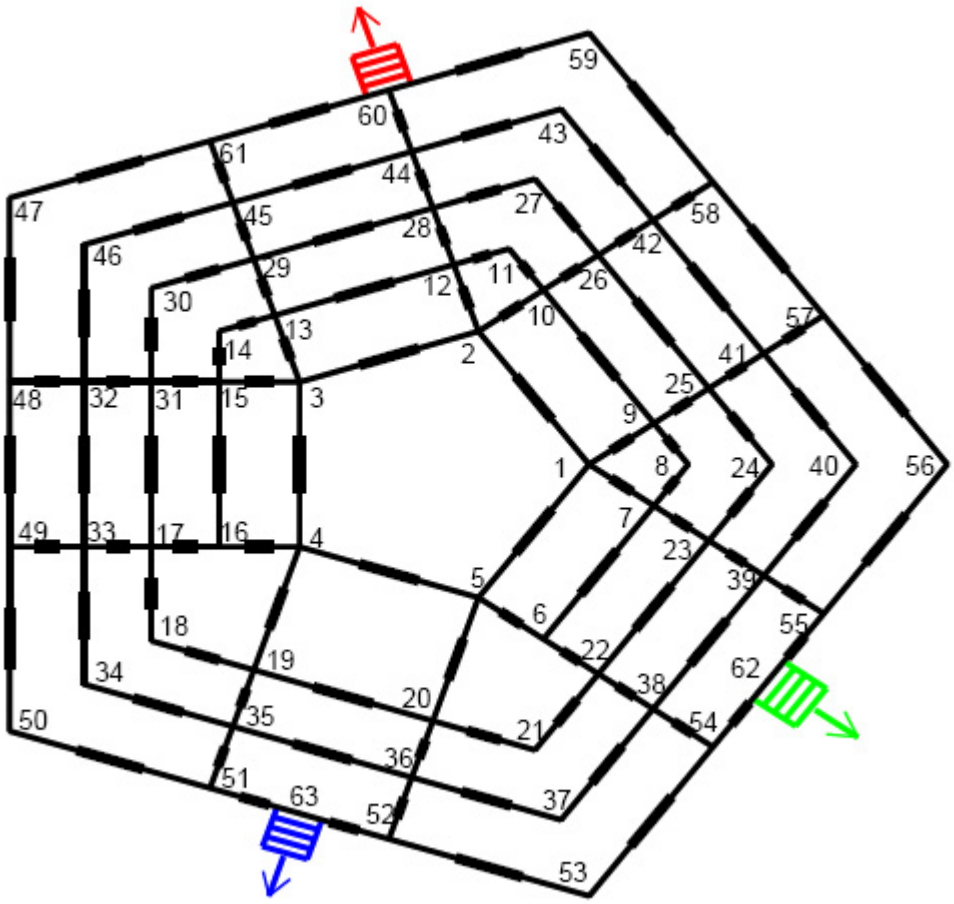

Figure 2.4: Nodes and Edges in the pentagon layout

Since the actual dimensions for the building were not available from the website, we obtained the relative positions of the nodes by actually measuring the distances with a scale in Figure 2.3. These scaled measurements were used to generate the schematic representation shown in Figure 2.4. In this figure the nodes and edges of the pentagon layout are indicated. The figure shows that there are 63 nodes with nodes 60, 62 and 63 being the exit nodes. Also shown are the sections on the edges by alternate thick and thin lines used to represent the edges. As can be seen for the current example every edge is divided into 3 sections. The division of edges into sections facilitates identification of the densities in different sections that could potentially be different and computing the corresponding section weight as well as enables the routing on the unresolved edges.

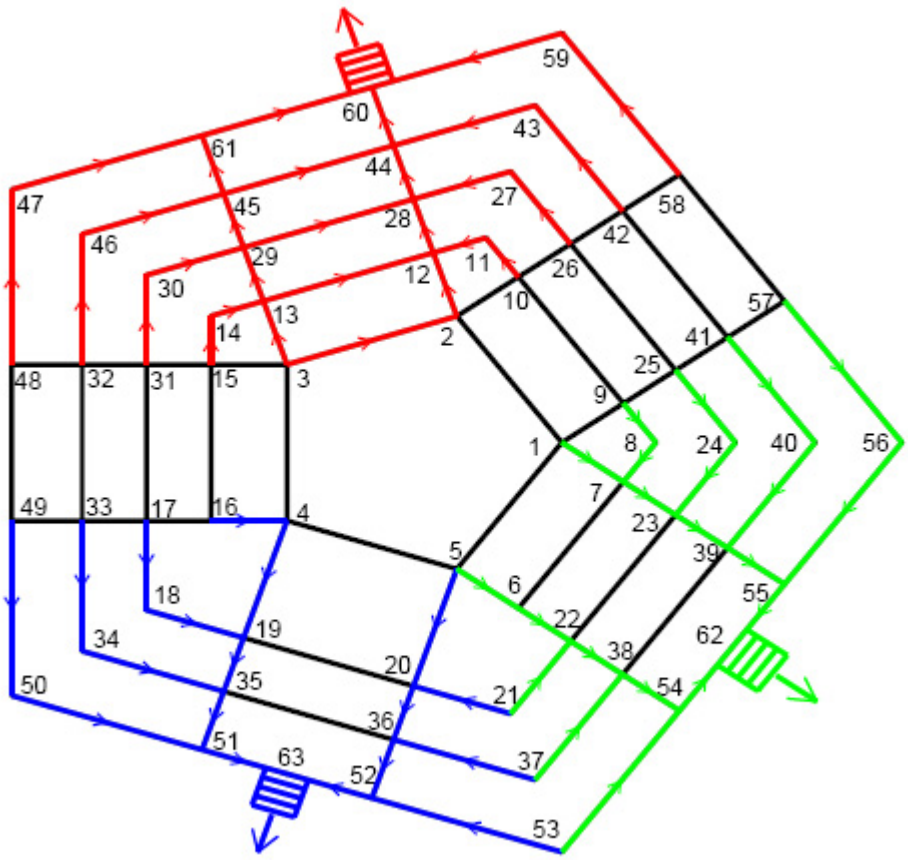

Figure 2.5: Shortest paths from nodes in the pentagon layout

In the current example, it is assumed that edge weights are proportional to the edge lengths and independent of the pedestrian density. The latter assumption is, of course, not necessary if measurements of the pedestrian density can be made. The relative values of different edge weights were obtained by using the nodal co-ordinates and the nodal connectivity data in Figure 2.3. These define some elements of the 63 x 63 edge weight matrix. For the remaining elements of this matrix are chosen as infinity, representing no direct connectivity between those nodes.

In Figure 2.5 we show the shortest paths from all the nodes to the closest exits. The shortest paths leading to different exits are shown in different colors. Shortest paths leading to node 60 are shown in red, shortest paths leading to exit 62 are shown in green and shortest paths leading to node 63 are shown in blue. It is noted that there

are several non-unique multiple paths in the network and the program can detect these paths. That is, they all have the same traversing lengths, and any of these paths can be chosen. For this example problem, there are several multiple paths starting from nodes 3, 13, 29 and 45 that lead to the same exit at node 60. For example shortest path starting from node 15 to node 60 can be either of $15-14-13-29-45-61-60$ or $15-14-13-12-28-44-60$, both pass through the node 13. Depending upon the layout, there could also be two or more shortest paths to different exits from a single location. For example, there are two shortest paths, starting at nodes 5,21,37 and 53 that either lead to exit 62 or 63.

In Figure 2.5 we also note that there are several edges such as those connecting the nodes $\{4,5\}$, $\{17,31\}$, $\{22,23\}$ etc. that do not have a direction associated with them as they did not fall on any shortest path. To evacuate pedestrians on such edges we divide them into sections and assign a routing direction to each of these sections. The basis for assigning the direction to a section of the edge is done using equation (2.5) given in Sec. 2.5. In Figure 2.6 the directions on the sections of these unresolved edges are shown in black arrows. The sections which point in the same direction are shown by the same arrow. The points from which the pedestrian move in opposite directions on these edges are also shown and were calculated according to the algorithm defined by equation (2.5).

Next we show some examples of the shortest paths when one or more nodes on the layout become impassable because of some problem in the building at or near those locations. In Figure (2.7), we show the path when node 44 is damaged. In Figure 2.8 shortest paths are shown when nodes 28, 44, 51 and 61 are damaged and hence can not be used for pedestrian passage. In order to make a comparison of how the paths change we show in Figures 2.9 and 2.10 some of the paths originating from the same nodes in the damaged and the undamaged case. Figure 2.9 shows a comparison when only node 44 is damaged and Figure 2.10 shows the comparison when nodes 28, 44, 51 and 61 are damaged.

The results for exits from multiple floors are shown in the next two figures for the damaged and undamage cases. We have the same node numbering for both the floors as both floor problems are solved independently. The layout assumes that the nodes where the stairwells from nodes 60 and 62 on the second floor meet the first floor are

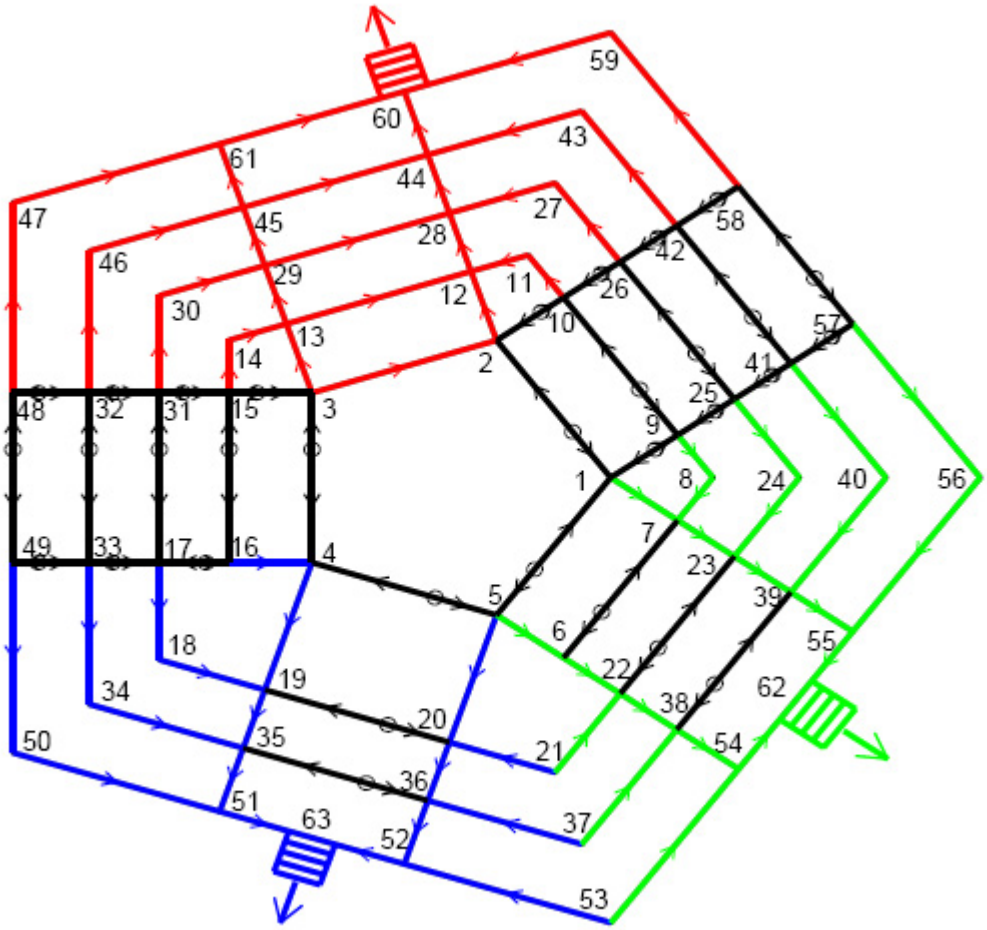

Figure 2.6: Shortest paths from nodes and along unresolved edges in the pentagon layout

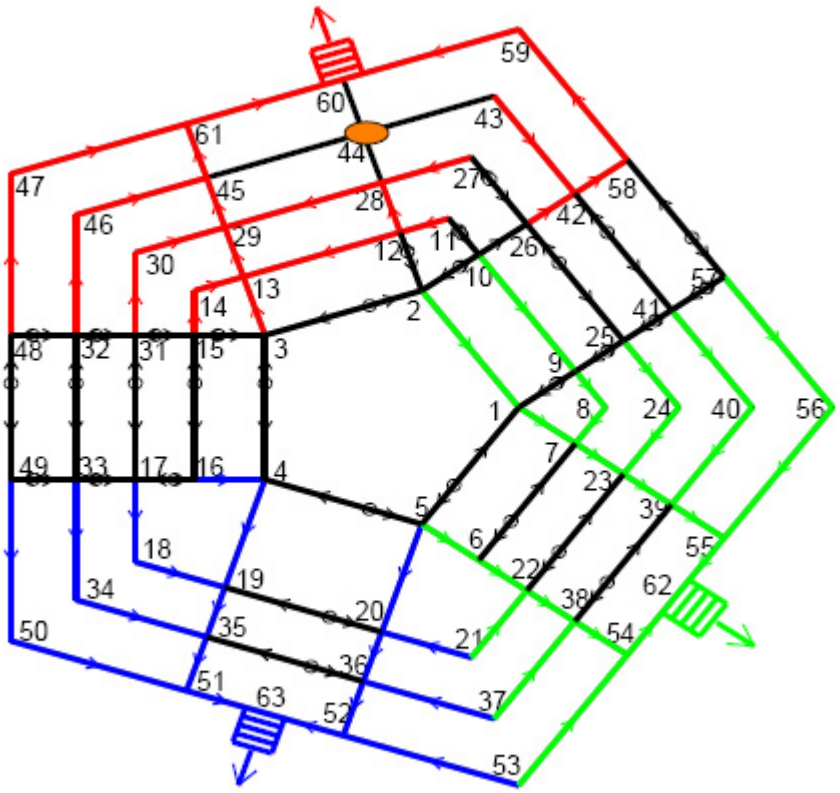

Figure 2.7: Shortest paths from nodes and along unresolved edges in the pentagon layout if damage occurs at node 44

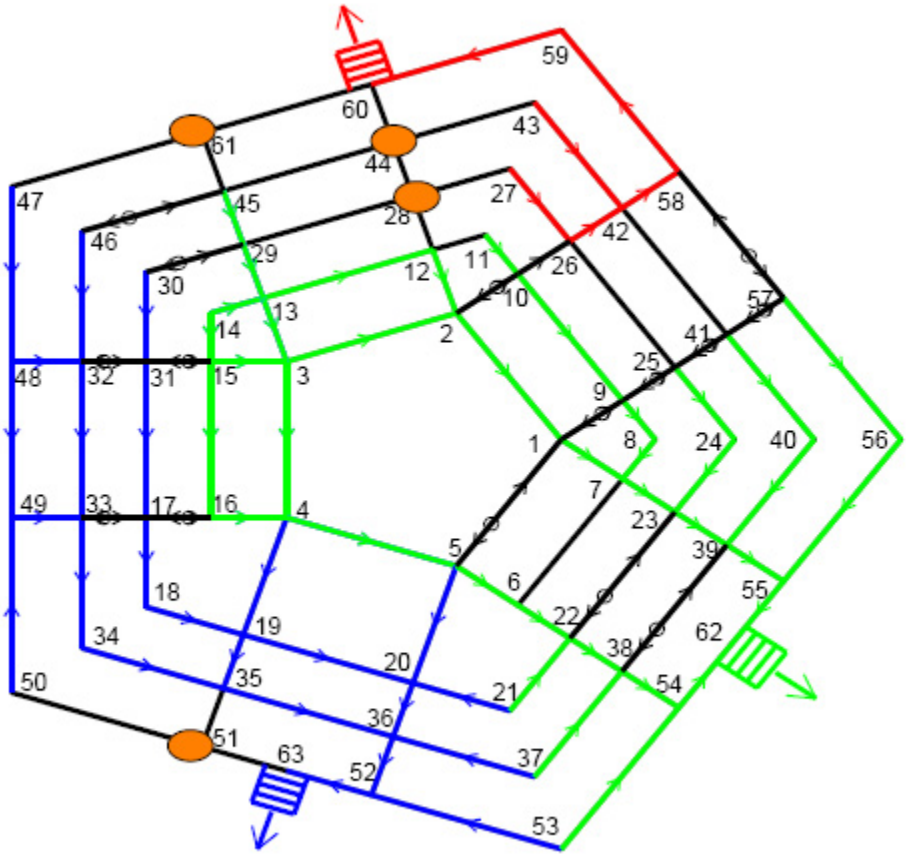

Figure 2.8: Shortest paths from nodes and along unresolved edges in the pentagon layout if damage occurs at nodes 44,61,28 and 51

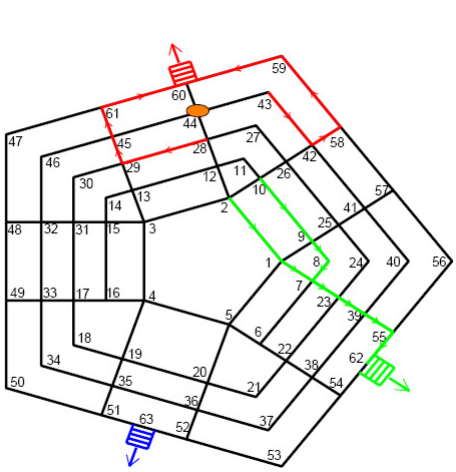

(a) Some shortest paths when node 44 is damaged

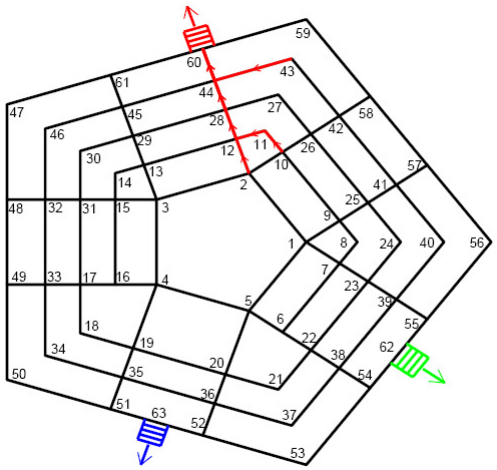

(b) The same shortest paths as above in the undamaged state

Figure 2.9: Comparison of some of the shortest paths when node 44 is damaged with the undamaged state

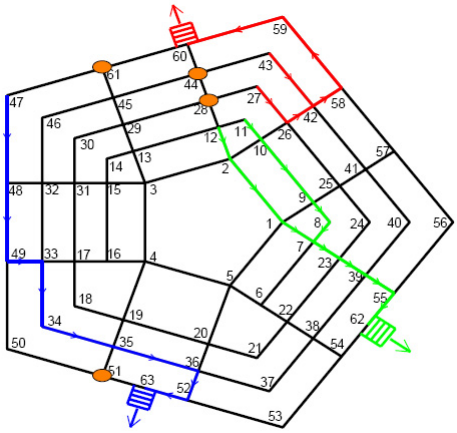

(a) Some shortest paths when nodes 44,28,61 and 51 are damaged

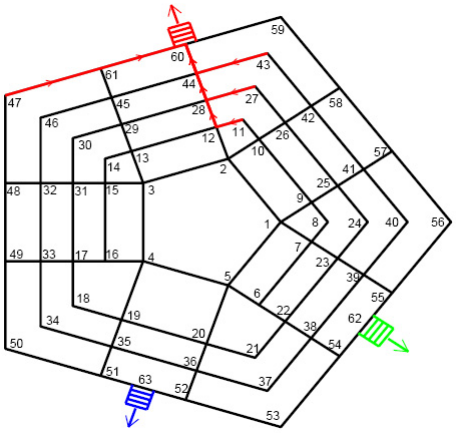

(b) The same shortest paths as above in the undamaged state

Figure 2.10: Comparison of some of the shortest paths when nodes 44, 28, 61 and 51 are damaged with the undamaged state

not the exit points at the first floor. In fact on floor 1 the exits are assumed to be nodes 48, 57 and 63 where as on floor 2 the exits are assumed to be nodes 60, 62 and 63. In Figure 2.11 we show the shortest paths on floor 1 and floor 2 for the undamaged case. In Figure 2.12 we show the evacuation paths from the same starting points but for the cases of damage at nodes 41 and 56 on the first floor and at node 44 on the second floor.

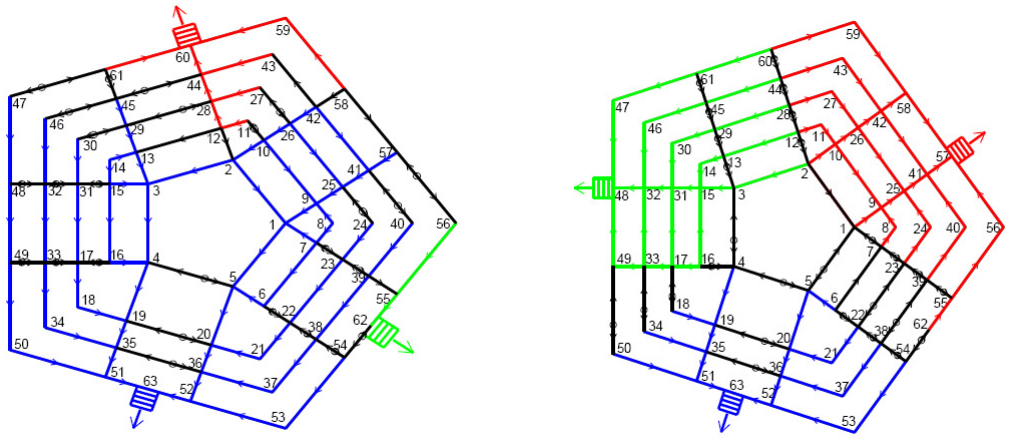

(a) Shortest paths on floor 2 in the undamaged state. Exits assumed at nodes 60,62 and 63

(b) Shortest paths on floor 1 in the undamaged state. Exits assumed at nodes 48, 57 and 63

Figure 2.11: Routing in a pentagon layout for 2 floors.

—

2.8.1 Additional Distance Covered in an Unguided Evacuation on a Damaged Route

In this section we show the importance of recomputing the shortest paths in real time based on the jamming and the layout damage data and conveying it to the evacuating population. In Table 2.8.1 we show the distance to be covered from some of the nodes (column 1) to the nearest exit using the shortest path for the undamaged (column 2), the damaged with guidance (D.G.) (column 3) and the damaged without guidance(D.W.G) (column 4) case. In the damage without guidance case it is assumed that the evacuees follow the undamaged shortest path till a node that is adjacent to

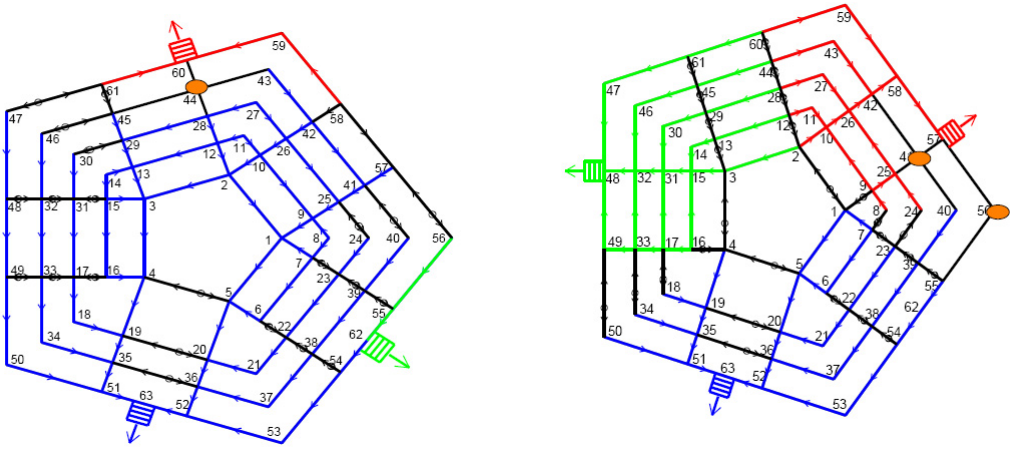

(a) Shortest paths on floor 2 in the damaged state. Exits assumed at nodes 60,62 and 63. Damage at node 44

(b) Shortest paths on floor 1 in the damaged state. Exits assumed at nodes 48, 57 and 63. Damage at nodes 41 and 56

Figure 2.12: Routing in a damaged pentagon layout for 2 floors.

the damaged node and from that node onwards follow the damaged shortest path. Though this assumption is unrealistic still it does give us a lower bound on the distance that an evacuee would have to travel in the case of layout damage without real time routing guidance. Thus the distances stated in column 4 of Table 2.8.1 are the least distances the pedestrians would travel in the damage without guidance (D.W.G.) case. Typically the distances will be much more and the paths to the exits would be found out by the evacuees by haphazard trial and error. The effects of panic and chaos ensuing from such a situation could be enormous. Column 5 of Table 2.8.1 is the % of additional distance that has to be covered for the damage without guidance case with respect to the damage with guidance case. As can be seen even for the case of lower bound on the distance traveled in the unguided case the additional distance percentages are considerably high. This strongly nessacitates the need for guided evacuation with recomputation of shortest paths in real time.

2.9 Chapter Summary

This chapter describes the problem of pedestrian evacuation along a shortest or quickest path from a complex network of interconnected corridors on a floor and interconnected

col. 1	col. 2	col. 3	col. 4	col. 5
node	undamaged	D.G	D.W.G.	% diff
2	3.80	7.50	9.60	28.02
3	6.27	9.97	15.63	56.78
4	5.03	7.50	7.50	0
10	4.27	7.98	10.08	26.35
15	6.75	11.02	12.55	13.86
31	7.15	10.85	16.52	52.18
32	7.55	11.26	16.92	50.31
48	7.99	12.23	17.75	45.19
42	5.09	6.50	10.61	63.34
26	4.68	7.39	10.21	38.20

Table 2.1: Shortest path values for the undamaged, damaged with guidance (D.G.) and the damaged without guidange (D.W.G.) case for nodes in column 1. Column 5 shows the % difference in the damaged with guidance (D.G.) and the damaged without guidance (D.W.G.) case. The exact units of distance are not known as the measurements were made on a scaled layout.

floors in a multi-story building. Framework of the pedestrian routing is formulated, and solved using the dynamic programming. The basic elements of the dynamic programing as applied to the calculation of the shortest path are described. The problems of single exit, multiple exits, and multiple floors are solved. The approach calculates the shortest distance or time to the exits and the corresponding path that the evacuees need to follow. The example results are presented to show the application of the approach to a realistic complex evacuation situation by considering the problem of evacuation from Pentagon. Shortest paths from different points of the building to the nearest exits are calculated and shown schematically. The cases for normal evacuation where all the links and nodes are usable for evacuation, as well the cases when certain nodes of the building are not accessible due to damage, are presented.

The approach in this chapter can be used to define the static routes for a complex building plan. It can also be used to used to define the re-routing plans if any portion

of the building network becomes unaccessible. This re-routing can also be done at intermittent time intervals in a pseudo dynamic sense by updating the edge weights using the real time congestion data. This would obviously result in an extremely efficient evacuation. However very advanced optical or pressure sensors would have to be used in order to generate the real time congestion data.

Chapter 3

Corridor Evacuation Control

3.1 Introduction

In the previous chapter, a shortest path calculation methodology was presented for the routing of pedestrians from a network of interconnected corridors and floors in an emergency evacuation situation. As input data this methodology needed the time estimates to traverse the corridor or the edge weights. These edge weights have to be evaluated assuming either free flow of pedestrians or model based density dependent flow. This typically involves finding the flow speed in the corridor and dividing the length of the corridor with the flow speed.

However in addition to routing, the pedestrian flow in an evacuation situation needs to be regulated. However, in the corridors adjacent to an exit we should expect high levels of congestion. In such case it may be necessary to regulate the pedestrian speed to avoid jamming and ensuing panic. The objective of the following study is thus to examine the flow conditions under an evacuation scenario for such exit corridors, and see if any controls can be exercised to avoid jamming and to expedite the evacuation.

The chapter is organized as follows. In Sec. 3.2 is presented the flow model for a corridor divided into sections. This flow model will be used subsequently to simulate the uncontrolled cases and develop, analyze and simulate the controls for various flow scenarios. Specifically we consider three flow scenarios that can be linked to various phases of evacuation, namely end, middle and beginning. In Sec. 3.3, 3.4 and 3.5 we outline the specifications of the uncontrolled flows, develop and analyze the control

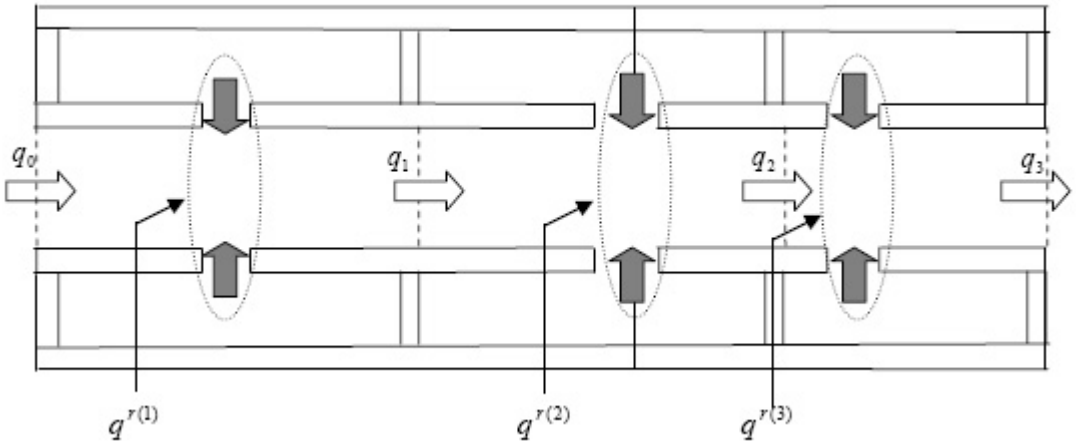

Figure 3.1: Flow in a corridor divided into sections

for these flow scenarios and make a comparison of the uncontrolled and the controlled flow case using numerical simulation for each of these flow scenarios. In Sec. 3.6 we summarize the content of the chapter.

3.2 Pedestrian Flow Model in a Corridor

In this section we develop equations for pedestrian flow in an exit corridor based on conservation of mass (pedestrians). A physical model of an exit corridor considered here consists of a corridor with pedestrian mass distributed along its length and pedestrian input from back and rooms adjacent to the corridor. The pedestrians are assumed to exit the corridor freely without any congestion at the exit end. A more general case in which a corridor is a part of a network is considered in the next chapter. To account for density variation along the length, the corridor is divided into sections, and each section is assumed to have a uniform pedestrian density. The schematic representation of such a corridor divided into sections and receiving flow input from the back and adjacent rooms is shown in Figure 3.1. The corridor in Figure 3.1 is divided into 3 sections. However we develop the equations for a general case of an n section corridor. Also we are assuming that the pedestrian flow in the corridor is one dimensional. That is, the pedestrian flow does not have a significant lateral component as compared to

its longitudinal component.

Let q_0 be the pedestrian input flow from the back. Let the room discharge into the i^{th} section be denoted by $q^{r(i)}$. This parameter denotes the rate at which the pedestrians enter the section i from all the rooms connected to the section. For the i^{th} section, let q_{i-1} and q_i be the rates at which the people get in and get out of the rear and front ends of the section, respectively. Let ρ_i denote the pedestrian density for the i^{th} section. This represents the number of pedestrians per unit length of the corridor. Writing the conservation of mass (pedestrians) equation for this section we get:

$$(\Delta\rho_i)L_i = (q_{i-1} - q_i + q^{r(i)})\Delta t. \tag{3.1}$$

where $\Delta\rho_i$ is an infinitesimal change in the section density ρ_i in an infinitesimal change in time Δt. Dividing equation (3.1) by Δt and in the limit letting Δt go to 0, we get the the following ordinary differential equation governing the evolution of the section pedestrian density:

$$\dot{\rho}_i = \frac{q_{i-1} - q_i + q^{r(i)}}{L_i}. \quad 1 \leq i \leq n \tag{3.2}$$

It is a common observation that pedestrian velocity is a function of pedestrian density. The more jammed the pedestrians are, *i.e.* the higher the pedestrian density, the lower the flow speed. It is observed that at a certain high pedestrian density called the jam density the pedestrians cannot move, that is the flow velocity becomes zero. It is, thus, apparent that the pedestrian velocity model should include the dependence of the velocity on the pedestrian density considering the parameter of the jam density. The jam density being the density at which the pedestrians or the traffic entities cannot move would depend on the sizes of the pedestrians as well as on the corridor width.

In the studies involving flow of traffic, a simple model called the Greensheilds model (Greenshields, 1935) is quite often used to describe the flow velocity and flow density relationship. For the pedestrian flow problem we propose to use the same model described by the following equation:

$$v = \left(1 - \frac{\rho}{\rho_m}\right) v_f. \tag{3.3}$$

This model assumes a linearly decreasing relationship between the pedestrian velocity v and pedestrian density ρ. The parameter v_f in equation (3.3) is the free flow velocity and the parameter ρ_m is the jam density. The free flow velocity is the velocity at

pedestrian density $\rho = 0$. This represents the speed at which a single pedestrian can move if her/his motion is not obstructed by other pedestrians. The jam density ρ_m represents the density at which the pedestrian flow speed $v = 0$. The jam density parameter for a corridor can be computed by assigning a circular area to every pedestrian that corresponds to a typical pedestrian size and finding the maximum number of such circles that can be packed in the corridor. This number divided by the length of the corridor would give the jam density of the corridor. However this elementary approach would need experimental verification. This density also represents the highest level of pedestrian congestion possible in a corridor. Using the velocity given by equation (3.3) we can get the following relationship between the pedestrian flow discharge q and the pedestrian density ρ :

$$q = \rho v = \rho \left(1 - \frac{\rho}{\rho_m}\right) v_f. \tag{3.4}$$

In Figure 3.2(a) is shown the plot of velocity v/s density for the Greenshields model and in Figure 3.2(b) is shown the plot of discharge v/s density for the Greenshields model. It can be seen that the average velocity v linearly decreases with respect to the density ρ and the discharge q varies quadratically with respect to the density ρ for a constant value of free flow velocity v_f. From Figure 3.2(b) we can see that maximum or critical discharge for the Greenshields model corresponds to a density of $\rho_{cr} = \frac{\rho_m}{2}$. This maximum discharge for the Greenshields model is given by:

$$q_m = \frac{\rho_m v_f}{4}. \tag{3.5}$$

Using the density-discharge relationship given by equation (3.4) for the outflow discharge q_i corresponding to section density ρ_i in equation (3.2) we get the following equations governing the evolution of pedestrian densities ρ_i for $1 \leq i \leq n$:

$$\dot{\rho}_1 = \frac{q_0 + q^{r(1)} - \rho_1 \left(1 - \frac{\rho_1}{\rho_m}\right) v_{f_1}}{L_1} \tag{3.6}$$

$$\dot{\rho}_i = \frac{q^{r(i)} + \rho_{i-1} \left(1 - \frac{\rho_{i-1}}{\rho_m}\right) v_{f_{i-1}} - \rho_i \left(1 - \frac{\rho_i}{\rho_m}\right) v_{f_i}}{L_i}. \quad 2 \leq i \leq n \tag{3.7}$$

It is noted that in equation (3.6) the term q_0 is the inflow discharge parameter into the corridor and hence it cannot be stated in terms of any section density.

Jam density ρ_m is a parameter that depends on a specific corridor and needs to be determined experimentally. However as we would like to generate numerical results

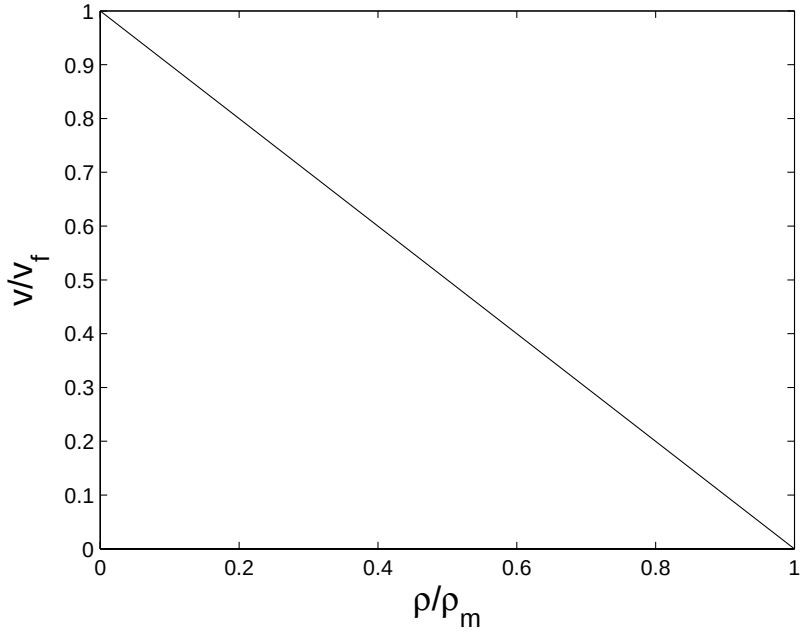

(a) Average velocity v in terms of the density ρ using the Greenshields model

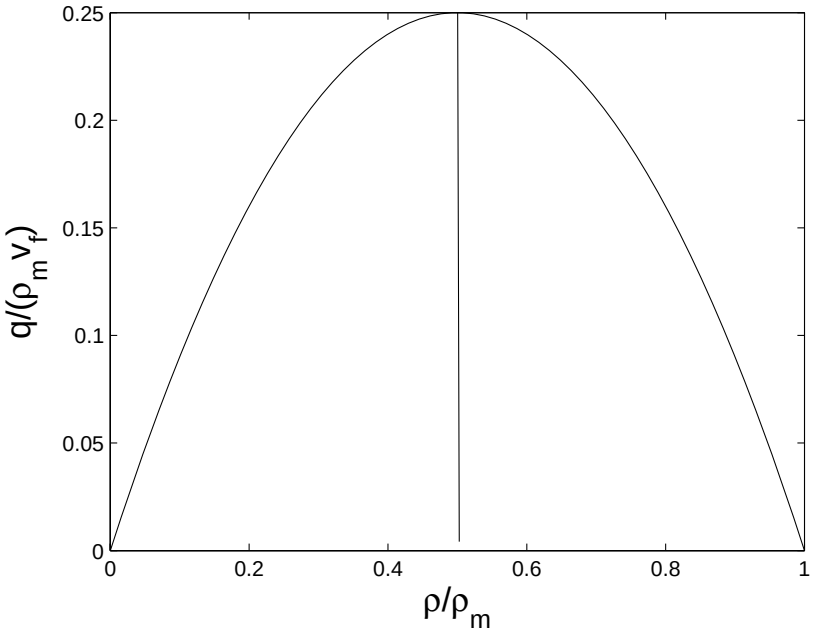

(b) Discharge q in terms of the density ρ using the Greenshields model

Figure 3.2: Velocity and Discharge v/s density for the Greenshields model.

independent of this parameter we normalize the equations (3.6) and (3.7). In order to do this we divide these equations with the jam density ρ_m and obtain the following equations:

$$\dot{\tilde{\rho}}_1 = (\tilde{q}_0 + \tilde{q}^{r(1)} - \tilde{\rho}_1(1-\tilde{\rho}_1)\tilde{v}_{f_1})b_1 \tag{3.8}$$

$$\dot{\tilde{\rho}}_i = (\tilde{q}^{r(i)} + \tilde{\rho}_{i-1}(1-\tilde{\rho}_{i-1})\tilde{v}_{f_{i-1}} - \tilde{\rho}_i(1-\tilde{\rho}_i)\tilde{v}_{f_i})b_i. \tag{3.9}$$

In equation (3.8) and (3.9) the quantities with tilde denote the normalized quantities. The normalized density $\tilde{\rho}_i$ is defined as:

$$\tilde{\rho}_i = \frac{\rho_i}{\rho_m}.$$

This represents the actual density as a fraction of the jam density. The normalized free flow velocity is expressed as the ratio of the free flow velocity v_{f_i} to the length of the corridor L and is defined as:

$$\tilde{v}_{f_i} = \frac{v_{f_i}}{L}.$$

It denotes the actual free flow velocity in terms of lengths of corridor per unit time. The normalized values of the input discharge $\tilde{q}_0$ and the room discharge, $\tilde{q}^{r(i)}$ are defined as :

$$\tilde{q}_0 = \frac{q_0}{\rho_m L}.$$

$$\tilde{q}^{r(i)} = \frac{q^{r(i)}}{\rho_m L}.$$

where $\rho_m L$ is the maximum number of pedestrians that can be filled up in a corridor. Thus $\tilde{q}_0$ is the fraction of the maximum number of pedestrians $\rho_m L$ that flow into the corridor from its back end. Likewise $\tilde{q}^{r(i)}$ denotes the fraction of the maximum number of pedestrians $\rho_m L$ that flow into the section i per unit time from the adjoining rooms. The normalization constants b_i in equations (3.8) and (3.9) are the ratios of the length of the corridor to those of the sections i. They are given by:

$$b_i = \frac{L}{L_i}. \quad 1 \leq i \leq n$$

In the analysis that follows the equations (3.8) and (3.9) are the state equations and the normalized section densities $\tilde{\rho}_i$ for sections $1 \leq i \leq n$ are the state variables. The section densities ρ_i have to be always non-negative and cannot exceed the jam density.

Thus the normalized section densities which are the state variables must satisfy the following bounds at all times:

$$0 \leq \tilde{\rho}_i \leq \frac{\rho_m}{\rho_m} = 1 \tag{3.10}$$

To control the flow in the corridor we will use the normalized free flow velocities $\tilde{v}_{f_i}$ in different sections, normalized room discharges $\tilde{q}^{r(i)}$ in different sections and the normalized rear input discharge $\tilde{q}_0$ as the control variables. That is, the control algorithm will calculate these variables which then will be used to regulate the pedestrian flow. We assume that the free flow velocities can be made to vary between 0 and a certain maximum value v_{f_m}, resulting in the following bounds on this variable:

$$0 \leq \tilde{v}_{f_i} \leq \tilde{v}_{f_m} = \frac{v_{f_m}}{L}. \tag{3.11}$$

We also need to impose bounds on the normalized section room discharges $\tilde{q}^{r(i)}$ and the normalized rear input discharges $\tilde{q}_0$. We assume that the maximum rear input discharge that can get into the corridor is given by the maximum discharge corresponding to the Greenshields model. This is given by equation (3.5). This discharge when normalized by the maximum number of pedestrians $\rho_m L$ results in:

$$\tilde{q}_m = \frac{\frac{\rho_m v_{f_m}}{4}}{\rho_m L} = \frac{\tilde{v}_{f_m}}{4} \tag{3.12}$$

We assume a unidirectional rear input discharge q_0, meaning that the pedestrians cannot be sucked out from behind. Hence $q_0 \geq 0$. Likewise we assume that the rooms do not act as pedestrian absorbers. We assume that the maximum discharge from all the rooms in the corridor will equal the maximum discharge given by the Greenshields model in equation (3.5). As there are n sections in the corridor hence the maximum discharge into each section will have an upper bound that corresponds to $\frac{q_m}{n}$. Thus the bounds on the normalized discharges are given by:

$$0 \leq \tilde{q}_0 \leq \tilde{q}_m \tag{3.13}$$

$$0 \leq \tilde{q}^{r(i)} \leq \frac{\tilde{q}_m}{n} \tag{3.14}$$

The model developed in this section is used to develop control algorithm for three evacuation cases described in the sequel. The evacuation control cases described are progressively more complex as more control inputs need to be managed. The flow cases that we investigate are:

1. **No rear input discharge and no room discharge.** This can be expected to be the case towards the very end of the evacuation process, when there are no pedestrians left to enter from behind and no pedestrians left in the adjoining rooms.

2. **Rear input discharge but no room discharge.** This case can be expected to happen sometime in the middle of the evacuation process when the pedestrians in the adjoining rooms have evacuated but there are still pedestrians entering the corridor from its rear end.

3. **Rear input discharge and room discharge.** This would be the evacuation scenario in the very beginning when there are pedestrians entering the corridor from the rear end as well as from the adjoining rooms.

For each case we first describe the uncontrolled flow scenario followed by the development of the control algorithm. Then for each case, the numerical results are obtained by simulation for different flow parameters of section densities, free flow velocities and discharge quantities. These results are then compared for the uncontrolled and controlled cases to demonstrate the advantages of affecting the pedestrian control.

3.3 Case 1: No rear discharge and no room discharge case.

This would be the case towards the end of the evacuation process when there are no pedestrians left to enter the corridor from the adjoining rooms as well as from its rear end. Thus in this case we have:

$$\tilde{q}_0 = 0 \tag{3.15}$$

$$\tilde{q}^{r(i)} = 0 \;\; 1 \leq i \leq n. \tag{3.16}$$

The state equations (3.8) and (3.9) for this case correspondingly become:

$$\dot{\tilde{\rho}}_1 = (-\tilde{\rho}_1(1-\tilde{\rho}_1)\tilde{v}_{f_1})b_1 \tag{3.17}$$

$$\dot{\tilde{\rho}}_i = (\tilde{\rho}_{i-1}(1-\tilde{\rho}_{i-1})\tilde{v}_{f_{i-1}} - \tilde{\rho}_i(1-\tilde{\rho}_i)\tilde{v}_{f_i})b_i \tag{3.18}$$

From equations (3.17) and (3.18) it is apparent that the only control input parameters available in this case would be the normalized section free flow velocities $\tilde{v}_{f_i}$. As mentioned before, next we develop the characteristics of pedestrian flow for two different scenarios: (a) panic driven uncontrolled flow, (b) controlled flow regulated by proper adjustment of free flow velocities in different corridor sections. This is followed by the comparison of the numerical simulation result obtained for the two flow scenarios.

3.3.1 The uncontrolled flow

In an uncontrolled flow scenario, we expect that the pedestrian would try to move with the maximum possible speed. In terms of our control variable, it means that the normalized free flow velocity in each section is equal to its maximum value. That is,

$$\tilde{v}_{f_i} = \tilde{v}_{f_m} \quad 1 \leq i \leq n. \tag{3.19}$$

This can happen in panic driven situation. This unregulated movement may cause jamming of people in some sections. When a section reaches its jam density,ρ_m, we assume that flow in this section will completely stop as indicated by equation (3.3). This would even happen at a non-zero free flow velocity. However, notionally set the free flow velocity in section i that gets jammed, $\tilde{v}_{f_i} = 0$, indicating the stoppage of flow. An important consequence of a section i of a corridor getting jammed would be that the pedestrians in the preceding section $i-1$ will not be able to move as their forward motion is completely blocked. This would happen even if the density in section $i-1$, $\tilde{\rho}_{i-1} \leq 1$, or the section $i-1$ is not jammed. Thus in order to account for this stoppage of motion in the section $i-1$ we set the free flow velocity in that section $\tilde{v}_{f_{i-1}} = 0$. We have used this approach to generate the numerical simulation results for the uncontrolled case.

Here we mention that in reality, we can expect that there will be some diffusion of the pedestrians which will eventually ease the congestion. So the evacuation situation will not be as extreme as described in the previous paragraph. However, we are not interested in refining the uncontrolled flow model by including the diffusion. The simulation results obtained with or without diffusion will show a considerable interruption of the flow. Furthermore the objective of this study is to develop controls to avoid the congestion, thus we will not worry about the precise nature of uncontrolled evacuation

considering the diffusion.

3.3.2 The controlled flow

In this section we develop a controlled flow scenario in which we regulate the free flow velocities in different sections. The control objective are the asymptotic stability of the state equations, (3.17) and (3.18), ensuring that no jamming occurs in any of the sections and the control variables $\tilde{v}_{f_i}$ remain within bounds. Asymptotic stability of the state equations implies that not only the normalized section densities $\tilde{\rho}_i$, which are the state variables in our problem remain within certain bounds of the zero state corresponding to $\tilde{\rho}_i = 0$ for $1 \leq i \leq n$ but also that they approach $\tilde{\rho}_i = 0$ for $1 \leq i \leq n$ asymptotically.

The theory of dynamics and control of the linear systems is well developed and well understood. However, our state equations (3.17) and (3.18) are non-linear and hence the stability concepts developed for the linear systems cannot be directly used for our case. One strategy that is often adopted to develop control for nonlinear systems is based on the concept of feedback linearization explained in the text books on control (Slotine and Li, 1991 ; Khalil, 1996 ; Nijmeijer and van der Schaft, 1990). In this section, we use this concept to present a feedback control method that uses the current value of the state and computes the control such that the resulting state equations are linear. We note that by choosing the normalized section free flow velocity to be:

$$\tilde{v}_{f_i} = \frac{k_i}{1 - \tilde{\rho}_i} \tag{3.20}$$

we can achieve this precisely. Here $k_i > 0$ is the control gain corresponding to section i. If we substitute the control in equation (3.20) in the flow equations (3.17) and (3.18) we obtain the following system of equations:

$$\dot{\tilde{\rho}}_1 = -k_1 b_1 \tilde{\rho}_1$$

$$\dot{\tilde{\rho}}_i = k_{i-1} b_i \tilde{\rho}_{i-1} - k_i b_i \tilde{\rho}_i. \tag{3.21}$$

Thus by using the control of equation (3.20) we are able to convert the non-linear equations (3.17) and (3.18) in state and control variables to linear equations (3.21) in the state variables $\tilde{\rho}_i$. We also note that the control variable $\tilde{v}_{f_i}$ in equation (3.20) depends on the state variable $\tilde{\rho}_i$. Thus this is a feedback control that linearizes the

system of governing differential equations. From equation (3.3), it is noted that this form of control renders the normalized section flow velocity $\tilde{v}(\rho)$ to be a constant value equal to k.

3.3.3 Stability under control

A question that naturally arises is if this feedback linearization scheme creates a stable system. We investigate this issue in the case of constant gain for all the sections. Thus for our analysis here we assume $k_i = k$, for all $1 \leq i \leq n$. For the system to remain asymptotically stable, the pedestrian densities should remain bounded under the application of this control and should progressively approach 0 as the time t approaches ∞. Herein we derive the conditions on parameters b_i to achieve this stability. Later in the Sec. 3.3.3 it is shown that for the equal section case the stability criteria are automatically satisfied.

The flow equations (3.20) with constant gain $k > 0$ for all the sections $1 \leq i \leq n$ can be written in the matrix form as:

$$\dot{\tilde{\rho}} = -k\mathbf{B}\tilde{\rho}. \tag{3.22}$$

In this equation $\mathbf{B}$ is a $n \times n$ matrix which has the following form:

$$\mathbf{B} = \begin{bmatrix} b_1 & & & & & & \\ -b_2 & b_2 & & & & & \\ 0 & -b_3 & b_3 & & & & \\ 0 & & -b_4 & b_4 & & & \\ . & & & & . & & \\ . & & & & & . & \\ . & . & . & . & . & -b_n & b_n \end{bmatrix} \tag{3.23}$$

The system of equations (3.22) is asymptotically stable if the matrix $-k(\mathbf{B^T} + \mathbf{B}) < 0$ (i.e. is negative definite) (Rugh, 1996). Since $k > 0$ this is equivalent to $(\mathbf{B^T} + \mathbf{B}) > 0$ (positive definite). This requires that $\mathbf{D} = \frac{\mathbf{B^T}+\mathbf{B}}{2} > 0$. The form which D assumes for

a general n dimensional system is as follows:

$$\mathbf{D} = \begin{bmatrix} b_1 & -\frac{b_2}{2} & & & & & \\ -\frac{b_2}{2} & b_2 & -\frac{b_3}{2} & & & & \\ 0 & -\frac{b_3}{2} & b_3 & -\frac{b_4}{2} & & & \\ 0 & & -\frac{b_4}{2} & b_4 & . & & \\ . & & & . & . & . & \\ . & & & & . & . & -\frac{b_n}{2} \\ . & . & . & . & . & -\frac{b_n}{2} & b_n \end{bmatrix}. \tag{3.24}$$

For $\mathbf{D} > 0$ it is necessary that all determinants D_i of the sub-matrices $\mathbf{D}_i$ of matrix $\mathbf{D}$ be greater than 0. The sub-matrices $\mathbf{D}_i$ are the square matrics of dimension $i \times i$ in the upper left corner of matrix $\mathbf{D}$. For the given structure of $\mathbf{D}$ we observe the following recurrence relation for D_i:

$$\begin{aligned} D_1 &= b_1 \\ D_2 &= b_1 b_2 - \frac{b_2^2}{4} \\ D_i &= b_i D_{i-1} - \frac{b_i^2}{4} D_{i-2} \quad 3 \leq i \leq n. \end{aligned} \tag{3.25}$$

$\mathbf{D}_i > 0$ if $\forall \;\; 1 \leq j \leq i \;\; D_j > 0$. This implies the following inequality relations for b_i's :

$$\begin{aligned} b_1 &> 0 \\ b_2 &< 4b_1 \\ b_i &< \frac{4D_{i-1}}{D_{i-2}}. \;\; \forall 3 \leq i \leq n \end{aligned} \tag{3.26}$$

Thus if we choose b_i such that the inequalities (3.26) are satisfied then $\mathbf{D} > 0$ (positive definite) and the system is stable. This in-turn implies that the section lengths L_i have to be chosen such that the inequalities (3.26) are satisfied.

Stability in the Equal Section Case

For the special case of the equal length section, we note that $b_i = \frac{L}{(L/n)} = n$. Thus the recurrence relation equation (3.25) assumes the following form:

$$D_1 = b_1 = n$$

$$D_2 = b_1 b_2 - \frac{b_2^2}{4} = \frac{3n^2}{4} \tag{3.27}$$

$$D_i = b_i D_{i-1} - \frac{b_i^2}{4} D_{i-2} = n(D_{i-1} - \frac{n}{4} D_{i-2}) \quad 3 \leq i \leq n.$$

By simple mathematical induction we can prove that:

$$D_i = n^i \frac{i+1}{2^i} > 0 \quad 1 \leq i \leq n \tag{3.28}$$

This means that for $b_i = n \quad \forall \quad 1 \leq i \leq n$, the system is asymptotically stable for equal length section if the sections gains $k_i = k$ for all $1 \leq i \leq n$.

This implies that the densities in the sections will not grow unbounded. Rather they approach 0 asymptotically at $t \to \infty$, as is shown in the following section.

3.3.4 Boundedness of control and no jamming

In this section it is shown that the control, corresponding to the normalized free flow velocities $\tilde{v}_{f_i}$ given by equation (3.20) for the case of constant gains $k_i = k$ for all sections $1 \leq i \leq n$ never crosses its bounds specified by equation (3.11) as long as the initial pedestrian densities are are below a certain prescribed value. It is noted that as $k > 0$ the the control specified by equations (3.20) is positive for all $1 \leq i \leq n$. Thus for this form of the control the lower bound of the control is automatically satisfied. Now we proceed to prove that so long as the initial normalized section densities $\tilde{\rho}_i$ are below a certain value the upper bound for controls $\tilde{v}_{f_i}$ specified by equation (3.11) is automatically satisfied. This upper bound from equation (3.11) is denoted by $\tilde{v}_{f_m}$. For the normalized free flow velocities $\tilde{v}_{f_i}$ (control parameters) to remain below its upper bound we need the following condition to be satisfied:

$$\tilde{v}_{f_i} = \frac{k}{1 - \tilde{\rho}_i} \leq \tilde{v}_{f_m} \tag{3.29}$$

Readjusting the inequalities (3.29) results in the following inequalities in terms of the state variables to ensure boundedness of control:

$$\tilde{\rho}_i \leq \left(1 - \frac{k}{\tilde{v}_{f_m}}\right) = \mu \quad 1 \leq i \leq n. \tag{3.30}$$

Conditions given by equations (3.30) are sufficient for keeping all the control variables v_{f_i} under the upper bound limit $\tilde{v}_{f_m}$ specified in equations (3.11). Thus our goal is

now to find the initial conditions under which the state variables $\tilde{\rho}_i$ remain below the value of μ. At this point we prove that if $\tilde{\rho}_i(0) \leq \mu$ then $\tilde{\rho}_i(t) \leq \mu$ for $0 \leq t \leq \infty$ if gains $k_i = k$ for all $0 \leq i \leq n$. Application of the feedback linearizing control given by equation (3.20) to these state equations with section wise constant gains $k_i = k$ for all $0 \leq i \leq n$ results in the following equations:

$$\dot{\tilde{\rho}}_1 = -kb_1\tilde{\rho}_1$$

$$\dot{\tilde{\rho}}_i = kb_i\tilde{\rho}_{i-1} - kb_i\tilde{\rho}_i. \tag{3.31}$$

From the 1^{st} equation of (3.31):

$$\dot{\tilde{\rho}}_1 = -kb_1\tilde{\rho}_1 \leq 0$$

This implies

$$\tilde{\rho}_1(t) \leq \tilde{\rho}_1(0) \leq \mu \ \ \forall \ \ 0 \leq t \leq \infty \tag{3.32}$$

Thus the proposition is proved for $\tilde{\rho}_1$. Now we prove the proposition for $\tilde{\rho}_k \ \ 2 \leq k \leq n$. We have for all $2 \leq k \leq n \ \ \tilde{\rho}_k(0) \leq \mu$. This implies that all the values of $\tilde{\rho}_k$ start from a value lower than μ. Let k be one such section $2 \leq k \leq n$ for which at $t = \tau$, $\tilde{\rho}_k(\tau) = \mu$, while all the other densities are either equal to or below μ. Thus for any other section $j \neq k$ for $1 \leq j \leq n$ we have $\tilde{\rho}_j \leq \tilde{\rho}_k$. Specifically we have $\tilde{\rho}_{k-1} \leq \tilde{\rho}_k$. Thus from equation (3.21) we get:

$$\dot{\tilde{\rho}}_k(\tau) = kb_k(\tilde{\rho}_{k-1}(\tau) - \tilde{\rho}_k(\tau)) \leq 0 \tag{3.33}$$

This implies

$$\tilde{\rho}_k(\tau + \delta\tau) \leq \tilde{\rho}_k(\tau) = \mu \tag{3.34}$$

for $\delta\tau \to 0$. Hence $\forall \ 2 \leq k \leq n \ \ \tilde{\rho}_k(t) \leq \mu \ \ \forall \ \ 0 \leq t \leq \infty$. This in view of equations (3.29) and (3.30) implies that no control variable $\tilde{v}_{f_i}$ for $1 \leq i \leq n$ would cross the upper bound $\tilde{v}_{f_m}$ for the state feedback linearizing control given by equation (3.21) for section wise constant gain $k_i = k$ for $1 \leq i \leq n$. In proving this we have equivalently proved that equation (3.30) is true for this control. This implies that $\tilde{\rho}_i \leq \mu \leq 1$, which is the condition for boundedness of control as well as no jamming.

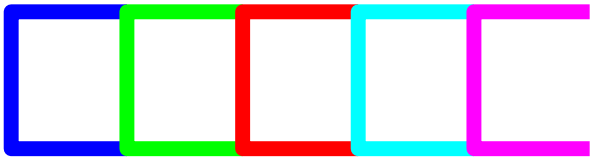

Figure 3.3: 5 sections of the corridor indicated in different colors. These colors will be used to plot various values corresponding to the sections.

3.3.5 Numerical Simulation

In this section we present and compare the numerical simulation results for the uncontrolled and controlled scenarios for case 1 flow conditions. We consider a corridor divided into 5 equal length sections like the one displayed in Figure 3.3. The colors of the sections displayed in that figure are used to plot the results corresponding to those sections. We assume the length of the corridor $L = 50m$ for our simulation. We assume the maximum free flow velocity to be $1.5m/s$. This would result in the normalized free flow velocity attaining its maximum value of $\tilde{v}_{f_m} = \frac{v_{f_m}}{L} = 0.03$. The results are presented in terms of the normalized state and control quantities. We choose relatively high initial normalized section densities in order to bring out a good comparison of the controlled and the uncontrolled flow situation. For this particular simulation, we choose a uniform value of $\tilde{\rho}_i^0 = 0.8$. For the controlled simulation case we are assuming the same gains value for all the sections. Specifically we choose $k_i = k = 0.0057 < 0.006$. The value of 0.006 is the maximum value of k that can be chosen according to equation (3.29) corresponding to $\tilde{\rho}_i^0 = 0.8$ to maintain the boundedness of the section free flow

velocities.

In Figures 3.4(a) and 3.4(b) we show the evolution of the normalized densities for the uncontrolled and controlled flow scenarios, respectively. The black dashed line in the figures indicate the critical normalized density of 0.5 or density corresponding to maximum discharge for a given free flow velocity. From the uncontrolled flow results shown in Figure 3.4(a) we observe that the normalized section densities in section 2 and section 4 reach the normalized jam density value of 1 within about 20 s and 30 s from the start, respectively. In such situations, the pedestrians in the preceding sections cannot move due to stoppage of flow. Thus after section 2 gets jammed about 20 s from the start the pedestrians in section 1 cannot move. As there is no inflow of pedestrians into section 1, the density in this section freezes to its value at the time section 2 gets jammed. After section 4 gets jammed in about 30 s from the start the pedestrians in section 3 cannot move. However as section 2 has already jammed at this point in time hence there is no inflow of pedestrians into this section either. Hence the section density in section 3 freezes at this point in time when section 4 gets jammed. This freezing of densities to their respective values in section 1 and 3 can be seen in Figure 3.4(a). In contrast to this situation, the normalized section density evolution in the controlled case is much better as can be seen in Figure 3.4(b). The density values steadily drop from a high value of 0.8 and asymptotically approach 0. There is no occurrence of jamming as was proved for this control.

In Figures 3.5(a) and 3.5(b), we show the plots of time evolution of the control variable of the free flow velocity for the uncontrolled and controlled cases, respectively. As explained in the section on uncontrolled flow, the free flow velocities in all the sections start at a maximum values. Then as a section get jammed the free flow velocity in that section and the preceding section become 0. This is clearly seen from Figure 3.5(a) that the lines corresponding to section 2 and section 4 drop off to 0 from their maximum value at the same times as the sections get jammed. The lines corresponding to section 1 and section 3 are hidden behind the lines for sections 2 and 4. The free flow velocity in the 5^{th} or the last section remains at its maximum value throughout as the density in this section never reaches the jam density; in fact it steadily decays to 0. In contrast to the above situation, the free flow velocities for the controlled case shown in Figure 3.5(b) change gradually and remain within their

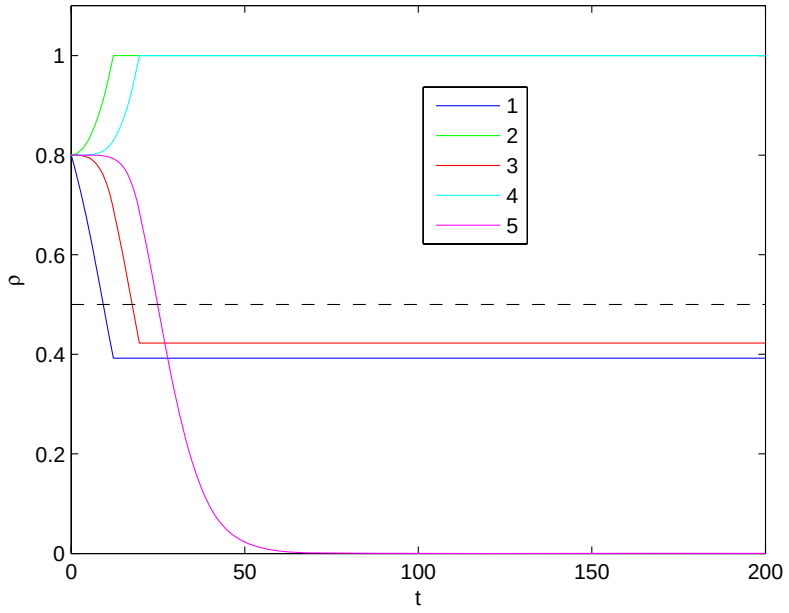

(a) Normalized section density $\tilde{\rho}_i$ in the uncontrolled case

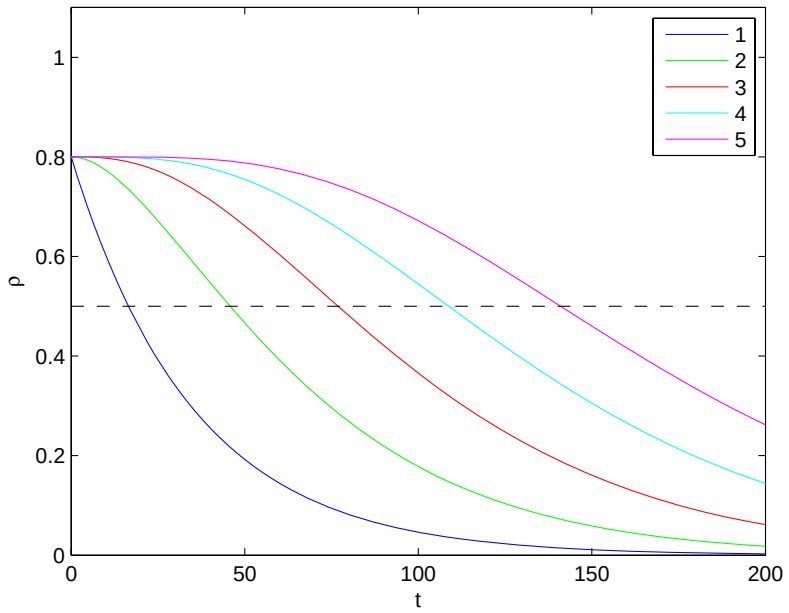

(b) Normalized section density $\tilde{\rho}_i$ in the controlled case

Figure 3.4: Normalized corridor section densities $\tilde{\rho}_i$ for all sections in the controlled and the uncontrolled case of flow scenario 1.

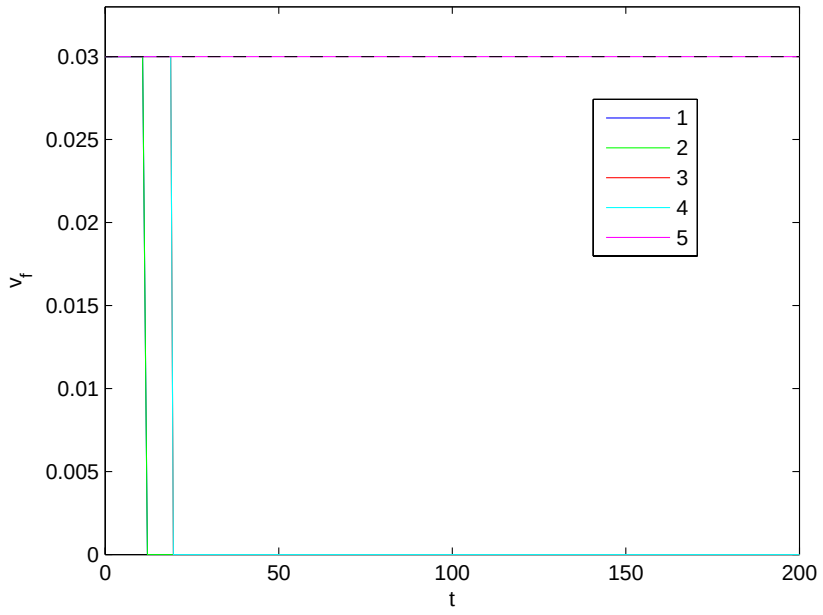

(a) Normalized section free flow velocity $\tilde{v}_{f_i}$ in the uncontrolled case

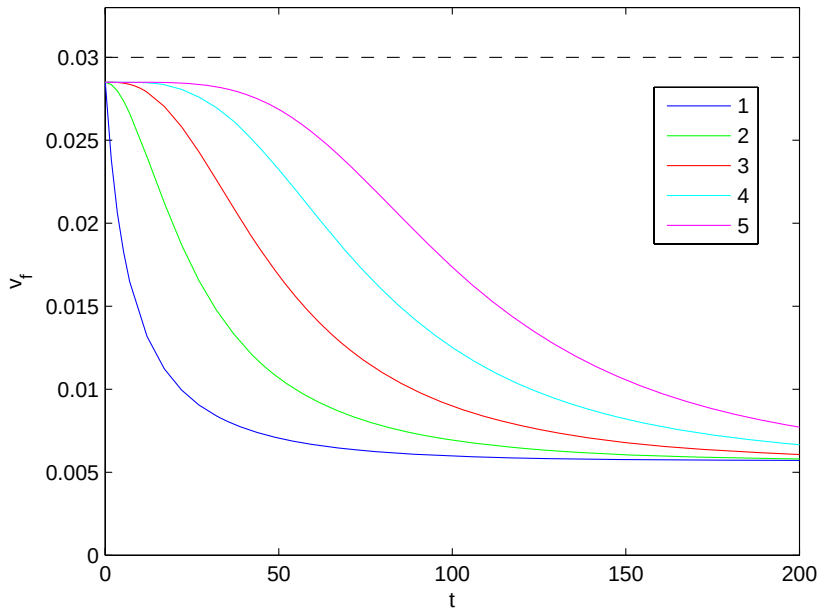

(b) Normalized section free flow velocity $\tilde{v}_{f_i}$ in the controlled case

Figure 3.5: Normalized corridor section free flow velocity $\tilde{v}_{f_i}$ for all sections in the controlled and the uncontrolled case of flow scenario 1.

specified bounds. This happens because the gains were chosen to ensure the bounded ness requirement.

In Figure 3.6 is shown a comparison of the exit discharges in the controlled and the uncontrolled cases. It can be seen that in the controlled case the discharge remains

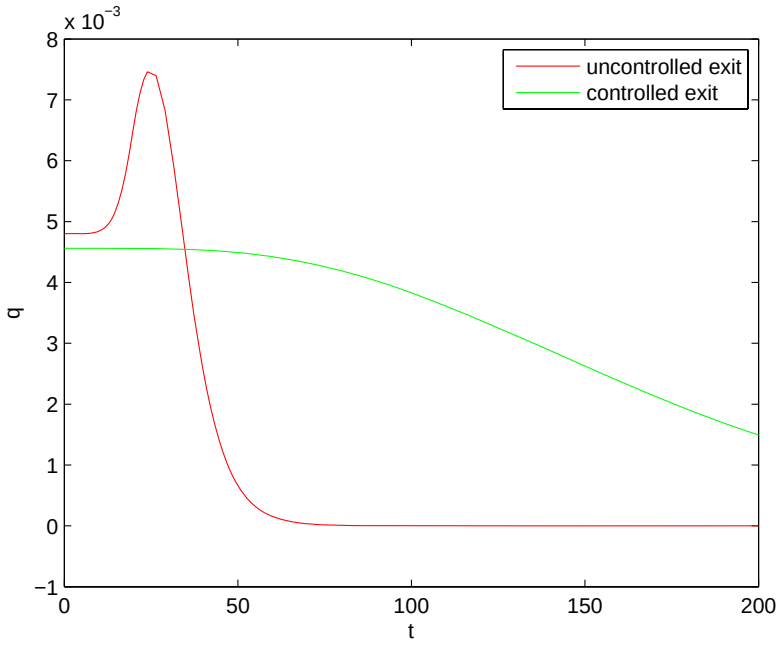

Figure 3.6: Normalized exit discharge in the controlled and the uncontrolled case.

consistently at reasonably high non-zero values while for the uncontrolled case it suddenly peaks to the critical value when the density in the last section, section 5 crosses the critical normalized density value of 0.5, and then suddenly drops to zero as flow from the sections behind section 4 gets blocked due to jamming in section 4. Thus from the above figures and discussion it is apparent that in the uncontrolled flow the sections get jammed and blocked while in the controlled flow the flow conditions are far better and the densities smoothly approach 0.

3.4 Case 2: Rear input discharge but no room discharge.

This flow scenario would occur sometime after the start of the evacuation process from the building but sometime before the end phase described in flow scenario 1 when there are no pedestrians in the rooms adjoining the corridors however there are pedestrians still entering from its rear end. The normalized section room discharges for all sections are set to 0 as there are no pedestrians occupying the rooms adjacent to the sections. Thus we have:

$$\tilde{q}^{r(i)} = 0 \;\; 1 \leq i \leq n. \tag{3.35}$$

In this case the state equations (3.8) and (3.9) become:

$$\dot{\tilde{\rho}}_1 = (\tilde{q}_0 - \tilde{\rho}_1(1-\tilde{\rho}_1)\tilde{v}_{f_1})b_1 \tag{3.36}$$

$$\dot{\tilde{\rho}}_i = (\tilde{\rho}_{i-1}(1-\tilde{\rho}_{i-1})\tilde{v}_{f_{i-1}} - \tilde{\rho}_i(1-\tilde{\rho}_i)\tilde{v}_{f_i})b_i \quad 2 \leq i \leq n \tag{3.37}$$

From equations (3.36) and (3.37) it is apparent that the control parameters available for this scenario are $\tilde{q}_0$ and $\tilde{v}_{f_i}$ for sections $1 \leq i \leq n$. Using these parameter we first state what we predict in a panic driven uncontrolled flow for this flow scenario. This is done by assigning the values to the control input variables in the absence of an explicit control. After this we develop the control for this flow scenario. Then we compare the results from the simulation of the controlled and the uncontrolled flow scenarios.

3.4.1 Uncontrolled flow

As in the previous flow case in this case too we expect the normalized free flow velocities in all the sections to be at their maximum value. This can be expected to happen due to the panic resulting from the evacuation situation. This is represented in terms of the normalized free flow velocities as:

$$\tilde{v}_{f_i} = \tilde{v}_{f_m}. \tag{3.38}$$

We also expect the pedestrians to enter at rear end of the corridor at a maximum rate which we assume to be limited by the maximum normalized value of the discharge in the corridor as determined by the Greenshield's model. That is,

$$\tilde{q}_0 = \tilde{q}_m. \tag{3.39}$$

Thus for simulating the flow in uncontrolled scenario, we assume the initial values of the control variables $\tilde{v}_{f_i}$ and $\tilde{q}_0$ to be their maximum values indicated in equations (3.38) and (3.39). However if the density in any section reaches jam density we assume that the flow in that section stops completely. In such as case we notionally set the free flow velocity $\tilde{v}_{f_i}$ in section i that gets jammed equal to 0. (As discussed before, in reality we can expect some pedestrians diffusion to ease the jam, but we do not wish to refine our uncontrolled model to include this.) An important consequence of a section $i \geq 2$ of a corridor getting jammed is that the pedestrians in the preceding section $i-1$ will not be able to move forward. This would happen even if the density in section $i-1$, $\tilde{\rho}_{i-1} \leq 1$, or the section $i-1$ is not jammed. Thus in order to account for this stoppage of motion in the section $i-1$ we set the free flow velocity in that section $\tilde{v}_{f_{i-1}} = 0$. In case the first section ($i = 1$) gets jammed, we analogously we set the rear end input discharge into the corridor $\tilde{q}_0 = 0$ as it precede the 1^{st} section.

3.4.2 Controlled Flow

In controlling the flow for this case, our objective is to attain the exponential convergence of the normalized section densities $\tilde{\rho}_i$ in every section i to the critical normalized density $\frac{1}{2}$ corresponding to the Greenshields model. This would ensure that for a given free flow velocity the corresponding discharge is approaching the critical discharge exponentially. In order to achieve this we need the time derivatives of the section densities $\tilde{\rho}_i$ to satisfy the following:

$$\dot{\tilde{\rho}}_i = -k_i(\tilde{\rho}_i - \frac{1}{2}) \quad 1 \leq i \leq n \tag{3.40}$$

where k_i is the control gain parameter. The time derivatives of the normalized section densities $\tilde{\rho}_i$ are also given by equations (3.36) and (3.37) and are different from those in equation (3.40). Thus our objective will be to manipulate the control variables $\tilde{v}_{f_i}$ and $\tilde{q}_0$ such that the right hand sides of (3.36) and (3.37) equal those of (3.40). Thus we are manipulating the control input in such a way that the right hand side of equations (3.36) and (3.37) that was nonlinear in state and control variables is now equal to the right hand sides of equations (3.40) that is linear in the state variables. This process is called as feedback linearization. In order to do this, the control variables $\tilde{v}_{f_i}$ and $\tilde{q}_0$

need to satisfy the following equations:

$$(\tilde{q}_0 - \tilde{\rho}_1(1-\tilde{\rho}_1)\tilde{v}_{f_1})b_1 = -k_1(\tilde{\rho}_1 - \frac{1}{2}) \quad (3.41)$$

$$(\tilde{\rho}_{i-1}(1-\tilde{\rho}_{i-1})\tilde{v}_{f_{i-1}} - \tilde{\rho}_i(1-\tilde{\rho}_i)\tilde{v}_{f_i})b_i = -k_i(\tilde{\rho}_i - \frac{1}{2}) \quad 2 \leq i \leq n \quad (3.42)$$

These are n independent equations with $n+1$ unknown control variables. To solve this, we can formulate an optimization problem the solution of which satisfies equations (3.41) and (3.42), the bounds (3.11) and (3.13) on the control variables $\tilde{v}_{f_i}$for $\tilde{q}_0$ and at the same time optimizes a certain objective function of the control variables. In an optimization routine the objective function that is maximized is commonly referred to as the payoff function and the objective function that is minimized is referred to as the cost function. A good payoff function will be the rear inflow discharge into the corridor to speed up the evacuation process. That is, we solve a optimization problem at every time instant that maximizes the control parameter $\tilde{q}_0$. We note that equations 3.41 and 3.42 are linear in the control variables $\tilde{q}_0$ and $\tilde{v}_{f_i}$. Our payoff function $\tilde{q}_0$ is also a linear function of the control variables. Such an optimization problem can be conveniently solved by linear programming. Typically the linear programming problem is formulated as a minimization problem for a cost function. Maximizing a function of variables is, however, equivalent to minimizing its negative. Thus our linear programming problem can be posed as the minimization of $-\tilde{q}_0$. This linear programming problem can be stated as:

Minimize $-\tilde{q}_0$

subject to

$(\tilde{q}_0 - \tilde{\rho}_1(1-\tilde{\rho}_1)\tilde{v}_{f_1})b_1 = -k_1(\tilde{\rho}_1 - \frac{1}{2})$.....3.41

$(\tilde{\rho}_{i-1}(1-\tilde{\rho}_{i-1})\tilde{v}_{f_{i-1}} - \tilde{\rho}_i(1-\tilde{\rho}_i)\tilde{v}_{f_i})b_i = -k_i(\tilde{\rho}_i - \frac{1}{2}) \quad 2 \leq i \leq n$.....3.42

$0 \leq \tilde{v}_{f_i} \leq \tilde{v}_{f_m} \quad 1 \leq i \leq n$.....3.11

$0 \leq \tilde{q}_0 \leq \tilde{q}_m$.....3.13

(3.43)

The solution of this linear programming problem at every time instant defines our control variables. We note that for any optimization problem there is a risk of running into constraints that are infeasible. This can happen if the control gains are arbitrarily

selected. In case, the imposed constraints are infeasible or become infeasible as the evacuation proceeds, then we need to adjust the gains k_i such that the constraints become feasible. This procedure is described in the next sub-section.

For the moment we assume that the constraints of the linear programming problem, equation (3.43) are feasible. In this case there will exist a solution to this problem. We will show that the solution of this problem will also maximize the free flow velocities in all the sections, $\tilde{v}_{f_k}$ for $1 \leq k \leq n$ subject to all the constraints. For this we show that it is equivalent to maximize the the input discharge $\tilde{q}_0$ and the free flow velocity in any section k, $\tilde{v}_{f_k}$. In order to do this we divide all the equations (3.41) and (3.42) by b_i for each $1 \leq i \leq k$ and add them up. In doing this all the terms except $\tilde{q}_0$ and $\tilde{\rho}_k(1-\tilde{\rho}_k)\tilde{v}_{f_k}$ cancel out on the left hand side. Shifting the term $\tilde{\rho}_k(1-\tilde{\rho}_k)\tilde{v}_{f_k}$ to the right hand side, results in the following:

$$\tilde{q}_0 = \tilde{\rho}_k(1-\tilde{\rho}_k)\tilde{v}_{f_k} + \sum_{i=1}^{k} -\frac{k_i}{b_i}(\tilde{\rho}_i - \frac{1}{2}). \tag{3.44}$$

In equation (3.44) we observe that the term $\sum_{i=1}^{k} -\frac{k_i}{b_i}(\tilde{\rho}_i - \frac{1}{2})$ does not depend on the variables of the linear programming problem (3.43), which are the control variables, $\tilde{v}_{f_i}$ and $\tilde{q}_0$. Hence as far as the optimization problem is concerned the terms $\tilde{q}_0$ and $\tilde{\rho}_k(1-\tilde{\rho}_k)\tilde{v}_{f_k}$ differ by a constant term. Thus maximizing $\tilde{q}_0$ is equivalent to maximizing $\tilde{\rho}_k(1-\tilde{\rho}_k)\tilde{v}_{f_k}$ for every section, k, $1 \leq k \leq n$. Also since the coefficient of $\tilde{v}_{f_k}$, $\tilde{\rho}_k(1-\tilde{\rho}_k)$ does not depend on any of the optimization variables and is positive, maximizing $\tilde{q}_0$ equivalently results in maximizing $\tilde{v}_{f_k}$ for every section, k, $1 \leq k \leq n$. Thus the control given by the solution of the linear programming problem equation, (3.43) achieves both the tracking of the section densities $\tilde{\rho}_i$ to the critical density of $\frac{1}{2}$ as well as maximizes the free flow velocities in all the sections $\tilde{v}_{f_k}$ while satisfying the bound constraints of all the controls. This ensures a high exit discharge as the factors increasing the discharge namely, the nearness of the exit density to the critical density $\tilde{\rho}_{cr} = \frac{1}{2}$ and high value of exit free flow velocity $\tilde{v}_{f_n}$ are attained by the tracking and the optimization problem respectively. The highest possible discharge or the critical discharge occurs at $\tilde{\rho}_{cr} = \frac{1}{2}$ and $\tilde{v}_{f_n} = \tilde{v}_{f_m}$. However we cannot assure that $\tilde{v}_{f_n} = \tilde{v}_{f_m}$ in the solution of this linear programming problem.

3.4.3 Gain scaling for infeasible constraints.

In this section we describe a strategy to adjust the gains in case the constraints (equality and bound) in the linear programming problem equation, (3.43) are infeasible. The idea is rooted in the fact that the equality constraints equations (3.41) and (3.42) are linear in the control variables $\tilde{v}_{f_i}$ and $\tilde{q}_0$. We can exploit this fact by making the observation that if $(\tilde{v}_{f_i})^0$ and $(\tilde{q}_0)^0$ satisfy the equalities (3.41) and (3.42) with gains $k^0_{\rho_i}$ then $\frac{(\tilde{v}_{f_i})^0}{\nu}$ and $\frac{(\tilde{q}_0)^0}{\nu}$ satisfy the equalities (3.41) and (3.42) with gains $\frac{k^0_{\rho_i}}{\nu}$. Thus in case the constraints (equality and bound) in the linear programming problem equation, (3.43) are infeasible then we find a solution $(\tilde{q}_0)^0 \geq 0$ and $(\tilde{v}_{f_i})^0 \geq 0$ satisfying just the equalities (3.41) and (3.42) with gains $k^0_{\rho_i}$. Then we find a least scaling factor $\nu > 0$ such that $\frac{(\tilde{v}_{f_i})^0}{\nu}$ and $\frac{(\tilde{q}_0)^0}{\nu}$ not only satisfy the equalities (3.41) and (3.42) with gains $\frac{k^0_{\rho_i}}{\nu}$ but also the bounds given by equations (3.11) and (3.13). However the goal is to find the initial solution in such a way that the cumulative violation of the original bounds is a minimum.

First we show that there exists a solution $(\tilde{q}_0)^0 \geq 0$ and $(\tilde{v}_{f_i})^0 \geq 0$ for any set of gains $k^0_{\rho_i} > 0$ satisfying the equalities (3.41) and (3.42). In order to show this, we observe that if we divide equalities (3.41) and (3.42) with b_i and add the first k equations then we get the following result after minor readjustment:

$$\tilde{\rho}_k(1-\tilde{\rho}_k)(\tilde{v}_{f_k})^0 = (\tilde{q}_0)^0 - S_k \quad 1 \leq k \leq n, \tag{3.45}$$

where,

$$S_k = \sum_{j=1}^{k} -\frac{k^0_{\rho_j}}{b_j}(\tilde{\rho}_j - \frac{1}{2}), \tag{3.46}$$

is the term representing the summation of k terms on the right hand side. We note that $(\tilde{q}_0)^0$ appears in all the n equations (3.45). In order to ensure that $(\tilde{v}_{f_k})^0 > 0$ and $(\tilde{q}_0)^0 > 0$ choose $(\tilde{q}_0)^0 > 0$ such that:

$$(\tilde{q}_0)^0 \geq \max_{k=1}^{n} S_k. \tag{3.47}$$

This will ensure $\tilde{v}_{f_k} > 0$ for $1 \leq k \leq n$ in equations (3.45). Thus we have verified analytically that equations (3.41) and (3.42) have solutions $(\tilde{q}_0)^0 \geq 0$ and $(\tilde{v}_{f_i})^0 \geq 0$ for any set of gains $k^0_{\rho_i}$.

We now state the procedure to find the solution violating the bound in a minimum cumulative sense in case the constraints (equalities (3.41) and (3.42) and bounds

(3.11) and (3.13)) are infeasible with gains $k^0_{\rho_i}$. To achieve this, we formulate a linear programming problem. In order to do this, first we relax the upper bound on bound constraints given by equations (3.11) and (3.13) by shifting the upper bound all the way to ∞. This would result in the following set of new relaxed constraints:

$$0 \leq \tilde{v}_{f_i} \leq \infty \quad 1 \leq i \leq n \tag{3.48}$$

$$0 \leq \tilde{q}_0 \leq \infty. \tag{3.49}$$

Now we proceed to quantify the violation of the original upper bounds that were relaxed in the infeasible constraints of the linear programming problem given by equation (3.43) (equalities (3.41) and (3.42) and bounds (3.11) and (3.13)). In order to do this we introduce the slack and surplus variables. The slack variables represent the amount by which the original constraint has been satisfied and the surplus variables represent the amount by which the original upper bounds have been violated. We denote the slack variables corresponding to $\tilde{v}_{f_i}$ by $(\tilde{v}_{f_i})_{sl}$ and those corresponding to $\tilde{q}_0$ by $(\tilde{q}_0)_{sl}$. We denote the surplus variables corresponding to $\tilde{v}_{f_i}$ by $(\tilde{v}_{f_i})_{su}$ and those corresponding to $\tilde{q}_0$ by $(\tilde{q}_0)_{su}$. Both kinds of variables are non-negative. We need to introduce both kinds of variables since for a given relaxed upper bound the solution $\tilde{v}_{f_i}$ and $\tilde{q}_0$ can either satisfy or violate the original bound. The variables $\tilde{v}_{f_i}$ and $\tilde{q}_0$, their relaxed upper bounds $\tilde{v}_{f_m}$ and $\tilde{q}_m$ respectively and the slack and surplus variables are related by the following linear equalities:

$$\tilde{v}_{f_i} = \tilde{v}_{f_m} + (\tilde{v}_{f_i})_{su} - (\tilde{v}_{f_i})_{sl} \quad 1 \leq i \leq n \tag{3.50}$$

$$\tilde{q}_0 = \tilde{q}_m + (\tilde{q}_0)_{su} - (\tilde{q}_0)_{sl} \tag{3.51}$$

These additional equality constraints will have to be included in the new linear programming problem along with the original equalities (3.41) and (3.42). As non-negativity is the only requirement on the slack and surplus variables the bounds on the slack and surplus variables are as follows:

$$0 \leq (\tilde{v}_{f_i})_{sl} \leq \infty \quad 1 \leq i \leq n \tag{3.52}$$

$$0 \leq (\tilde{v}_{f_i})_{su} \leq \infty \quad 1 \leq i \leq n \tag{3.53}$$

$$0 \leq (\tilde{q}_0)_{sl} \leq \infty \tag{3.54}$$

$$0 \leq (\tilde{q}_0)_{su} \leq \infty \tag{3.55}$$

As surplus variables represent the constraint violation of the original bound, sum of all the surplus variables represent the cumulative constraint violation. We would like to minimize such cumulative constraint violations. Thus we can use the cumulative constraint violations, given by the following equation as a cost function that we wish to minimize:

$$g = \sum_{i=1}^{n} (\tilde{v}_{f_i})_{su} + (\tilde{q}_0)_{su}. \tag{3.56}$$

Since this cost function is a linear function of the problem variables, we can use the linear programming approach to solve for the variables in the equations (3.41) and (3.42) such that they minimize the constraints violations in a cumulative sense. This linear programming problem can be stated as:

Minimuze $g = \sum_{i=1}^{n} (\tilde{v}_{f_i})_{su} + (\tilde{q}_0)_{su}$.

Subject To

$(\tilde{q}_0 - \tilde{\rho}_1(1-\tilde{\rho}_1)\tilde{v}_{f_1})b_1 = -k_1(\tilde{\rho}_1 - \frac{1}{2})$.....3.41

$(\tilde{\rho}_{i-1}(1-\tilde{\rho}_{i-1})\tilde{v}_{f_{i-1}} - \tilde{\rho}_i(1-\tilde{\rho}_i)\tilde{v}_{f_i})b_i = -k_i(\tilde{\rho}_i - \frac{1}{2}) \quad 2 \leq i \leq n$.....3.42

$\tilde{v}_{f_i} = \tilde{v}_{f_m} + (\tilde{v}_{f_i})_{su} - (\tilde{v}_{f_i})_{sl} \quad 1 \leq i \leq n$.....3.50

$\tilde{q}_0 = \tilde{q}_m + (\tilde{q}_0)_{su} - (\tilde{q}_0)_{sl}$.....3.51

$0 \leq \tilde{v}_{f_i} \leq \infty \quad 1 \leq i \leq n$.....3.48

$0 \leq \tilde{q}_0 \leq \infty$.....3.49

$0 \leq (\tilde{v}_{f_i})_{sl} \leq \infty \quad 1 \leq i \leq n$.....3.52

$0 \leq (\tilde{v}_{f_i})_{su} \leq \infty \quad 1 \leq i \leq n$.....3.53

$0 \leq (\tilde{q}_0)_{sl} \leq \infty$.....3.54

$0 \leq (\tilde{q}_0)_{su} \leq \infty$.....3.55

(3.57)

The solution of the above problem given by equation (3.57) will provide $\tilde{v}_{f_i}$ and $\tilde{q}_0$ which violate the original bounds in a minimum cumulative sense. To obtain the scaling factor $(\nu)^0$ for the infeasible gains $k^0_{\rho_i}$ we scale the solution $\tilde{v}_{f_i}$ and $\tilde{q}_0$ by a factor ν such that it satisfies the original bounds given by equation (3.11) and (3.13). The minimum of all possible ν provides us the optimal scaling factor $(\nu)^0$ by which

the initially assumed value of the gain factor $k^0_{\rho_i}$ is adjusted to $\frac{k^0_{\rho_i}}{(\nu)^0}$ so that the original bounds become feasible.

3.4.4 Numerical Simulation

As done before for case 1, in this section we obtain the numerical results for Case 2 obtained according to the algorithms developed in the previous sections for the uncontrolled and controlled flow cases. The two sets of results are compared to demonstrate the merits of controlling the pedestrian flow.

We again consider a corridor divided into 5 equal length sections like the one displayed in Figure 3.3. The colors of the sections displayed in that Figure are again used to identify the results corresponding to those sections. Again we use the same physical parameters as in the previous case. That is, the length of the corridor $L = 50m$, the maximum free flow velocity to be $1.5m/s$ with corresponding maximum value of $\tilde{v}_{f_m} = \frac{v_{fm}}{L} = 0.03$. The upper limit on the discharge variable for this maximum free flow velocity, that is the maximum normalized discharge is $\tilde{q}_m = \frac{\tilde{v}_{fm}}{4} = 7.5 \times 10^{-3}$. We again use the normalized quantities in our simulation. In simulation, we choose the initial values of the section densities to be $\tilde{\rho}^0_1 = 0.6933$,$\tilde{\rho}^0_2 = 0.5850$,$\tilde{\rho}^0_3 = 0.2670$,$\tilde{\rho}^0_4 = 0.8000$ and $\tilde{\rho}^0_5 = 0.0290$. These are randomly spread values. For the controlled simulation, we use the same gain values for all the sections. Specifically we choose $k_i = k = \frac{1}{70} = 0.0143$. This value was found to render the linear programming problem given by equation (3.43) feasible.

First in Figures 3.7(a) and 3.7(b), we show the evolution of the normalized densities in different section for the uncontrolled and controlled flow scenarios, respectively. As seen from the results for the uncontrolled case in Figure 3.7(a), section 4 reaches jam density in about 20 s and section 1 reaches jam density in about 30 s. The normalized densities in section 2 and section 5 reach a value of 0. The normalized density in section 3 stabilizes at a value that is neither 0 nor jam value of 1. This is because the section 2 which immediately precedes this section reaches 0 density and the section 4 which immediately follows this section reaches jam density. Due to section 2 reaching a value of 0 there is no inflow into this section and due to section 4 reaching a jam value there is no out flow from section 3. Hence the density of section 3 freezes to a value between 0 and 1. The physical implication of this would be that the pedestrians

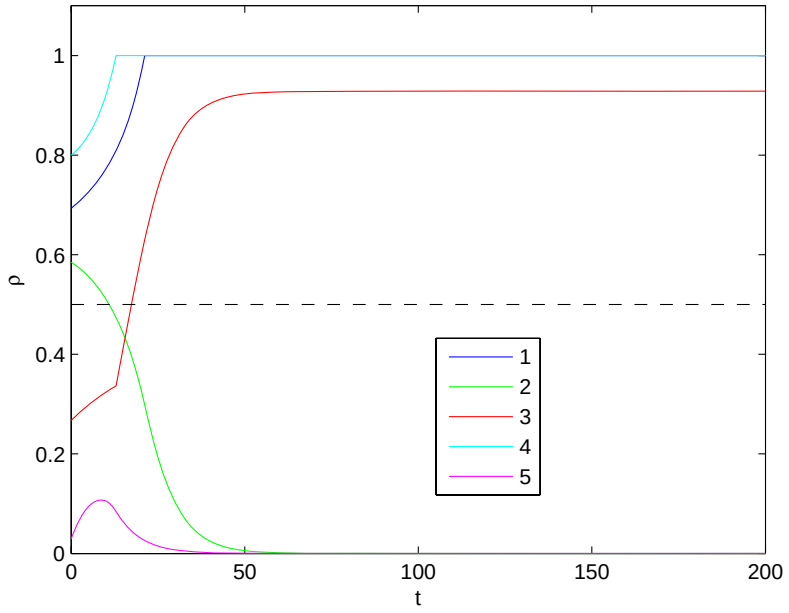

(a) Normalized section density $\tilde{\rho}_i$ in the uncontrolled case

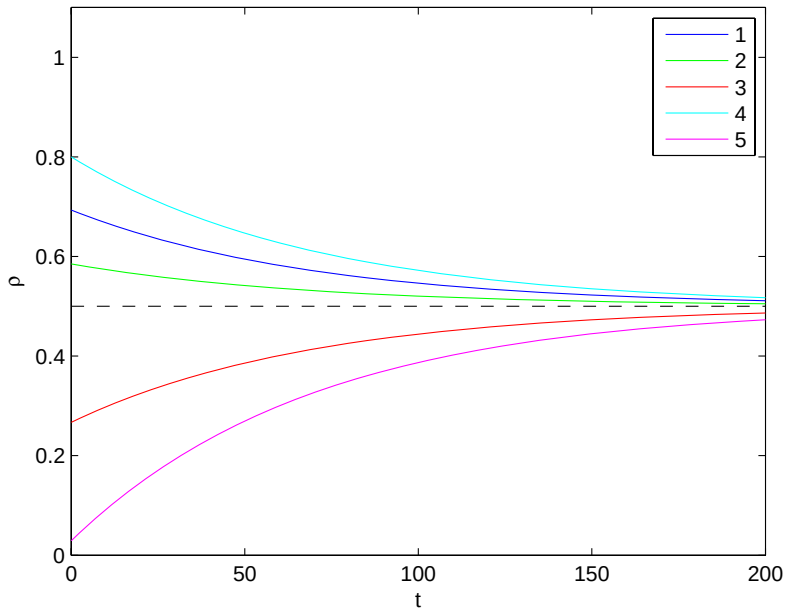

(b) Normalized section density $\tilde{\rho}_i$ in the controlled case

Figure 3.7: Normalized corridor section densities $\tilde{\rho}_i$ for all sections in the controlled and the uncontrolled case of flow scenario 2.

from section 2 get trapped in section 3 as they cannot proceed ahead as section 4 is blocked. In contrast to these results, we observe that for the controlled case, Figure 3.7(b), the pedestrian densities in all sections approach the critical normalized density of 0.5 exponentially without any jamming. That is, the control approach is effective in smooth regulation of the flow to achieve the optimum flow conditions.

In the next set of Figures 3.8(a) and 3.8(b) we show the evolution of the normalized free flow velocities in different section for the uncontrolled and controlled flow scenarios, respectively. The simulation results for the uncontrolled case (Figure 3.8(a)) show that the normalized free flow velocities in all sections start off at their maximum values, but then they drop off to a value of 0 in sections 1 and 4 as these sections get jammed. When section 4 gets jammed the normalized free flow velocity in section 3 also drops off to 0. It can be seen that the normalized free flow velocities in sections 2 and 5 never drop off to 0 and stay at their maximum value of 0.03. As section 5 is the last section hence it gets completely evacuated whereas the pedestrians in section 2 get trapped in section 3. These sudden changes of free flow velocity are, however, completely absent in the controlled scenario as seem from the simulation results in Figure 3.8(b). The normalized free flow velocities in this case all approach the maximum value and stay very close to this value for the most part of the simulation. This can be attributed to the fact that the normalized free flow velocities in all the sections are maximized as a result of maximizing the rear end input discharge in the linear programming problem. It can be seen that for section 5 the normalized free flow velocity in fact starts off from the maximum value but reduces slightly as the simulation proceeds.

In Figures 3.9(a) and 3.9(b) we show the evolution of the rear end input discharge for the uncontrolled and controlled scenarios, respectively. From the results of the uncontrolled scenario shown in Figure 3.9(a), we observe that the rear input discharge starts out at its maximum value but then suddenly it drops off to 0 when section 1 gets jammed resulting in the blockage of this flow. At this point the input discharge into this corridor is 0 thus the corridor is blocked to entering pedestrians. On the other hand for the controlled scenario (Figure 3.9(b)) we observe that the rear input discharge starts out at a relatively low value and then approaches its maximum value without any blockage. Thus, the active regulation of the input discharge and section velocities ensures that all all normalized section densities approach the critical densities (Figure

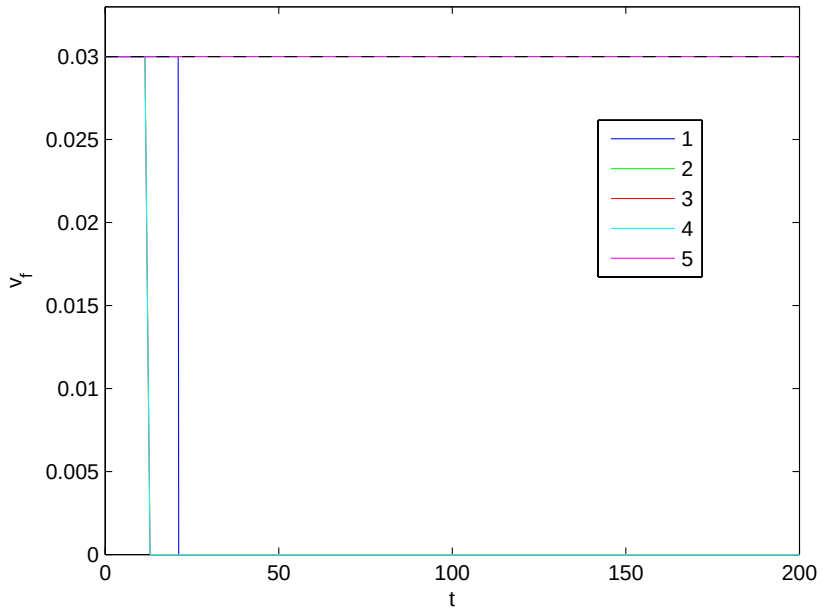

(a) Normalized section free flow velocity $\tilde{v}_{f_i}$ in the uncontrolled case

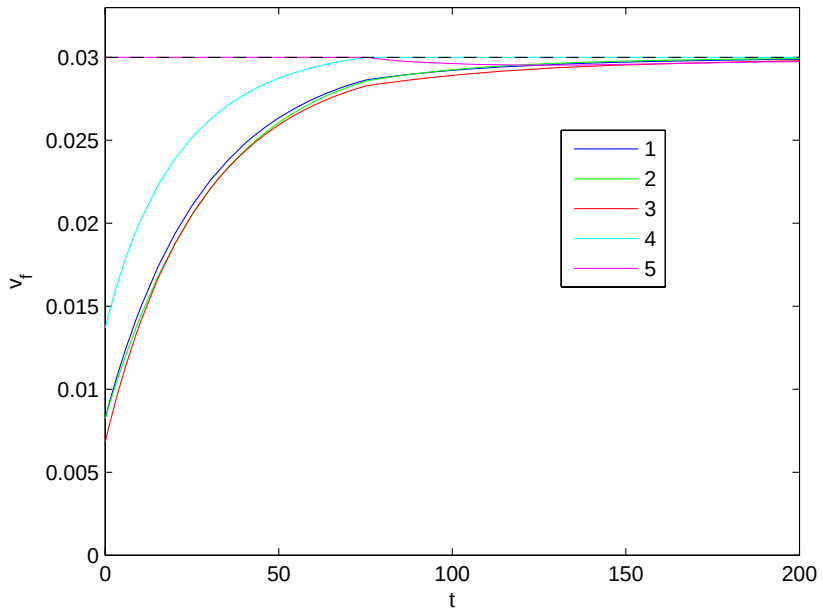

(b) Normalized section free flow velocity $\tilde{v}_{f_i}$ in the controlled case

Figure 3.8: Normalized corridor section free flow velocity $\tilde{v}_{f_i}$ for all sections in the controlled and the uncontrolled case of flow scenario 2.

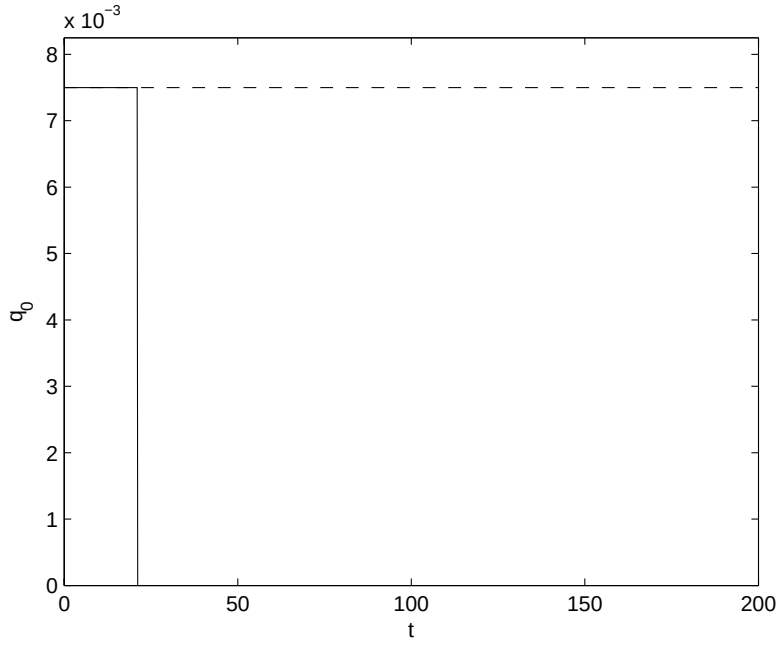

(a) Normalized rear end input discharge $\tilde{q}_0$ in the uncontrolled case

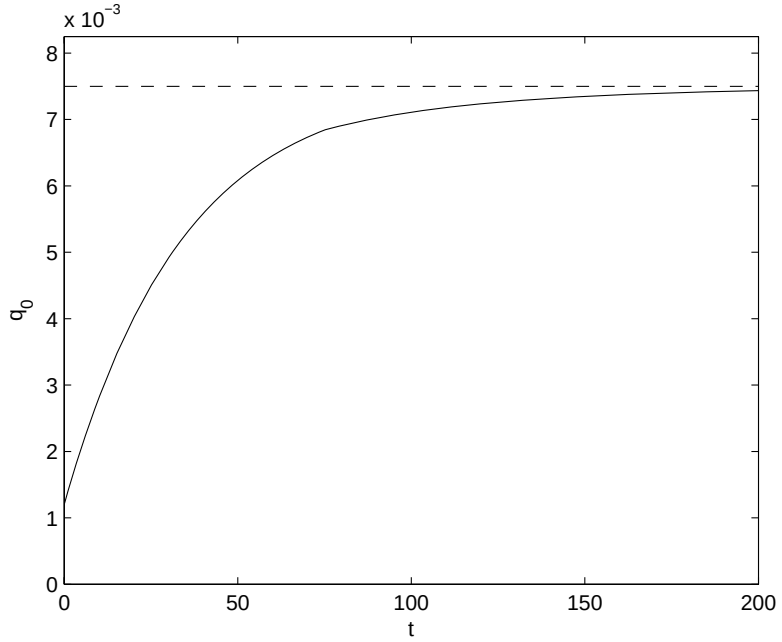

(b) Normalized rear end input discharge $\tilde{q}_0$ in the controlled case

Figure 3.9: Normalized corridor rear end input discharge $\tilde{q}_0$ in the controlled and the uncontrolled case of flow scenario 2.

3.7(b)) along with the free flow velocities in all sections being near their maximum values (Figure 3.8(b)).

In Figure 3.10 we compare the rear end input discharge (which is the only input discharge in this case) as well as the exit discharge for the uncontrolled and controlled scenarios. The results for the uncontrolled case are shown by red lines and those for

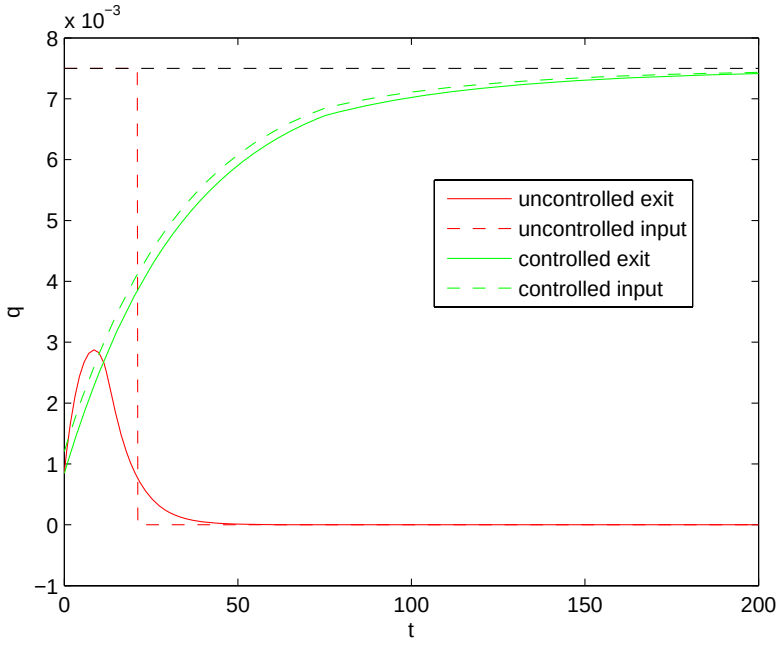

Figure 3.10: Normalized exit discharge and input discharge in the controlled and the uncontrolled case.

the controlled cae by the green lines. The results for the input discharges are the same as shown earlier in Figures 3.9(a) and 3.9(b). For the uncontrolled scenario we note that the exit discharge remains low most of the times except for reaching a low peak at the start of the evacuation. The input discharge, however, starts at its maximum values but then it suddenly drops to 0 as section 1 get jammed. Thus, the unregulated flow approach is highly inefficient with regard to the evacuation of the pedestrians. In contrast, the flow conditions in the controlled case with regard to the input and output discharge are efficient and smooth. Both the exit and input discharges are close to each other, finally approaching each other at the evacuation progresses. They both approach the critical discharge which corresponds to the critical density and the

maximum free flow velocity, as the densities in all the sections approach the critical density and the section free flow velocities get very close to their maximum value.

3.5 Case 3: Rear input and room discharges.

This flow condition would occur in the beginning of the evacuation scenario when there are pedestrians entering from the rear end as well as from the rooms along the sections. In this section we describe the approach to control the flow for such a case by appropriately regulating all three variables namely: the free flow velocities $\tilde{v}_{f_i}$in different sections, the rear end input discharge $\tilde{q}_0$, and the discharges $\tilde{q}^{r(i)}$ from rooms into different sections. This is the most general case, and the state equations for this case are the original state equations (3.8) and (3.9) repeated below :

$$\dot{\tilde{\rho}}_1 = (\tilde{q}_0 + \tilde{q}^{r(1)} - \tilde{\rho}_1(1-\tilde{\rho}_1)\tilde{v}_{f_1})b_1 \tag{3.58}$$

$$\dot{\tilde{\rho}}_i = (\tilde{q}^{r(i)} + \tilde{\rho}_{i-1}(1-\tilde{\rho}_{i-1})\tilde{v}_{f_{i-1}} - \tilde{\rho}_i(1-\tilde{\rho}_i)\tilde{v}_{f_i})b_i \tag{3.59}$$

As before, we will first describe the evolution of the flow for both the uncontrolled and controlled scenarios. This will be followed by the comparison of the numerical simulation for the two scenarios.

3.5.1 Uncontrolled flow

As done before, we assume that in the uncontrolled case, the pedestrian would try to move the maximum possible speed according to the densities in different sections. Such an action implies that the free flow velocities in all sections initially start at their maximum values. That is,

$$\tilde{v}_{f_i} = \tilde{v}_{f_m}. \tag{3.60}$$

We also expect the pedestrians to enter the corridor from the rear as well as from adjoining rooms at the maximum rate. This situation can be represented by assigning the maximum possible value to the normalized rear end input discharge as well as the room discharges as follows:

$$\tilde{q}_0 = \tilde{q}_m. \tag{3.61}$$

$$\tilde{q}^{r(i)} = \tilde{q}_m. \quad 1 \leq i \leq n. \tag{3.62}$$

Thus for the uncontrolled flow scenario we use the equations (3.60), (3.61) and (3.62) to determine the time evolution from equations (3.58) and (3.59). However if any of the section i reaches jam density then we assume that the flow in that section stops completely. As before, we notionally set the free flow velocity in that section to 0 indicating the stoppage of flow. In reality there will be a diffusion of pedestrian, but as discussed earlier we do not intend to include this in the study the uncontrolled flow. A direct consequence of a section i getting jammed will be that the section room discharge associate with it $\tilde{q}^{r(i)} = 0$. This would happen as the pedestrians from adjoining rooms will not be able to enter the section which is jammed. Another important consequence of a section $i \geq 2$ getting jammed would be that the pedestrians in the preceding section $i-1$ will not be able to move as their forward motion is completely blocked. This would happen even if the density in section $i-1$, $\tilde{\rho}_{i-1} \leq 1$, or the section $i-1$ is not jammed. Thus in order to account for this stoppage of motion in the section $i-1$ we set the free flow velocity in that section $\tilde{v}_{f_{i-1}} = 0$. In case the first section ($i = 1$) gets jammed, we set the rear end input discharge into the corridor $\tilde{q}_0 = 0$.

3.5.2 Controlled flow

The control procedure to be developed in this section follows essentially the same line as in Case 2 described in the previous section. As was discussed for Case 2, our control objective is to attain the exponential convergence of the normalized section densities $\tilde{\rho}_i$ in every section i to the critical normalized density value of $\frac{1}{2}$ corresponding to the Greenshield model. Approaching this critical density ensures that for a given free flow velocity, the corresponding discharge is approaching the critical discharge exponentially. To achieve the exponential convergence we need the time derivatives of the section densities $\tilde{\rho}_i$ need to satisfy the following:

$$\dot{\tilde{\rho}}_i = -k_i(\tilde{\rho}_i - \frac{1}{2}) \quad 1 \leq i \leq n \tag{3.63}$$

However the time derivatives of the normalized section densities $\tilde{\rho}_i$ are given by equations (3.58) and (3.59) and are different from those in equation (3.63). However by manipulating the control variables $\tilde{q}_0$ (input discharge at the rear end), $\tilde{v}_{f_i}$ (section free flow velocities), and $\tilde{q}^{r(i)}$ (room discharge in sections) in the right hand side of equations (3.58) and (3.59) they can be made equal to the right hand side of equation

(3.63). That is, the control inputs variables need to satisfy the following equations:

$$(\tilde{q}_0 + \tilde{q}^{r(1)} - \tilde{\rho}_1(1-\tilde{\rho}_1)\tilde{v}_{f_1})b_1 = -k_1(\tilde{\rho}_i - \frac{1}{2}) \quad (3.64)$$

$$(\tilde{q}^{r(i)} + \tilde{\rho}_{i-1}(1-\tilde{\rho}_{i-1})\tilde{v}_{f_{i-1}} - \tilde{\rho}_i(1-\tilde{\rho}_i)\tilde{v}_{f_i})b_i = -k_i(\tilde{\rho}_i - \frac{1}{2}) \quad (3.65)$$

That is, we have manipulated the control inputs in such a way that the right hand sides of equations (3.58) and (3.59) that were nonlinear in state and control variables become equal to the right hand sides of equations (3.63) that are linear in the state variables. This process is called state feedback linearization.

Equations (3.64) and (3.65) are n independent equations with $2n+1$ unknown control variables. To solve for the control variables, we formulate an optimization problem the solution of which satisfies equations (3.64) and (3.65), the control bounds (3.11), (3.13) and (3.14) and at the same time optimizes a certain function of these control variables. As we would like to maximum the total inflow discharge into the corridor to speed up the evacuation process, we solve a optimization problem that maximizes this quantity. The total inflow discharge into the corridor comprises of the control variable of the input discharge $\tilde{q}_0$ at the rear end and room discharges $\tilde{q}^{r(i)}$ feeding into different corridor sections defining our payoff function f as follows:

$$f = \tilde{q}_0 + \sum_{i=1}^{n} \tilde{q}^{r(i)}. \quad (3.66)$$

We note that equations (3.64) and (3.65) are linear in the control variables $\tilde{q}_0$ and $\tilde{v}_{f_i}$ and $\tilde{q}^{r(i)}$. Also the payoff function in (3.66) is a linear function of the control variables. Thus the optimization problem consists of a linear payoff subject to linear equality and inequality constraints. This optimization problem can be conveniently solved by linear programming approach at every time step. Since a linear programming problem is typically formulated as a minimization problem, we can pose our problem

as minimization of $-f$. This linear programming problem is, thus, stated as:

$$
\begin{aligned}
&\text{Minimize } \; -f = -\tilde{q}_0 - \sum_{i=1}^{n} \tilde{q}^{r(i)} \\
&\text{Subject To} \\
&(\tilde{q}_0 + \tilde{q}^{r(1)} - \tilde{\rho}_1(1-\tilde{\rho}_1)\tilde{v}_{f_1})b_1 = -k_1(\tilde{\rho}_i - \frac{1}{2}) \text{.....3.64} \\
&(\tilde{q}^{r(i)} + \tilde{\rho}_{i-1}(1-\tilde{\rho}_{i-1})\tilde{v}_{f_{i-1}} - \tilde{\rho}_i(1-\tilde{\rho}_i)\tilde{v}_{f_i})b_i = -k_i(\tilde{\rho}_i - \frac{1}{2}) \quad 2 \leq i \leq n \text{.....3.65} \\
&0 \leq \tilde{v}_{f_i} \leq \tilde{v}_{f_m} \quad 1 \leq i \leq n \text{.....3.11} \\
&0 \leq \tilde{q}_0 \leq \tilde{q}_m \text{.....3.13} \\
&0 \leq \tilde{q}^{r(i)} \leq \frac{\tilde{q}_m}{n} \quad 1 \leq i \leq n \text{.....3.14}
\end{aligned}
\tag{3.67}
$$

The solution of this linear programming problem at every time instant gives us the control variable values. We note that for any optimization problem there is a risk of running into constraints that are infeasible. This can happen if the control gain parameter values are not properly selected. In such cases, we need to adjust the gains k_i such that the constraints become feasible. This procedure is outlined in the next section.

For the moment we assume that the constraints of the linear programming problem of equation (3.67) are feasible. In this case there will exist a solution to this problem. We will show that the solution of this problem will also maximize the free flow velocity in the last section, $\tilde{v}_{f_n}$ subject to all the constraints. For this we show that it is equivalent to maximizing the payoff function f given by equation (3.66) and the free flow velocity in the last section $\tilde{v}_{f_n}$. In order to do this we divide all the equations (3.64) and (3.65) by b_i for each $1 \leq i \leq n$ and add them up. In doing this all the terms except $\tilde{q}_0$, $\tilde{q}^{r(i)}$ and $\tilde{\rho}_n(1-\tilde{\rho}_n)\tilde{v}_{f_n}$ cancel out on the left hand side. Shifting the term $\tilde{\rho}_n(1-\tilde{\rho}_n)\tilde{v}_{f_n}$ to the right hand side, results in the following:

$$
\tilde{q}_0 + \sum_{i=1}^{n} \tilde{q}^{r(i)} = \tilde{\rho}_n(1-\tilde{\rho}_n)\tilde{v}_{f_n} + \sum_{i=1}^{n} -\frac{k_i}{b_i}(\tilde{\rho}_i - \frac{1}{2}). \tag{3.68}
$$

We observe that the linear payoff f given by equation (3.66) equals the left hand side of (3.68). Also note that the term $\sum_{i=1}^{n} -\frac{k_i}{b_i}(\tilde{\rho}_i - \frac{1}{2})$ does not depend on the variables of the linear programming problem (3.67). Hence as far as the optimization problem is

concerned the payoff f which equals the terms on the left hand side and $\tilde{\rho}_n(1-\tilde{\rho}_n)\tilde{v}_{f_n}$ differ by a constant term. Thus maximizing f is equivalent to maximizing $\tilde{\rho}_n(1-\tilde{\rho}_n)\tilde{v}_{f_n}$. Also since the coefficient of $\tilde{v}_{f_n}$, $\tilde{\rho}_n(1-\tilde{\rho}_n)$ does not depend on any of the optimization variables and is positive, maximizing f equivalently results in maximizing $\tilde{v}_{f_n}$. Thus the control given by the solution of the linear programming problem (3.67) achieves both the tracking of the section densities $\tilde{\rho}_i$ to the critical density of $\frac{1}{2}$ as well as maximizes the free flow velocity in the last section $\tilde{v}_{f_n}$ while meeting the tracking objective and satisfying the bound constraints of all the controls. This ensures a high exit discharge as the factors increasing the discharge namely, the nearness of the exit density to the critical density $\tilde{\rho}_{cr} = \frac{1}{2}$ and high value of exit free flow velocity are attained by the tracking and the optimization problem simultaneously. This exit discharge may, however, be less than the highest possible discharge, or the critical discharge, which occurs when $\tilde{\rho}_{cr} = \frac{1}{2}$ and $\tilde{v}_{f_n} = \tilde{v}_{f_m}$. This is because we have been able to track the densities to the critical value of 1/2 but we cannot ensure that $\tilde{v}_{f_n} = \tilde{v}_{f_m}$ as it might result in some control values violating the control bounds.

3.5.3 Gain scaling for infeasible constraints

In this section we describe a strategy to adjust the gains in case the constraints (equality and bound) in the linear programming problem of equation (3.67) are infeasible. This strategy is similar to the one described in Sec. 3.4, except that now we have more control variables. The idea again exploits the linearity of the equality constraints in equations (3.64) and (3.65) in the control variables $\tilde{v}_{f_i}$, $\tilde{q}_0$ and $\tilde{q}^{r(i)}$. This linearity implies that if $(\tilde{v}_{f_i})^0$, $(\tilde{q}_0)^0$ and $(\tilde{q}^{r(i)})^0$ satisfy the equalities (3.64) and (3.65) with gains $k^0_{\rho_i}$ then $\frac{(\tilde{v}_{f_i})^0}{\nu}$, $\frac{(\tilde{q}_0)^0}{\nu}$ and $\frac{(\tilde{q}^{r(i)})^0}{\nu}$ satisfy the equalities (3.64) and (3.65) with gains $\frac{k^0_{\rho_i}}{\nu}$. Thus, in case the constraints (equality and bound) in the linear programming problem (3.67) are infeasible because of an improper selection of gains $k^0_{\rho_i}$ then we find a solution $(\tilde{q}_0)^0 \geq 0$, $(\tilde{v}_{f_i})^0 \geq 0$ and $\tilde{q}^{r(i)} > 0$ satisfying just the equalities (3.64) and (3.65) with these values of the gains $k^0_{\rho_i}$. Then we find a least scaling factor $\nu > 0$ such that $\frac{(\tilde{v}_{f_i})^0}{\nu}$ and $\frac{(\tilde{q}_0)^0}{\nu}$ not only satisfy the equalities (3.64) and (3.65) with gains $\frac{k^0_{\rho_i}}{\nu}$ but also the bounds (3.11), (3.13) and (3.14). However the goal is to find the initial solution in such a way that the cumulative violation of the original bounds is a minimum.

We now describe the procedure to find the optimal solution violating the original

bounds such that the cumulative violations of the original bounds is minimum. For this we formulate a linear programming problem as follows. First we relax the upper bound on all the bound constraints of equations (3.11), (3.13) and (3.14) by shifting the upper bound all the way to ∞, resulting in to the following set of new relaxed constraints:

$$0 \leq \tilde{v}_{f_i} \leq \infty \quad 1 \leq i \leq n \tag{3.69}$$

$$0 \leq \tilde{q}_0 \leq \infty \tag{3.70}$$

$$0 \leq \tilde{q}^{r(i)} \leq \infty \quad 1 \leq i \leq n \tag{3.71}$$

Next we proceed to quantify the violations of the original bounds that were relaxed. In order to do this we introduce a slack and a surplus variable corresponding to each bound that has been relaxed. As the upper bound on all the control variables is relaxed hence we need to introduce a slack and a surplus variable corresponding to each variable. The slack variables denote the amount by which the original constraint has been satisfied and the surplus variable denotes the amount by which the original bound has been violated. Each of the slack and the surplus variables satisfy the non-negativity constraint. Let the slack variables corresponding to $\tilde{v}_{f_i}$, $\tilde{q}_0$ and $\tilde{q}^{r(i)}$ be denoted by $(v_{f_i})_{sl}$, $(q_0)_{sl}$ and $(q^{r(i)})_{sl}$ respectively. Let the surplus variables corresponding to $\tilde{v}_{f_i}$, $\tilde{q}_0$ and $\tilde{q}^{r(i)}$ be denoted by $(v_{f_i})_{su}$, $(q_0)_{su}$ and $(q^{r(i)})_{su}$ respectively. The non-negativity of the slack and the surplus variables results in the following bound constraints on them:

$$0 \leq (v_{f_i})_{sl} \leq \infty \quad 1 \leq i \leq n \tag{3.72}$$

$$0 \leq (v_{f_i})_{su} \leq \infty \quad 1 \leq i \leq n \tag{3.73}$$

$$0 \leq (q_0)_{sl} \leq \infty. \tag{3.74}$$

$$0 \leq (q_0)_{su} \leq \infty. \tag{3.75}$$

$$0 \leq (q^{r(i)})_{sl} \leq \infty \quad 1 \leq i \leq n \tag{3.76}$$

$$0 \leq (q^{r(i)})_{su} \leq \infty \quad 1 \leq i \leq n \tag{3.77}$$

As the slack and the surplus variables represent the amount by which a relaxed constraint has been satisfied or violated respectively hence we have the following equality relations between the variables, the original upper bound and the slack and the surplus

variables:

$$\tilde{v}_{f_i} = \tilde{v}_{f_m} + (v_{f_i})_{su} - (v_{f_i})_{sl} \quad 1 \leq i \leq n \tag{3.78}$$

$$\tilde{q}_0 = \tilde{q}_m + (q_0)_{su} - (q_0)_{sl} \tag{3.79}$$

$$\tilde{q}^{r(i)} = \tilde{q}_m + (q^{r(i)})_{su} - (q^{r(i)})_{sl} \quad 1 \leq i \leq n \tag{3.80}$$

In order to find the solution to the equations (3.64) and (3.65) that violates the original bounds in a minimum cumulative sense we formulate a linear programming problem using the above defined slack and surplus variables. As the individual surplus variables define the amount by which a relaxed constraint has been violated hence the sum of all the surplus variables denotes the cumulative constraint violations. Thus the cost to be minimized in the new linear programming problem is:

$$g = (q_0)_{su} + \sum_{i=1}^{n}((v_{f_i})_{su} + (q^{r(i)})_{su}). \tag{3.81}$$

As the slack and surplus variables are involved, in addition to the original equalities (3.64) and (3.65) the equalities (3.78), (3.79) and (3.80) also need to be satisfied. Also the bounds corresponding to the slack and surplus variables given by equations (3.72), (3.73), (3.74), (3.75), (3.76) and (3.77) need to be satisfied in addition to the relaxed bounds on the original variables given by equations (3.69), (3.70) and (3.71). The complete linear programming problem, that we propose to solve to obtain the solution

is:

Minimize

$$g = (q_0)_{su} + \sum_{i=1}^{n}((v_{f_i})_{su} + (q^{r(i)})_{su})$$

Subject To

$$(\tilde{q}_0 + \tilde{q}^{r(1)} - \tilde{\rho}_1(1-\tilde{\rho}_1)\tilde{v}_{f_1})b_1 = -k_1(\tilde{\rho}_i - \frac{1}{2}) \quad \text{.....3.64}$$

$$(\tilde{q}^{r(i)} + \tilde{\rho}_{i-1}(1-\tilde{\rho}_{i-1})\tilde{v}_{f_{i-1}} - \tilde{\rho}_i(1-\tilde{\rho}_i)\tilde{v}_{f_i})b_i = -k_i(\tilde{\rho}_i - \frac{1}{2}) \quad 2 \leq i \leq n \text{.....3.65}$$

$$\tilde{v}_{f_i} = \tilde{v}_{f_m} + (v_{f_i})_{su} - (v_{f_i})_{sl} \quad 1 \leq i \leq n \text{.....3.78}$$

$$\tilde{q}_0 = \tilde{q}_m + (q_0)_{su} - (q_0)_{sl} \text{.....3.79}$$

$$\tilde{q}^{r(i)} = \tilde{q}_m + (q^{r(i)})_{su} - (q^{r(i)})_{sl} \quad 1 \leq i \leq n \text{.....3.80}$$

$$0 \leq \tilde{v}_{f_i} \leq \infty \quad 1 \leq i \leq n \text{.....3.69}$$

$$0 \leq \tilde{q}_0 \leq \infty \text{.....3.70}$$

$$0 \leq \tilde{q}^{r(i)} \leq \infty \quad 1 \leq i \leq n \text{.....3.71}$$

$$0 \leq (v_{f_i})_{sl} \leq \infty \quad 1 \leq i \leq n \text{.....3.72}$$

$$0 \leq (v_{f_i})_{su} \leq \infty \quad 1 \leq i \leq n \text{.....3.73}$$

$$0 \leq (q_0)_{sl} \leq \infty \text{.....3.74}$$

$$0 \leq (q_0)_{su} \leq \infty \text{.....3.75}$$

$$0 \leq (q^{r(i)})_{sl} \leq \infty \quad 1 \leq i \leq n \text{.....3.76}$$

$$0 \leq (q^{r(i)})_{su} \leq \infty \quad 1 \leq i \leq n \text{.....3.77}$$

(3.82)

The solution of this problem given by equation (3.82) will violate the original bounds in a minimum cumulative sense. To obtain the scaling factor $(\nu)^0$ for the infeasible gains $k^0_{\rho_i}$ we scale the components of the solution corresponding to $\tilde{v}_{f_i}$,$\tilde{q}_0$ and $\tilde{q}^{r(i)}$ by a factor $\nu > 0$ such that it satisfies the original bounds given by equations (3.11), (3.13) and (3.14). The minimum of all possible $\nu > 0$ would give us the optimal scaling factor $(\nu)^0$. The feasible gain that would make the original bound feasible is then equal to $\frac{k^0_{\rho_i}}{(\nu)^0}$.

3.5.4 Numerical Simulation

In this section we present the numerical simulation results obtained for the uncontrolled and controlled scenarios for case 3 where the corridor receives input from back as well as input from the connecting rooms. We again consider the same corridor divided into 5 equal length sections like the one displayed in Figure 3.3. Again the colors of the sections displayed in that figure are used to plot the results corresponding to those sections. We assume same physical parameters as in the Sec. 3.4: the length of the corridor $L = 50m$; the maximum free flow velocity v_{f_m}= $1.5m/s$ with corresponding normalized value of $\tilde{v}_{f_m} = \frac{v_{f_m}}{L} = 0.03$; the normalized maximum discharge $\tilde{q}_m = \frac{\tilde{v}_{f_m}}{4} = 7.5 \times 10^{-3}$;the initial pedestrian densities in different section as $\tilde{\rho}_1^0 = 0.6933$, $\tilde{\rho}_2^0 = 0.5850$, $\tilde{\rho}_3^0 = 0.2670$, $\tilde{\rho}_4^0 = 0.8000$ and $\tilde{\rho}_5^0 = 0.0290$. All room discharges are bound by the maximum value $\tilde{q}_m$. For the controlled simulation case we assume the same gains value for all the sections as $k_i = k = \frac{1}{250} = 4 \times 10^{-3}$. Again we present the results in terms of normalized quantities.

First we present the results for the evolution of the normalized densities in different sections in Figures 3.11(a) and 3.11(b) for the uncontrolled and controlled flow scenarios, respectively. The results for the uncontrolled scenario shown in the top part of the Figure 3.11(a) clearly show that all sections except section 5 reach the jam density. Section 4 reaches jam density in about 10 s from the start of the evacuation, section 1 in about 15 s, section 3 in about 30 s and section 2 in about 140 s. While section densities in sections 1, 3 and 4, continually increase till they reach the jam density, density in section 2 initially decreases and then suddenly starts increasing towards the jam density. It should be noted that once section 4 gets jammed the flow behind this section gets completely obstructed. Since every section receives input from the connected rooms, the density in a section behind the jammed section would eventually reach the jam density. It is seen that the density in section 5 stabilizes at a constant value as pedestrian can exit uninterrupted from this section. This constant density value is sustained by the room discharge feeding into this section; this is also its maximum value limited by the section discharge capacity. Such blockages of the sections, however, never happens in the controlled flow scenario (Figure 3.11(b)); all section densities approach the normalized critical density 0.5 exponentially, thus ensuring a smooth flow.

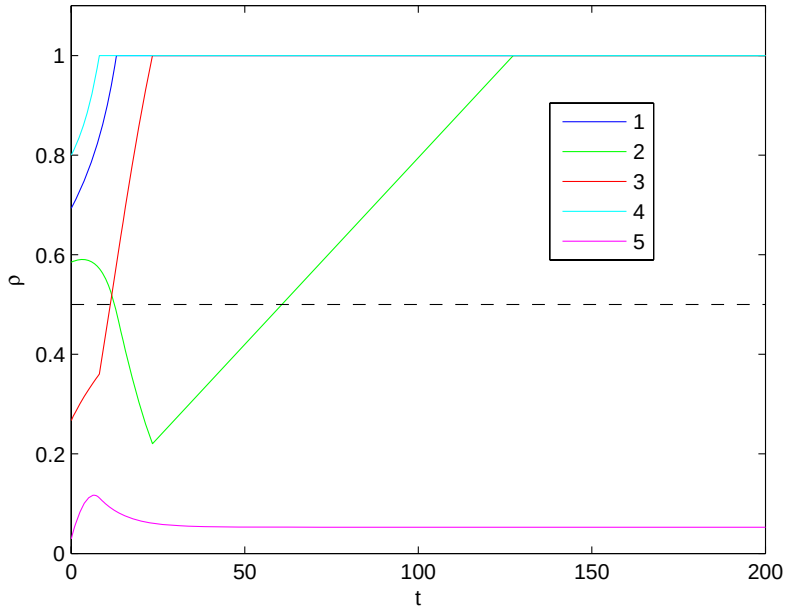

(a) Normalized section density $\tilde{\rho}_i$ in the uncontrolled case

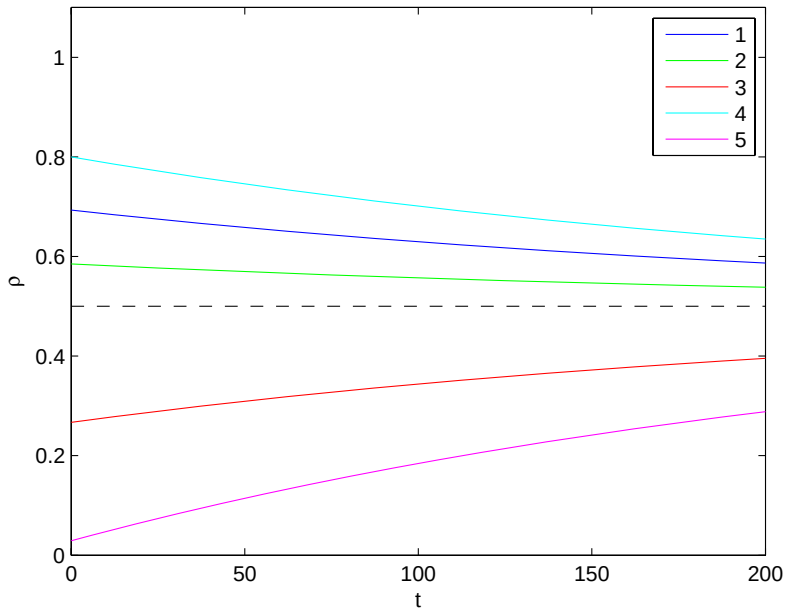

(b) Normalized section density $\tilde{\rho}_i$ in the controlled case

Figure 3.11: Normalized corridor section densities $\tilde{\rho}_i$ for all sections in the controlled and the uncontrolled case of flow scenario 3.

The next set of figures, Figures 3.12(a) and 3.12(b), show the evolution of the normalized free flow velocities in different sections for the uncontrolled and controlled scenarios, respectively. From the results for the uncontrolled case shown in Figure 3.12(a), we observe that as sections 1, 2, 3 and 4 get jammed the normalized free flow velocities in them fall to 0 from their initial maximum values with which they start. Section 5 never gets jammed, and its free flow velocity constantly remains at its maximum value. The line for section 3 is not visible as is concealed by line for section 4; when section 4 gets jammed the free flow velocities in both the sections fall to 0. For the controlled case, on the other hand the free flow velocities in all sections change gradually to ensure a smooth uninterrupted flow. The free flow velocity section 5 reaches the maximum possible values. This is a desirable consequence of control as it ensures the highest possible exit discharge corresponding to the given exit density.

In the next set of two Figures 3.13(a) and 3.13(b) we show how the rear end input discharge evolves in the uncontrolled and controleed scenarios, respectively. The results for the uncontrolled scenario shown in Figure 3.13(a) cleary indicate that the rear end input discharge falls off to 0 as soon as the section 1 gets blocked. On the other hand the rear end discharge gradually increases to a high value of about half of the maximum possible value (critically discharge) without interruption in controlled scenario, Figure 3.13(b). Thus the corridor remains available to accept input all the time in the controlled scenario.

In Figures 3.14(a) and 3.14(b), we show the evolution of the normalized room discharges in different corridor sections for the uncontrolled and controlled cases. The results for the uncontrolled scenario given in Figure 3.14(a) show that room inputs to sections 1, 2, 3 and 4 cease as soon as these sections get jammed. Section 5 being next to the exit is able to accept pedestrians from connected rooms at maximum rate. In the controlled scenario, on the other hand, the corridor sections are able to accept the input from rooms throughout the simulation. The control algorithms is clearly effective in controlling the discharge values to remain with the established bounds.

In last Figure 3.15 we show the plots for the exit discharge and the total input discharge obtained for the uncontrolled and controlled scenarios. The red lines show the results for the uncontrolled case and the green lines for the controlled case. In the uncontrolled flow scenario, we observe that the total input discharge (from the rear end

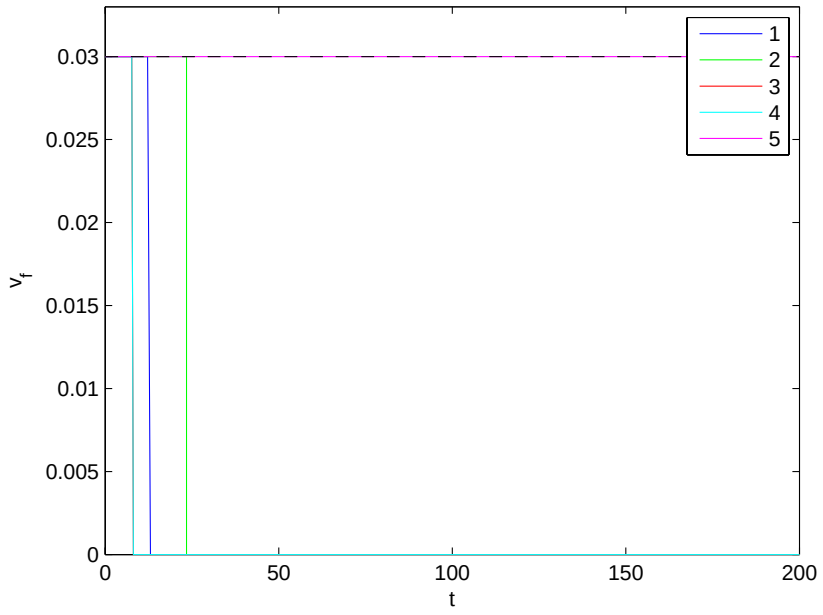

(a) Normalized section free flow velocity $\tilde{v}_{f_i}$ in the uncontrolled case

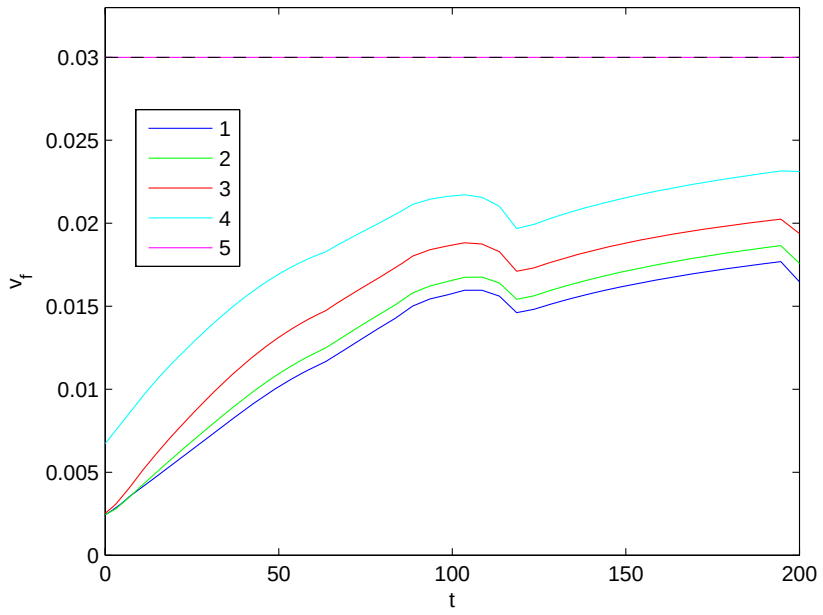

(b) Normalized section free flow velocity $\tilde{v}_{f_i}$ in the controlled case

Figure 3.12: Normalized corridor section free flow velocity $\tilde{v}_{f_i}$ for all sections in the controlled and the uncontrolled case of flow scenario 3.

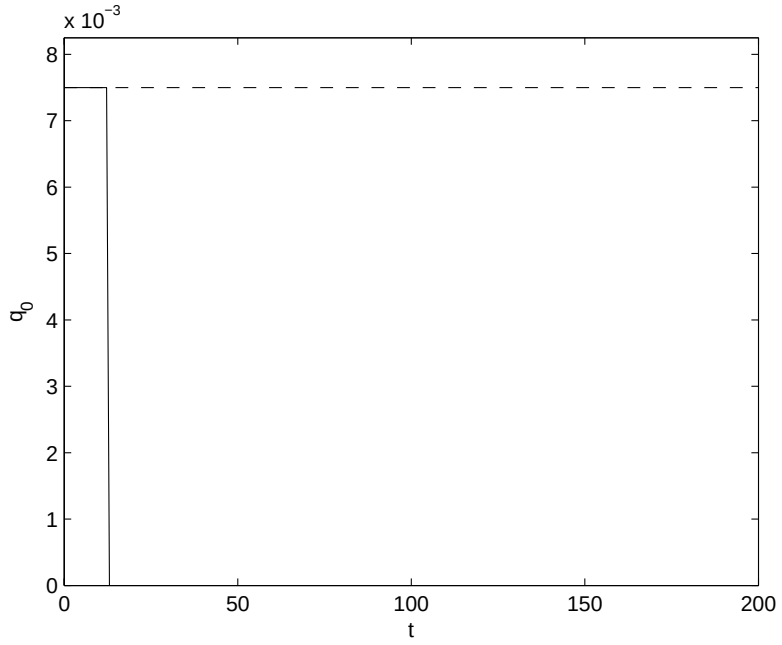

(a) Normalized rear end input discharge $\tilde{q}_0$ in the uncontrolled case

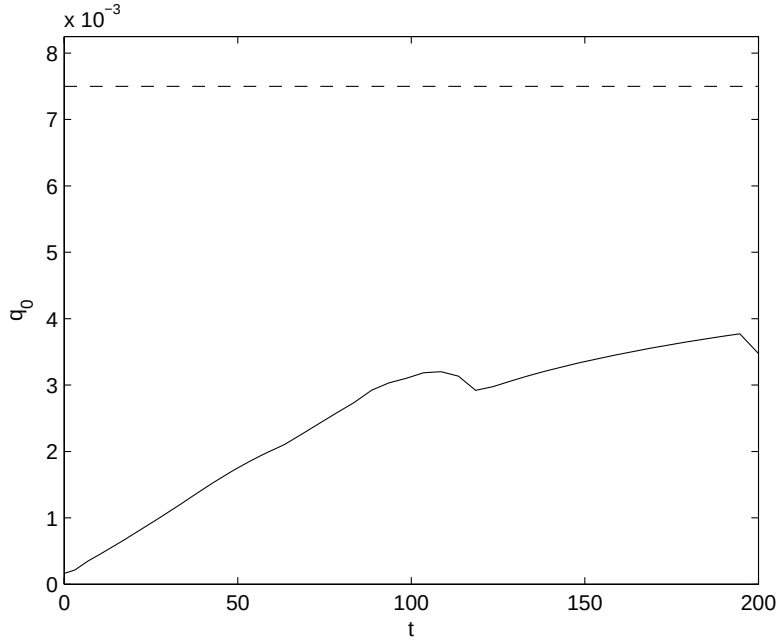

(b) Normalized rear end input discharge $\tilde{q}_0$ in the controlled case

Figure 3.13: Normalized corridor rear end input discharge $\tilde{q}_0$ in the controlled and the uncontrolled case of flow scenario 3.

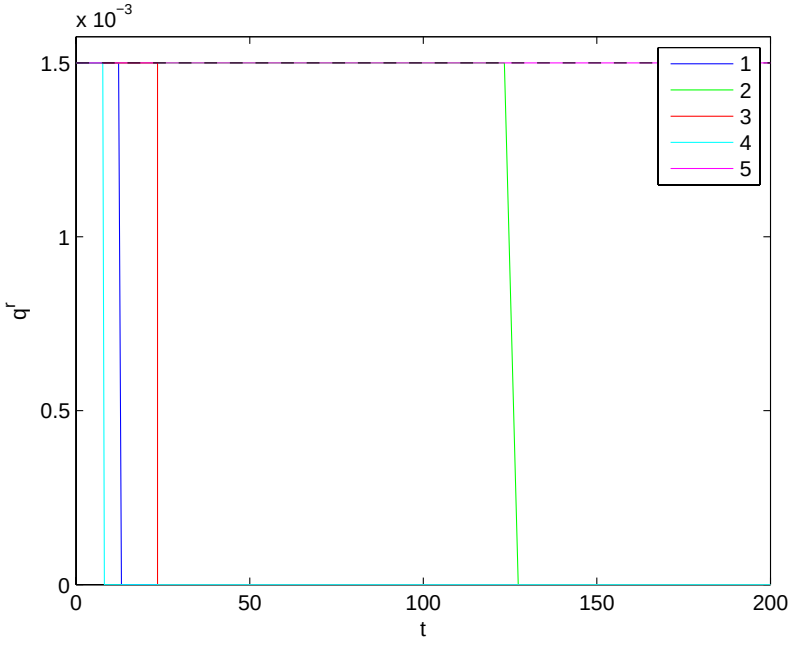

(a) Normalized section room input discharge $\tilde{q}^{r(i)}$ in the uncontrolled case

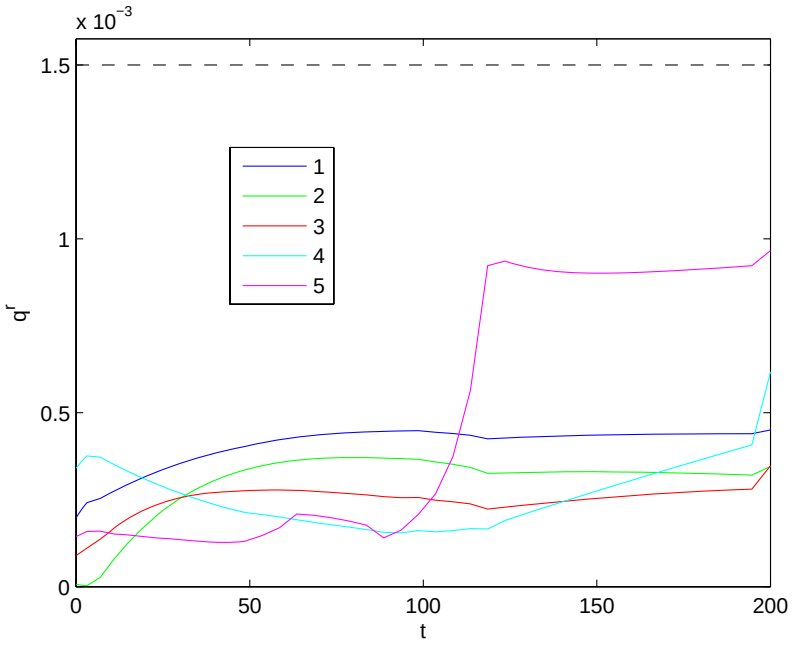

(b) Normalized section room input discharge $\tilde{q}^{r(i)}$ in the controlled case

Figure 3.14: Normalized corridor section room input discharge $\tilde{q}^{r(i)}$ for all sections in the controlled and the uncontrolled case of flow scenario 3.

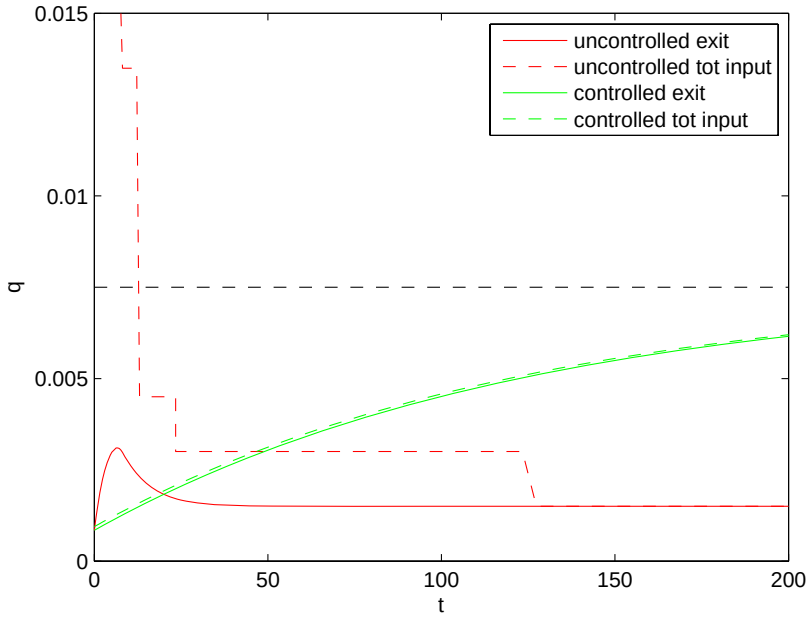

Figure 3.15: Normalized exit discharge and total input discharge in the controlled and the uncontrolled case.

and rooms) starts with its maximum possible value, but then it drops off in four steps to a value equal to maximum room discharge in section 5. The first drop coincides with the blocking of section 4, and is equal to the maximum room discharge in this section. The second drop which is relatively larger than the other steps occurs when section 1 gets jammed which also blocks in input from the back; the magnitude of this drop is equal to the sum of the room discharge in section 1 plus the rear end input. The third drop occurs when section 3 gets blocked and the last drop occurs when section 2 gets blocked. Both the drops are equal to the maximum possible room discharge in the respective sections. The final value of the total input discharge for the uncontrolled case is equal to the maximum possible room discharge from section 5 which remains open throughout. The figure also shows the exit discharge, which is noted to remain at a low value throughout, with its final value being equal to the final exit discharge which is the room discharge from section 5.

The results for the controlled case are, however, are quite different from those of the uncontrolled case. The total input discharge to the system and the exit discharge from

the system are seen to vary smoothly and increasing gradually to the maximum value in the last section. We also note that input and exit discharge are very close to each other initially and finally they approach the same maximum value asymptotically. The total input the system is slightly higher than the exit discharge in the initial stages. The difference between these two values is equal to slight accumulation of pedestrians in the system. However, the proposed control provides a good balance between the input and exit discharges emphasizing the smooth evolution of the flow without any undesirable congestion.

3.6 Chapter Summary

In this chapter we describe the flow of pedestrians in a single corridor as a prelude to the study presented in the following chapter. The corridor is divided into sections to be able to consider the variability in the pedestrian density in different sections. The pedestrian density evolution in corridor sections is defined by ordinary differential equations. Three cases of increasing complexity are considered. In the first case, the corridor is occupied with pedestrian but there is no input discharge either from the rooms or the rear end. The second case includes the input from the rear end of the corridor but not from the rooms. Third case finally considers the input from the back as well as input from the rooms in every section. These cases describe the possible flow scenarios that are likely to develop in an exit corridor at the end, middle and beginning of evacuation from a network of corridors. For each case the numerical results describing the evolution of different flow representing quantities are obtained for the uncontrolled and controlled scenarios. The uncontrolled scenario assumes that pedestrians are likely to move at the fastest possible speed considering density in the corridor sections. Also the flow discharges from the rooms and the rear end are assumed to be at their maximum value. This is a likely flow scenario in panic situation. When a section gets jammed, it prevents flow of people in the jammed section. It also blocks the flow from the immediately preceding section. In the controlled scenario, we control the flow by regulating the free flow velocity, input from the back and also the input from the rooms in to the corridor. The results for the uncontrolled case for all flow representing quantities show that flow gets interrupted within a few seconds of starting

because of jamming at different places. However, it does not happen in the controlled scenario and the flow evolves gradually to the maximum possible level of pedestrian evacuation. This clearly demonstrates the effectiveness of the proposed pedestrian control approaches.

Chapter 4

Evacuation control on a directed corridor network

4.1 Introduction

To define the shortest paths to different exits in a multi-exit network of corridors, in Chapter 2 we treated the network as a connected planner graph. A graph can be thought of as a collection of points (called nodes) connected by line segments (called edges). In our analysis the edges represented the corridors and the nodes their intersections. This shortest path analysis for such a multi-exit layout then defined the directed subgraphs for each exit separately. A directed subgraph is nothing but a part of the original graph consisting of nodes and directed edges from each node. A sequence of directed edges from a node in the subgraph defined the shortest path from that node to the subgraph exit node. The edges that did not fall on a shortest path were called as the unresolved edges. To identify the direction of movement of pedestrians on such edges, each such edge was divided into multiple sections and each section was assigned a direction towards either of the end nodes of that edge. This resulted in the edge getting divided onto 2 parts based on the node to which the pedestrian traffic was directed.

This shortest path procedure was applied to a complicated layout of the Pentagon shown in Figure 4.1, reproduced here from Chapter 2. This was obtained from `http://www.hqda.army.mil/aoguide/Pentagon_Map.htm`.The results of short-

est path analysis for the pentagon layout are presented in Figure 4.2 which is reproduced from Chapter 2. The results of shortest path analysis for the pentagon layout are presented in Figure 4.2 which is reproduced from Chapter 2. For convenience in visualization we assign a color to every exit and use the same color for the shortest path directed edges. Also shown in black color in this figure are the unresolved edges with a node identified in the their middle by small circles. This node separates the flow directions on the unresolved edges. By the shortest path analysis, thus a multi-exit graph was decomposed into multiple single-exit directed subgraphs; each such subgraph represents a flow control layout for pedestrian evacuation to an exit.

In the development of these shortest paths in Chapter 2, however, no attempt was made to regulate the pedestrian traffic based on the pedestrian density along the edges. Even when we do real time routing of pedestrians along the shortest-time-to-exit routes we only use the density based time estimates to traverse an edge of the graph. Thus the routing procedure developed in Chapter 2 does not concern with regulating the flow velocities and discharges which are critical to ensure smooth pedestrian flows.

In this chapter, therefore, we propose a procedure to control the flow of pedestrians on a directed network by regulating the flow parameters like pedestrian velocities and discharges to avoid undue congestion that might develop in a panic driven rush to evacuate. This can be done independently for each uncoupled flow layouts (directed subgraphs) corresponding to each exit, such as those shown in Figure 4.2. Thus the content of this chapter can be viewed as a sequel to that of Chapter 2. Our main objective will be to evacuate as many people as possible out of network without the development of any jam.

To develop the control we model the pedestrian flow evolution in the network by a system of ordinary differential equations. These equations model the flow from a macroscopic perspective and ignore the microscopic details concerning individual evacuees. They include the dependence of the pedestrian velocity and pedestrians discharge on the link densities. For this we use the Greenshields model used in Chapter 3 earlier. A similar model is used to estimate exit velocity from a link based on the accumulation of the pedestrians at the corners. The flow is controlled by appropriately regulating the nodal input discharge into the links, the free-flow velocity in the links and the cumulative room discharges in the links. Due to the restrictions on human

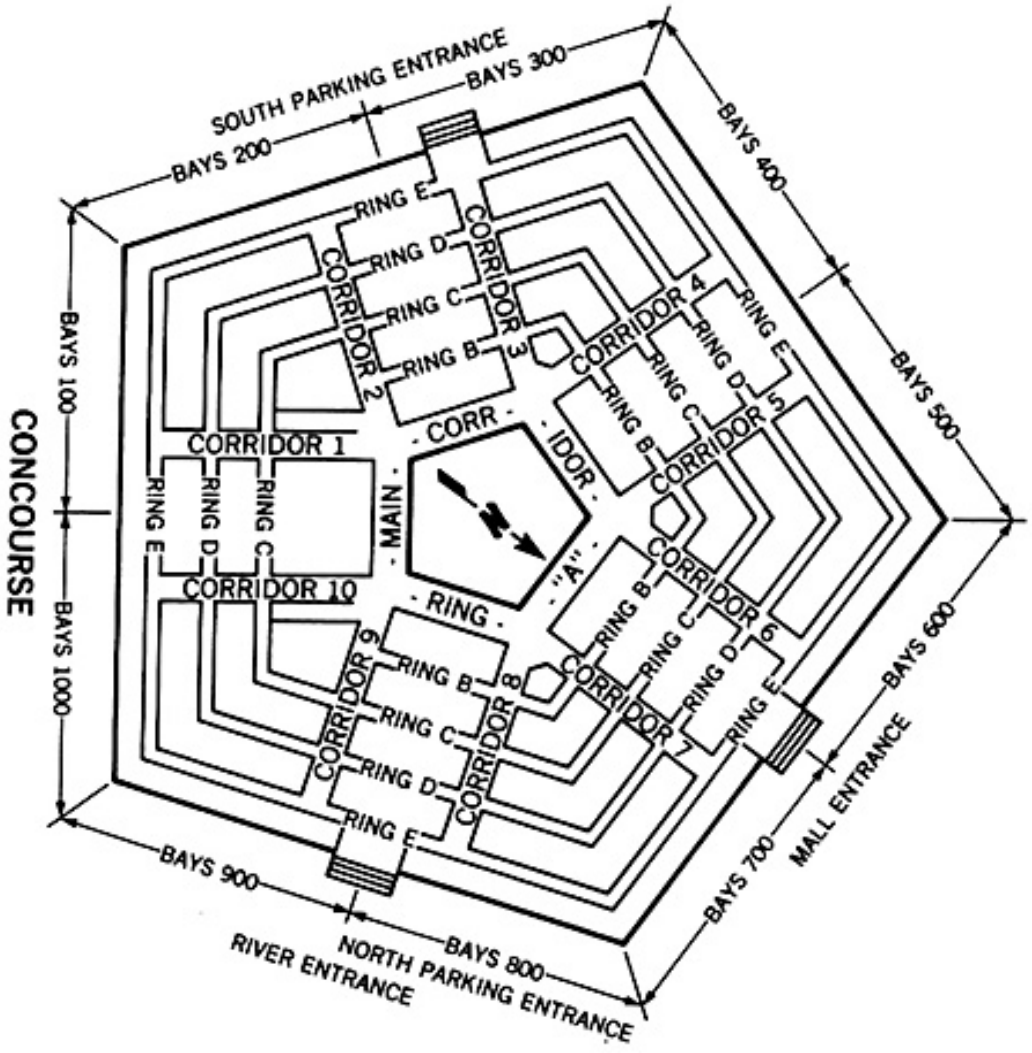

Figure 4.1: Pentagon corridor network

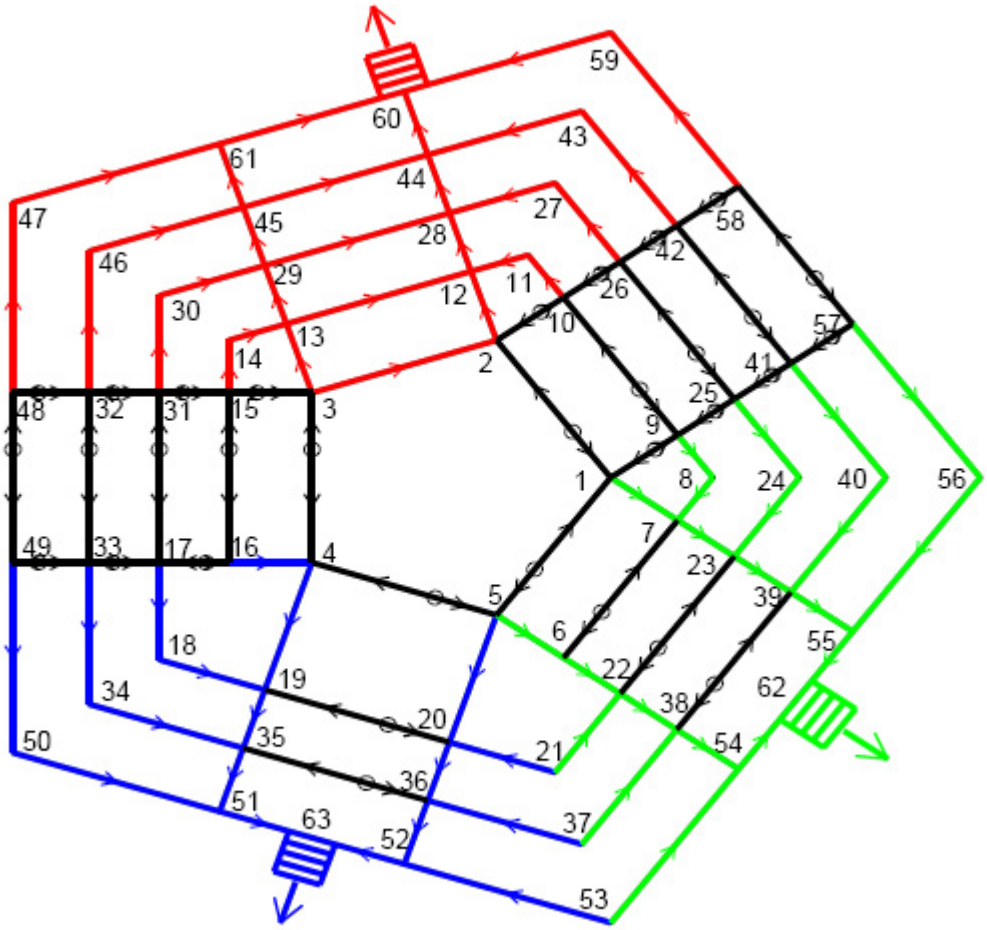

Figure 4.2: Shortest path analysis for the pentagon layout

capabilities in executing the control commands upper and lower bounds on the control inputs are imposed. For the given pedestrian flow equations, the control variables that achieve the tracking objectives while satisfying the bounding constraints are computed by solving a linear optimization problem at every stage. The key feature of our control methodology is that we are able to achieve the objectives of tracking and maximizing the total room discharge within the stated constraints, and thus making the control practically implementable.

The sections in this chapter are organized as follows: In Sec. 4.2 a control oriented macroscopic pedestrian flow model is developed for a corridor network. In Sec. 4.3 the uncontrolled flow scenario is described with the developed equations. The main objective of this section is to assign values to the control variables in absence of any explicit control scheme. These values are then used in the simulation to show that uncontrolled pedestrian flow is likely to develop jamming in several links which stalls and interrupts the pedestrian evacuation. In Sec. 4.4 a control methodology based on the equations formulated in Sec. 4.2 is developed. The method of feedback linearization is used and the optimal solution for the control variables is obtained by linear programming. Various results concerning the flow control variables resulting from this control are derived. In the feedback linearization, some values are assumed for the control gain parameters. For these assumed values for the gain parameters, however, there may not be a feasible solution for the control variables in the linear programming approach. In Sec. 4.5, therefore, a method is proposed to scale the control gains to obtain feasible optimal solution by linear programming. In Sec. 4.6 a local control algorithm is proposed at the link level that fine tunes the network control of cumulative edge room discharge. This has special relevance for pedestrian evacuation from long corridors with several feeding rooms. It is observed that the local control variables that are consistent with the global network control can be obtained without affecting the latter. In Sec. 4.7 the numerical results for the example problem of the Pentagon layout are obtained and the clear advantages of controlling the pedestrian evacuation over the uncontrolled evacuation scenario are demonstrated . In Sec. 4.8 various important aspects covered in the chapter are summarized.

4.2 Model Formulation

In this section we develop an analytical model for the pedestrian flow on a directed network of corridors with a single exit. As mentioned above such a directed network of corridors can be treated as a directed graph on which we can find a sequence of directed edges from every node to the exit node. Let the nodes be numbered $\{1, 2, ..., n\}$, with n being the total number of nodes and the n^{th} node being the exit node. Let us denote the set of all the nodes by Z. We identify every edge by an ordered pair of nodes (t, h) where t is the tail node and h is the head node. Let E denote a set of all the edges (t, h) in the directed graph under consideration. We consider a graph with e edges. For every node to be connected to the exit node with a sequence of directed edges we need atleast one directed edge coming out of every node except the exit node. Thus we have $e \geq n - 1$.

In a directed subgraph with single exit, we have three types of nodes:

1. The initial or the starting nodes. These are the nodes that have at least one outgoing edge and no incoming edge. Set of all these nodes is denoted by T_o

2. The exit node. This node has at least one incoming edge and no outgoing edge. n^{th} node is the exit node.

3. The interior nodes. These are the nodes that have at least one incoming edge and at least one outgoing edge. Set of all these nodes is denoted by T

We explain these 3 types of node using Figure 4.7, which is also the figure we use to demonstrate our simulations. In this figure the layout corresponding to the red shortest path subgraph of the pentagon layout is highlighted. It consists of the red shortest path edges and the parts of unresolved edges that point into the nodes of the red shortest path subgraph, denoted with black arrows. The concept of unresolved edges in the context of shortest path analysis of the network of corridors is explained in Chapter 2 section 2.5. The tail nodes of the unresolved edges are highlighted using black circles in Figure 4.7. Observe that these nodes have no incoming edges and at least one outgoing edge. Hence these nodes denoted by black circles for this particular layout constitute the nodes in the set T_o which denotes the initial nodes. Nodes 26 to 43 in Figure 4.7 belong to the set T_o for this layout. Observe that node 44 in Figure

4.7 is the exit node. This node has 3 incoming edges and no outgoing edge. As we are considering single exit layouts hence there will only be one exit node. Nodes 1 to 25 in Figure 4.7 have both incoming as well as outgoing edges associated with them. Hence these nodes are the interior nodes that belong to the set T. Let n_T be the number of nodes in set T.

Each one of the directed edges of the graph is assumed to have a 1-D flow in the prescribed direction. This is a reasonable assumption as the width of the corridor is typically small as compared to the length and the flow in the lateral direction is almost negligible. For the macroscopic modeling of the flow in the corridor we consider the average pedestrian density in a link to be a representative parameter. This is tantamount to assuming uniform pedestrian density in the link. The average pedestrian density on a link is the number of pedestrians on the link divided by the length of the link. We assume a linearly decreasing relationship between the link flow velocity v and the average pedestrian density ρ on a link given by the Greenshields model of traffic flow:

$$v = v_f \left(1 - \frac{\rho}{\rho_m}\right), \tag{4.1}$$

In equation (4.1) the parameter v_f is the free flow velocity and the parameter ρ_m is the pedestrian jam density.

The free flow velocity, v_f as the name suggests is the velocity when density $\rho = 0$, or the velocity in the un-congested state. That is,it is the maximum velocity with which a pedestrian can move. We are assuming that the free flow velocity parameter can be regulated using appropriate instructions. We are assuming a maximum value of v_{f_m} for this parameter. The jam density ρ_m is the density at which the pedestrian velocity equals 0. The jam density could be different for different corridors depending on their width. However, here to simplify the analytical development we assume that all corridors in the layout have the same width, which is the case in most situations. Thus, herein, we assume that the jam density ρ_m is the same for all the corridors.

Corresponding to the flow velocity given by equation (4.1) above the flow discharge q is given by:

$$q = \rho v = \rho \left(1 - \frac{\rho}{\rho_m}\right) v_f. \tag{4.2}$$

Note that the discharge q is quadratic in the density ρ. The plot of discharge v/s density is given in Figure 4.3. It should be noted that the maximum or the critical

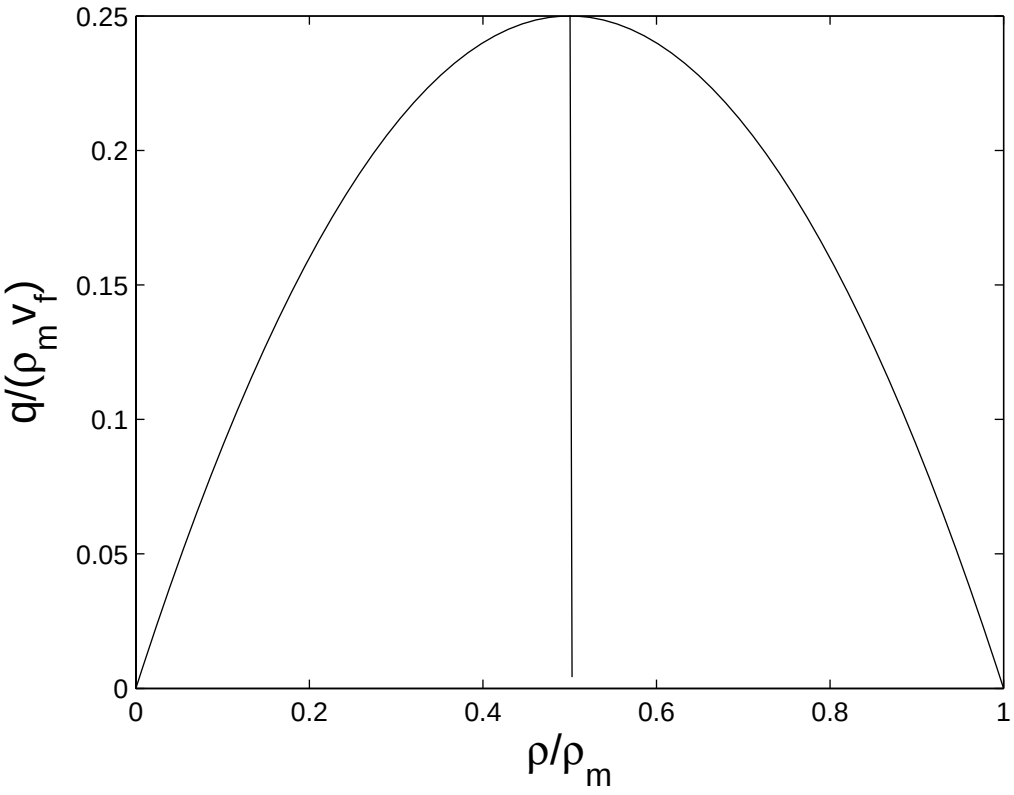

Figure 4.3: Discharge as a function of density in the Greensheilds model

discharge for a given value of free flow velocity occurs at $\rho = \frac{\rho_m}{2}$ from Figure 4.3. Thus we call $\frac{\rho_m}{2}$ the critical density and denote it by ρ_{cr}. For the maximum possible free flow velocity v_{f_m} this critical discharge corresponds to the maximum possible discharge for any density and any free flow velocity. This maximum possible discharge in the link is given by:

$$q_m = \frac{\rho_m v_{f_m}}{4} \tag{4.3}$$

For a link (t, h) let $\rho_{t,h}$ denote the average pedestrian density on that link. To compute the output discharge from a link, we need to know the exit velocity at the head node of the link. It is noted that the exit velocity at the head node of the link would be affected by the pedestrian congestion at the head node. For the interior nodes that belong to set T as described above we can expect some pedestrians to accumulate at these node due to differing rates of arrival and departure at the node (intersection) as well as due to the initial accumulation of pedestrians at these nodes. Due to this

accumulation of pedestrians at the nodes we should expect a slow down in the exit velocity from the links relative to the average velocity given by the Greenshields model in equation (4.1). At the moment there is no literature available that would quantify this slow down in an efficient manner that can be useful to develop control. To include the effect of this slow down on the flow in link (t,h) at the head node h, we introduce a slow down factor $S(N_h)$ as function of the number of pedestrians N_h accumulated at the node h to get the exit velocity $v^e_{t,h}$ from link (t,h) as:

$$v^e_{t,h} = v_{t,h}\ S(N_h). \tag{4.4}$$

We define this slow down factor as a linearly decreasing function of the number of pedestrians at the node h, N_h:

$$S(N_h) = \left(1 - \frac{N_h}{N_m}\right). \tag{4.5}$$

wherein analogous to the jam density ρ_m in the Greenshields model, N_m here would be considered as the jam nodal pedestrian mass. To compute this, we could consider a representative area at a corner and fill it up with circles. The size of the circles would correspond to the floor area occupied by an average pedestrian. Thus the jam nodal pedestrian mass N_m would correspond to a packed state of the circles in the corner area. This is a elementary approach that needs to be experimentally verified. Although not necessary, to simplify the analytical formulation we assume that jam nodal mass N_m is the same for all nodes. Combining equations (4.1), (4.4) and (4.5) we get:

$$v^e_{t,h} = v_{f_{t,h}} \left(1 - \frac{\rho_{t,h}}{\rho_{m_{t,h}}}\right) \left(1 - \frac{N_h}{N_{m_h}}\right). \tag{4.6}$$

Next we derive the equation governing the evolution of the average edge density on a typical edge $(t,h) \in E$. Using the exit velocity in equation (4.6) we get the output discharge from edge (t,h) as:

$$q^{out}_{t,h} = \rho_{t,h}\ v^e_{t,h} = \rho_{t,h} \left(1 - \frac{\rho_{t,h}}{\rho_m}\right) \left(1 - \frac{N_h}{N_m}\right)\ v_{f_{t,h}}. \tag{4.7}$$

The input discharge into the edge (t,h) consists of 2 parts, namely the nodal input discharge $q_{t,h}$ at the tail node t into the edge (t,h) and the cumulative room discharge $q^r_{t,h}$ from the rooms aligned along the edge (t,h). The input and output discharges for

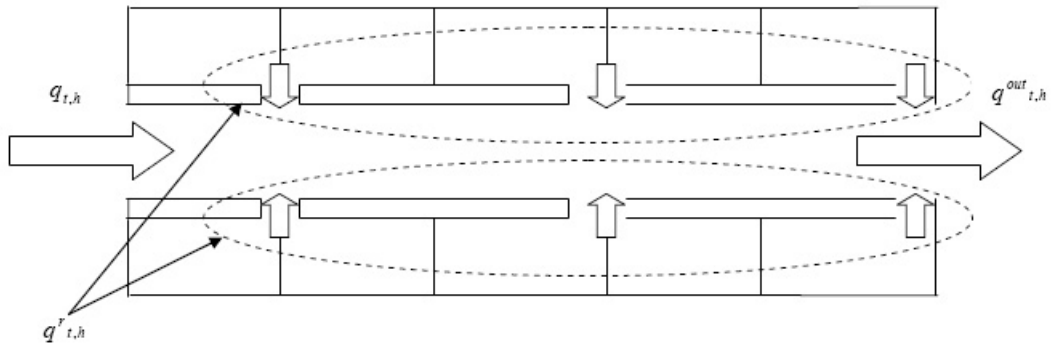

Figure 4.4: Input and output discharges in a corridor (edge) (t, h).

a corridor are shown schematically in Figure 4.4. Applying the conservation of mass (pedestrians) to edge (t, h) we obtain the equation defining the time evolution of the average density on the edge (t, h) as:

$$\dot{\rho}_{t,h} = \frac{q_{t,h} - q^{out}_{t,h} + q^{r}_{t,h}}{L_{t,h}}. \tag{4.8}$$

After substituting for $q^{out}_{t,h}$ from equation (4.7) we get the following equation representing the conservation of mass (pedestrians) for a link $(t, h) \in E$:

$$\dot{\rho}_{t,h} = \frac{q_{t,h} + q^{r}_{t,h} - \rho_{t,h} \left(1 - \frac{\rho_{t,h}}{\rho_{m_{t,h}}}\right) \left(1 - \frac{N_h}{N_{m_h}}\right) v_{f_{t,h}}}{L_{t,h}}. \tag{4.9}$$

Equation (4.9) is the equation governing the evolution of density in edge (t, h).

Next we derive the equation governing the evolution of the number of pedestrians N_i at a generic node i. The initial or start nodes as stated before have no incoming edges and have atleast one out going edge. Such nodes are indicated by black circles in Figure 4.7 which highlights the flow control layout corresponding to the red shortest path subgraph for the pentagon layout. As these nodes are located in the middle of the corridors, there is are no pedestrians accumulated on these nodes, that is, $N_k = 0$ for $k \in T_o$. Thus the conservation of mass (pedestrians) for these set of nodes with only outgoing edge implies,

$$q_{k,h} = 0 \quad (k, h) \in E \text{ and } k \in T_o. \tag{4.10}$$

The exit node, on the other hand only has incoming edges and no out going edge. We are assuming a free flow condition without obstruction at the exit node n, *i.e.* there is no accumulation of pedestrian at this node. This results in $N_n = 0$. The conservation of mass (pedestrians) at this node implies that the rate of inflow of the pedestrians at the exit node, n equals the rate of outflow at the exit node. The rate of outflow of the pedestrians at the exit node is the rate at which the pedestrians are egressing the network associated with that exit.

The interior nodes have both incoming and outgoing edges associated with them, as shown in Figure 4.5. For all such nodes $i \in T$ we can have $N_i > 0$ due to differing rates of arrival and departure as well as the initially accumulated pedestrians. Let I_i denote the set of nodes that have outgoing edges with head node i and let O_i denote a set of nodes that have incoming edges with tail node as i, as shown in Figure 4.5. Applying the conservation of mass (pedestrians) to such an interior node $i \in T$ we

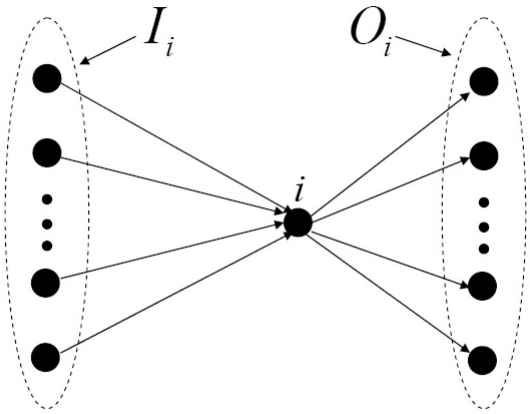

Figure 4.5: Incoming and outgoing edges for a node i.

obtain :

$$\dot{N}_i = \sum_{k \in I_i} \rho_{k,i} \left(1 - \frac{\rho_{k,i}}{\rho_m}\right) v_{f_{k,i}} \left(1 - \frac{N_i}{N_m}\right) - \sum_{j \in O_i} q_{i,j}. \tag{4.11}$$

This equation defines the evolution of the number of pedestrians at a generic node $i \in T$.

Note that the edge pedestrian density $\rho_{t,h}$ and the number of pedestrians accumulated at nodes $i \in T$ denoted by N_i describe the macroscopic pedestrian flow situation.

Thus these are the state variables of the problem. The variables $v_{f_{t,h}}$, $q_{t,h}$ and $q^r_{t,h}$ can be manipulated using appropriate instructions. Hence these are the control variables. As these control inputs are limited by the capability of the pedestrians we need to impose appropriate bounds on these. Earlier we denoted the maximum possible free flow velocity in a link to be v_{f_m}. This would hence be the upper bound on the link free flow velocities $v_{f_{t,h}}$. We assume a one directional flow on every link $(t,h) \in E$, *i.e.* the flow is always from the tail node t to the head node h and never the other way. This would impose a non-negativity restriction on the link free flow velocities $v_{f_{t,h}}$. Thus the bounds on the free flow velocity would be given by:

$$0 \leq \quad v_{f_{t,h}} \quad \leq v_{f_m}. \tag{4.12}$$

We assume that the input discharges on edges $(t,h) \in E$ namely the nodal input discharge $q_{t,h}$ and the cumulative room discharge $q^r_{t,h}$ are bounded by the critical discharge q_m given by equation (4.3). In an evacuation scenario we cannot expect to suck the pedestrian out of the tail node using any control command. Thus we have to impose a non-negativity constraint on the nodal input discharge $q_{t,h}$. We also have to impose a non-negativity constraint on the cumulative room discharge $q^r_{t,h}$. Thus the bounds on the input discharges would be given by:

$$0 \leq \quad q_{t,h} \quad \leq q_m \tag{4.13}$$

$$0 \leq \quad q^r_{t,h} \quad \leq q_m. \tag{4.14}$$

We do not know the parameters of jam density ρ_m and jam nodal pedestrian mass N_m as they need to be experimentally determined and verified. Thus we would like to do the control computation and obtain the simulation results in terms of normalized state and control variables that are proportional to the actual state and control variables. Thus we normalize the state variables $\rho_{t,h}$ with ρ_m and N_i for $i \in T$ with N_m and the control variables $v_{f_{t,h}}$ with L_m where L_m denotes maximum length of the corridor in a layout and the input discharges $q_{t,h}$ and $q^r_{t,h}$ with $\rho_m L_m$.

In order to do the above mentioned normalization we divide equation (4.9) by the jam density ρ_m and equation (4.11) by the jam nodal pedestrian mass N_m. After some algebraic manipulations this results in the following equations:

$$\frac{\dot{\rho_{t,h}}}{\rho_m} = \left(\frac{q_{t,h}}{\rho_m L_m}\right)\left(\frac{L_m}{L_{t,h}}\right) + \left(\frac{q^r_{t,h}}{\rho_m L_m}\right)\left(\frac{L_m}{L_{t,h}}\right) - \left(\frac{\rho_{t,h}}{\rho_m}\right)\left(1 - \frac{\rho_{t,h}}{\rho_m}\right)\left(\frac{v_{f_{t,h}}}{L_m}\right)\left(1 - \frac{N_h}{N_m}\right)\left(\frac{L_m}{L_{t,h}}\right) \tag{4.15}$$

$$\frac{\dot{N}_i}{N_m} = \sum_{k \in I_i} \frac{\rho_{k,i}}{\rho_m} \left(1 - \frac{\rho_{k,i}}{\rho_m}\right) \frac{v_{f_{k,i}}}{L_m} \left(1 - \frac{N_i}{N_m}\right) \left(\frac{\rho_m L_m}{N_m}\right) - \sum_{j \in O_i} \frac{q_{i,j}}{\rho_m L_m} \left(\frac{\rho_m L_m}{N_m}\right). \quad (4.16)$$

We set the following normalized variables:

$$\tilde{\rho}_{t,h} = \left(\frac{\rho_{t,h}}{\rho_m}\right) \quad (4.17)$$

$$\tilde{N}_h = \left(\frac{N_h}{N_m}\right) \quad (4.18)$$

$$\tilde{q}_{t,h} = \left(\frac{q_{t,h}}{\rho_m L_m}\right) \quad (4.19)$$

$$\tilde{q}^r_{t,h} = \left(\frac{q^r_{t,h}}{\rho_m L_m}\right) \quad (4.20)$$

$$\tilde{q}^r_i = \left(\frac{q^r_i}{\rho_m L_m}\right) \quad (4.21)$$

$$\tilde{v}_{f_{t,h}} = \left(\frac{v_{f_{t,h}}}{L_m}\right). \quad (4.22)$$

and the following normalization constants:

$$b_{t,h} = \left(\frac{L_m}{L_{t,h}}\right) \quad (4.23)$$

$$\mu = \left(\frac{\rho_m L_m}{N_m}\right). \quad (4.24)$$

Note that the normalization constants $b_{t,h}$ for edges $(t,h) \in E$ are the ratios of the length of the maximum edge to length of the edge $(t,h) \in E$ and the normalization constant μ is the ratio of the maximum number of pedestrians that can accumulate along the longest edge to the maximum number of pedestrians that can accumulate at a node. In terms of the normalized variables and normalization constants we can write equation (4.15) as:

$$\dot{\tilde{\rho}}_{t,h} = (\tilde{q}_{t,h} + \tilde{q}^r_{t,h} - \tilde{\rho}_{t,h}(1 - \tilde{\rho}_{t,h})(1 - \tilde{N}_h)\tilde{v}_{f_{t,h}})b_{t,h}. \quad (4.25)$$

and equation (4.16) as:

$$\dot{\tilde{N}}_i = (\sum_{k \in I_i} \tilde{\rho}_{k,i}(1 - \tilde{\rho}_{k,i})\tilde{v}_{f_{k,i}}(1 - \tilde{N}_i) - \sum_{j \in O_i} \tilde{q}_{i,j})\mu. \quad (4.26)$$

It should be noted that in terms of the normalized variables the jam density $\tilde{\rho_m} = \frac{\rho_m}{\rho_m} = 1$ and the jam pedestrian mass $\tilde{N}_m = \frac{N_m}{N_m} = 1$. The critical density described above in this section for the normalized variables will be $\tilde{\rho}_{cr} = \frac{\rho_{cr}}{\rho_m} = \frac{1}{2}$. Thus we do not need to know the specific parameters of jam density ρ_m and jam nodal pedestrian mass N_m in order to develop the control for or simulate equations (4.25) and (4.26). Thus we use these equations (4.25) and (4.26) as our state equations. In this case the state variables are $\tilde{\rho}_{t,h}$ for edges $(t,h) \in E$ and $\tilde{N}_i$ for interior nodes $i \in T$. The corresponding controls for these equations would be the normalized free flow velocity $\tilde{v}_{f_{t,h}}$, the normalized nodal input discharge $\tilde{q}_{t,h}$ and the normalized cumulative room discharge $\tilde{q}^r_{t,h}$. The bounds on these controls would be the scaled down bounds on the original controls given by given by inequalities (4.12), (4.13) and (4.14). Thus the bounds on the controls $\tilde{v}_{f_{t,h}}$, $\tilde{q}_{t,h}$ and $\tilde{q}^r_{t,h}$ will be given by:

$$0 \leq \quad \tilde{v}_{f_{t,h}} \quad \leq \tilde{v}_{f_m} = \frac{v_{f_m}}{L_m} \tag{4.27}$$

$$0 \leq \quad \tilde{q}_{t,h} \quad \leq \tilde{q}_m = \frac{q_m}{\rho_m L_m} \tag{4.28}$$

$$0 \leq \quad \tilde{q}^r_{t,h} \quad \leq \tilde{q}_m = \frac{q_m}{\rho_m L_m}. \tag{4.29}$$

These bounds will be used in proposing the uncontrolled flow scenario in Sec. 4.3 and explicitly imposed on the controls developed in Sec. 4.4.

4.3 Uncontrolled Flow Scenario

To examine what state of congestion will occur in a network if the pedestrian flow is not regulated, in this section we describe the uncontrolled evacuation flow scenario in the network for the flow model developed in the previous section. This involves assigning appropriate values to the control input variables $\tilde{v}_{f_{t,h}}$, $\tilde{q}_{t,h}$ and $\tilde{q}^r_{t,h}$ for $(t,h) \in E$ in absence of any explicit control.

Given the urgency of the evacuation in an emergency situation one can expect the pedestrians to move at a maximum possible speed in the corridors. This would result in the free flow velocity and hence the normalized free flow velocity for every link $(t,h) \in E$ attaining its maximum value:

$$\tilde{v}_{f_{t,h}} = \tilde{v}_{f_m}. \tag{4.30}$$

As people would try to rush out from the rooms as fast as possible, one can also expect the normalized cumulative corridor room discharge to attain its maximum value:

$$\tilde{q}^r_{t,h} = \tilde{q}_m. \tag{4.31}$$

For the normalized nodal input discharge into every link $(t,h) \in E$ we assume it to be given by the normalized average link density $\tilde{\rho}_{t,h}$ and the maximum normalized free flow velocity $\tilde{v}_{f_m}$ using the Greenshields formula. This is because the pedestrians at a node would try to get into the links as fast as possible and their velocity would be governed by the Greenshields formula using the maximum possible free flow velocity v_{f_m}. Thus for the normalized nodal input discharge into link $(t,h) \in E$ from the node t we have the following relationship:

$$\tilde{q}_{t,h} = \tilde{\rho}_{t,h}(1 - \tilde{\rho}_{t,h})\tilde{v}_{f_m}. \tag{4.32}$$

However we note that these values given by equations (4.30), (4.31) and (4.32) would be applicable only as long as the density in the links is below the jam density ρ_m. If the density reaches jam density ρ_m then we can assume that the flow in that link would stop entirely. In more realistic situation, however, such a jam will eventually thin out because of the diffusion process; but in any case, a jam in a link will cause a considerable slow down in the pedestrian flow. Thus as alluded to earlier in Chapter 3 we do not wish to pursue any further refinement of the uncontrolled flow with diffusion but focus on developing controls that would avoid undesirable occurrences like jamming. Thus, herein, we assume that in a link $(t,h) \in E$ where the pedestrian density has reached the jam density, the input variables $\tilde{v}_{f_{t,h}}$, $\tilde{q}_{t,h}$ and $\tilde{q}^r_{t,h}$ for the link are all zero as the flow in the link stops. Also it should be noted that if the number of pedestrians at a node i is zero (that is $N_i = 0$, $i \in T$), then it might not be possible to send the discharge indicated by equation (4.32) into the unjammed links having i as their tail node. This would happen if the cumulative discharge coming into node i from all the links having their head node as i is less than the cumulative outgoing discharge computed using equation (4.32) for each unjammed link with tail node i. In that case the input discharge into the unjammed links having i as their tail node is computed by equally distributing the cumulative incoming discharge into node i into the unjammed links emanating from node i. However if the normalized input discharge resulting from

the above method is greater than the maximum possible normalized discharge $\tilde{q}_m$, then the input discharge is set to the maximum possible value $\tilde{q}_m$.

This algorithm is used to generate numerical results in Sec. 4.7 later.

4.4 Flow Control Methodology

The primary goal of an emergency evacuation procedure is to get maximum discharge of pedestrians smoothly out of a network without causing any jamming in the network. To achieve this, here we propose a control approach. In mathematical terms, the objectives of the proposed control methodology are as follows:

1. To achieve exponential convergence of the average density to the critical density *i.e.* the density corresponding to maximum discharge for a given free flow velocity in every link of the network.

2. To achieve exponential convergence of the number of pedestrians accumulated at the nodes or intersection of corridors of the network to 0.

3. To maximize the total discharge from the rooms on the network to the corridors at every instant of time while meeting the above 2 objectives. This will be shown to be equivalent to maximizing the total exit edge discharge or the total discharge out of the layout.

4. To explicitly meet the specified control bounds.

The first objective of tracking the critical density is to maximize the discharge in a link for a given free flow velocity as is shown in Sec. 4.2. For the Greenshield model assumed here, this normalized critical density is $\tilde{\rho}_{cr} = \frac{1}{2}$. The second objective of tracking the number of pedestrians at nodes to approach 0 maximizes the exit velocity from a link for a given value of the density and free flow velocity. Thus these two objectives are highly desirable from the network flow efficiency perspective. Maximizing the room discharge also ensures that most number of pedestrians enter the network and eventually get out of the system. The last objective of satisfying the control bounds is essential from the implementability point of view.

The state equations that we use to develop the control algorithm are equations (4.25) and (4.26). The state variables for these equations are $\tilde{\rho}_{t,h}$ for edges $(t,h) \in E$ and $\tilde{N}_i$ for nodes $i \in T$. The nodes $i \in T$ are the interior nodes. Note that there is a possibility of accumulation of pedestrians only on the interior nodes as discussed in Sec. 4.2. Hence only the normalized nodal pedestrian masses of these nodes are tracked to 0. For nodes $k \in T_0$ the nodal pedestrian mass is already 0 and free flow conditions assumed at the exit node n ensure that the nodal pedestrian mass at the exit node $N_n = 0$.

The control variables used for achieving the objectives are the normalized free flow velocities $\tilde{v}_{f_{t,h}}$, the normalized nodal input discharges $\tilde{q}_{t,h}$ and the normalized cumulative room discharges $\tilde{q}^r_{t,h}$ for every edge $(t,h) \in E$. From equation (4.10) we already know that for all initial nodes, $\tilde{q}_{k,h} = 0$ $(k,h) \in E$ $k \in T_o$. Hence these nodal input discharges are not the control variables in our problem.

To realize the exponential convergence mentioned above, we use the state feedback linearization approach. The state feedback linearization approach will manipulate the control input variables mentioned above such that the state time derivatives $\dot{\tilde{\rho}}_{t,h}$ and $\dot{\tilde{N}}_i$ attain the following values:

$$\dot{\tilde{\rho}}_{t,h} = -k_{\tilde{\rho}_{t,h}}(\tilde{\rho}_{t,h} - 1/2) \tag{4.33}$$

$$\dot{\tilde{N}}_i = -k_{N_i}(\tilde{N}_i). \ \forall i \in T \tag{4.34}$$

where $k_{\rho_{t,h}}$ and k_{N_i} are appropriately chosen gains. The solutions of equations (4.33) and (4.34) are:

$$\tilde{\rho}_{t,h}(\tau) = \frac{1}{2} + \left((\tilde{\rho}_{t,h})_0 - \frac{1}{2}\right) \exp(-k_{\rho_{t,h}}\tau) \tag{4.35}$$

$$\tilde{N}_i(\tau) = \tilde{N}_{i_0} \exp(-k_{N_i}\tau) \tag{4.36}$$

These equations ensure that exponentially the link densities $\tilde{\rho}_{t,h}$ approach $\rho_{cr} = 1/2$ for all $(t,h) \in E$ and the nodal pedestrian mass $\tilde{N}_i$ approach 0 for all $i \in T$. In order to realize the state feedback linearization, we need to equate the state time derivatives given by the state equations (4.25) and (4.26) with the intended state time derivatives given by equations (4.33) and (4.34) respectively. This would result in the following

equations that the control variables would have to satisfy at every time instant:

$$(\tilde{q}_{t,h} + \tilde{q}^r_{t,h} - \tilde{\rho}_{t,h}(1-\tilde{\rho}_{t,h})(1-\tilde{N}_h)\tilde{v}_{f_{t,h}})b_{t,h} = -k_{\rho_{t,h}}(\tilde{\rho}_{t,h} - 1/2) \quad (4.37)$$

$$(\sum_{k\in I_i} \tilde{\rho}_{k,i}(1-\tilde{\rho}_{k,i})\tilde{v}_{f_{k,i}}(1-\tilde{N}_i) - \sum_{j\in O_i} \tilde{q}_{i,j})\mu = -k_{N_i}(\tilde{N}_i). \quad \forall i \in T \quad (4.38)$$

Thus the tracking control problem boils down to finding a control vector at every time instant that satisfies the equality constraints (4.37) and (4.38) required for tracking and the control bounds (4.28), (4.27) and (4.29) required for implementability. For every edge $(t,h) \in E$ we have the control variables $\tilde{v}_{f_{t,h}}$ and $\tilde{q}^r_{t,h}$. These constitute a total of $2e$ control variables. We have the control variables $\tilde{q}_{t,h}$ defined for all edges $(t,h) \in E$ for which $t \in T$. Let the number of edges $(t,h) \in E$ for which $t \in T$ be e_T. Note that as the number of outgoing edges from every node in T is at least one hence $e_T \geq n_T$, where as defined in Sec. 4.2 n_T is the number of nodes in the set T. Thus the total number of control variables n_v in our problem are:

$$n_v = 2e + e_T \geq 2e + n_T. \quad (4.39)$$

The tracking equation (4.37) corresponds to every edge $(t,h) \in E$. Thus there are e equations corresponding to equation (4.37). The tracking equation (4.38) corresponds to every interior node $i \in T$. Thus there are n_T equations corresponding to equation (4.38). Thus the total number of equations n_e that need to be satisfied to achieve tracking are:

$$n_e = e + n_T. \quad (4.40)$$

From equations (4.39) and (4.40) it is obvious that the number of variables n_v in equations (4.37) and (4.38) are greater than the number of equations n_e. Thus the system of equations (4.37) and (4.38) is an over determinate system in the control variables. Multiple solutions exists that can satisfy these equations. However we are interested in finding a solution that satisfies the equations, the control bounds as well as optimizes some criteria. Thus we formulate an optimization problem in terms of the control variables $\tilde{v}_{f_{t,h}}$, $\tilde{q}^r_{t,h}$ for all $(t,h) \in E$ and $q_{t,h}$ for all $(t,h) \in E \text{and} t \in T$. These control variables then become the variables of optimization problem that needs to be solved at every stage. The solution to this optimization problem would give us the control values at every stage that ensure tracking, satisfy the bound constraints and optimize some objective function.

4.4.1 Optimization based control

As mentioned above we proceed with the development of optimization based control. We first formulate an objective function. This objective function can be constructed in multiple ways using the variables of the optimization problem in order to meet different optimality criteria. For the pedestrian evacuation control we would like that most number of pedestrians start the evacuation at every instant of time. This is equivalent to maximizing the total normalized discharge from all the rooms along the network to the corridors. This can be defined in terms of the control variables as the sum of the normalized cumulative room discharges $\tilde{q}^r_{t,h}$ for all edges $(t,h) \in E$. Thus our objective function f for the optimization problem is:

$$f = \sum_{(t,h)\in E} \tilde{q}^r_{t,h}. \tag{4.41}$$

As we intend to maximize this objective function it represents our payoff or utility function. Note that the equality constraints (4.37) and (4.38) are linear in the control variables. Also the objective function f is linear in the control variables. Along with satisfying the equalities (4.37) and (4.38) we also need to satisfy the bound constraints on the control variables given by inequalities (4.27), (4.28) and (4.29). Thus both our payoff function f and the constraints (equalities and bounds) are linear in the control variables which are also the variables of the optimization problem. Hence our optimization problem is a linear programming problem.

Typically the problem of linear programming is a minimization problem for a linear cost function. However the problem of maximizing a payoff f is the same as minimizing its negative *i.e.* $-f$. Thus we formulate the linear programming problem as minimization of a linear cost function $-f$. Hence the complete linear programming can be stated

as follows:

$$
\begin{aligned}
&\text{Minimize} - f = -\sum_{(t,h)\in E} \tilde{q}^r_{t,h}. \\
&\text{subject to} \\
&(\tilde{q}_{t,h} + \tilde{q}^r_{t,h} - \tilde{\rho}_{t,h}(1-\tilde{\rho}_{t,h})(1-\tilde{N}_h)\tilde{v}_{f_{t,h}})b_{t,h} = -k_{\rho_{t,h}}(\tilde{\rho}_{t,h} - 1/2) \quad \text{.....(4.37)} \\
&(\sum_{k\in I_i} \tilde{\rho}_{k,i}(1-\tilde{\rho}_{k,i})\tilde{v}_{f_{k,i}}(1-\tilde{N}_i) - \sum_{j\in O_i} \tilde{q}_{i,j})\mu = -k_{N_i}(\tilde{N}_i). \quad \forall i \in T \quad \text{.....(4.38)} \\
&0 \le \tilde{q}_{t,h} \le \tilde{q}_m \quad \text{.....(4.28)} \\
&0 \le \tilde{v}_{f_{t,h}} \le \tilde{v}_{f_m} \quad \text{.....(4.27)} \\
&0 \le \tilde{q}^r_{t,h} \le \tilde{q}_m \quad \text{.....(4.29)}
\end{aligned}
\tag{4.42}
$$

The linear programming problem of equation (4.42) can be solved using any standard linear programming software. We have used the "linprog" command in the optimization toolbox of matlab. The solution of this problem gives a control that achieves feedback linearization as well as meets the control constraints. However like any other optimization problem involving constraints, the linear programming problem of equation (4.42) may not have a feasible solution. This means that a solution satisfying all the constraints cannot be found. For our problem, this can occur if the control gain parameters are too high that in order to satisfy the equalities the control variables have to violate their bound constraints. If this were to happen then the values of the gain parameters $k_{\rho_{t,h}}$ and k_{N_i} would have to be adjusted. A systematic procedure to do this is outlined in Sec. 4.5. For our further analysis in this section we however assume that the constraints of the linear programming problem of equation (4.42) are feasible and thus a solution to the problem exists. Assuming that the solution to the linear programming problem of equation (4.42)exits we analyze the the linear programming problem to highlight some interesting facts about it.

Free flow velocity and cumulative edge room discharges on exit edges: For all the exit edges $(i,n) \in E$ we show in this section that either the corresponding normalized free flow velocity $\tilde{v}_{f_{i,n}} = \tilde{v}_{f_m}$ or the corresponding normalized cumulative room discharge $\tilde{q}^r_{i,n} = \tilde{q}_m$. It will be shown that if the former is true then the output discharge from the exit edge tracks the maximum possible discharge q_m given by equation (4.3). In case the later is true then it is self evident that the room input discharge

into the exit corridor is at its maximum value. This fact becomes evident when we inspect equation (4.37) for the exit edge (i,n). Noting that $N_n = 0$ and rearranging the equation we can write equation (4.37) as:

$$\tilde{q}^r_{i,n} = -\frac{k_{\rho_{i,n}}}{b_{i,n}}(\tilde{\rho}_{i,n} - \frac{1}{2}) - \tilde{q}_{i,n} + \tilde{\rho}_{i,n}(1 - \tilde{\rho}_{i,n})\tilde{v}_{f_{i,n}}. \tag{4.43}$$

This expression gives the expression for the normalized cumulative edge room discharge for the exit edge (i,n). As (i,n) is an exit edge $\tilde{v}_{f_{i,n}}$ appears only in one of the equality constraints (4.37) and (4.38) of the linear programming problem of equation (4.42). This is the equality constraint corresponding to the edge (i,n) in the equations (4.37) given by (4.43). Other than this equality constraint the control variables $\tilde{v}_{f_{i,n}}$ has to satisfy only the bounds given by equation (4.27). The control variable $\tilde{q}^r_{t,h}$ for any $(t,h) \in E$ appears only in one of the equality constraints (4.37) corresponding to edge (t,h) of all the equality constraints (4.37) and (4.38) of the linear programming problem of equation (4.42). Thus $\tilde{q}^r_{i,n}$ appears only in the equality constraint (4.37) corresponding to (i,n) given by equation (4.43). Along with this equality constraint $\tilde{q}^r_{i,n}$ has to satisfy the bounds given by equation (4.29).

The solution of the linear programming problem of equation (4.42) though formulated as a minimization problem implies that the total normalized room discharge is maximized. Thus the contribution from the normalized room discharge $\tilde{q}^r_{i,n}$ has to be maximized while satisfying the equality constraint (4.43) and the bound constraint in equation (4.29). Let us examine the last term, $\tilde{\rho}_{i,n}(1 - \tilde{\rho}_{i,n})\tilde{v}_{f_{i,n}}$ on the right hand side of equation (4.43). This is the only term on the right hand side containing $\tilde{v}_{f_{i,n}}$. Also note that $\tilde{v}_{f_{i,n}}$ appears linearly in this term with a positive coefficient $\tilde{\rho}_{i,n}(1 - \tilde{\rho}_{i,n})$. Thus in order to maximize the contribution of $\tilde{q}^r_{i,n}$ the solution of the linear programming problem of equation (4.42) will maximize $\tilde{v}_{f_{i,n}}$ while satisfying the equality (4.43) and the bound constraint of equation (4.27). As the only equality constraint consisting of either $\tilde{q}^r_{i,n}$ or $\tilde{v}_{f_{i,n}}$ is equation (4.43) of all the equality constraints (4.37) and (4.38) hence in increasing $\tilde{v}_{f_{i,n}}$ the only considerations are that $\tilde{v}_{f_{i,n}}$ itself satisfies bounds (4.27) and $\tilde{q}^r_{i,n}$ satisfies bounds (4.29). Thus the solution of the linear programming problem of equations (4.42) requires that either $\tilde{v}_{f_{i,n}} = \tilde{v}_{f_m}$ or $\tilde{q}^r_{i,n} = \tilde{q}_m$.

Next we observe that the last term of equation (4.43) $\tilde{\rho}_{i,n}(1 - \tilde{\rho}_{i,n})\tilde{v}_{f_{i,n}} \leq \tilde{q}_m$ as it corresponds to the normalized output discharge of the edge (i,n). It attains its maximum value $\tilde{q}_m$ when $\tilde{\rho}_{i,n} = \tilde{\rho}_{cr} = \frac{1}{2}$ and $\tilde{v}_{f_{i,n}} = \tilde{v}_{f_m}$. This value corresponds to the

upper bound of $\tilde{q}^r_{i,n}$ given by equation (4.29). Thus if the first 2 terms in the equation (4.43) $-\frac{k_{\rho_{i,n}}}{b_{i,n}}(\tilde{\rho}_{i,n}-\frac{1}{2})-\tilde{q}_{i,n}\leq 0$ then $\tilde{v}_{f_{i,n}}=\tilde{v}_{f_m}$ as the upper bound of $\tilde{q}^r_{i,n}$, $\tilde{q}_m$ cannot be violated. $-\frac{k_{\rho_{i,n}}}{b_{i,n}}(\tilde{\rho}_{i,n}-\frac{1}{2})\leq 0$ for $\tilde{\rho}_i\geq\frac{1}{2}$ and $\tilde{q}_{i,n}\geq 0$ by (4.28). This implies that for $\tilde{\rho}_i\geq\frac{1}{2}$, $-\frac{k_{\rho_{i,n}}}{b_{i,n}}(\tilde{\rho}_{i,n}-\frac{1}{2})-\tilde{q}_{i,n}\leq 0$ and hence $\tilde{v}_{f_{i,n}}=\tilde{v}_{f_m}$. However if $\tilde{\rho}_{i,n}<\frac{1}{2}$ then $-\frac{k_{\rho_{i,n}}}{b_{i,n}}(\tilde{\rho}_{i,n}-\frac{1}{2})>0$. Hence it is possible that $-\frac{k_{\rho_{i,n}}}{b_{i,n}}(\tilde{\rho}_{i,n}-\frac{1}{2})-\tilde{q}_{i,n}>0$. Thus we cannot be sure that $\tilde{v}_{f_{i,n}}=\tilde{v}_{f_m}$ as the upper bound of $\tilde{q}^r_{i,n}$, $\tilde{q}_m$ can be violated. In case the upper bound of $\tilde{q}^r_{i,n}$ gets violated by $\tilde{v}_{f_{i,n}}=\tilde{v}_{f_m}$ then we have $\tilde{q}^r_{i,n}=\tilde{q}_m$. However note that as $\tilde{\rho}_{i,n}<\frac{1}{2}$ comes close to $\frac{1}{2}$ the positive contribution of the term $-\frac{k_{\rho_{i,n}}}{b_{i,n}}(\tilde{\rho}_{i,n}-\frac{1}{2})$ will decrease. If it decreases to a point where $-\frac{k_{\rho_{i,n}}}{b_{i,n}}(\tilde{\rho}_{i,n}-\frac{1}{2})-\tilde{q}_{i,n}\leq 0$ then by the previous argument $\tilde{v}_{f_{i,n}}=\tilde{v}_{f_m}$. The exponential convergence ensured by the control implies that $\tilde{\rho}_{i,n}$ can come arbitrarily close to $\frac{1}{2}$ if the system runs long enough. Thus if the system runs long enough then we can be assured that $\tilde{v}_{f_{i,n}}=\tilde{v}_{f_m}$ even if initially $\tilde{v}_{f_{i,n}}<\tilde{v}_{f_m}$. The only reason why in some situations when $\tilde{\rho}_{i,n}<\frac{1}{2}$ the exit edge free flow velocity $\tilde{v}_{f_{i,n}}<\tilde{v}_{f_m}$ is that there isnt sufficient edge room discharge available for tracking the critical edge density of $\frac{1}{2}$ at the free flow velocity of $\tilde{v}_{f_{i,n}}=\tilde{v}_{f_m}$. Thus if we can relax the upper bound restriction on the cumulative edge discharge (possibly by making the room doors on the exit edges wider) then we increase the possibility of the exit edge free flow velocity attaining its maximum value. Another approach though not as desirable would be to reduce the exit edge gain $k_{\rho_{t,h}}$ and slow down the approach of the edge density to the critical density. Doing this would avoid the term $-\frac{k_{\rho_{i,n}}}{b_{i,n}}(\tilde{\rho}_{i,n}-\frac{1}{2})$ from making a relatively large positive contribution to the right hand side of equation (4.43) and avoiding $\tilde{v}_{f_{i,n}}=\tilde{v}_{f_m}$.

Now we show that if $\tilde{v}_{f_{i,n}}=\tilde{v}_{f_m}$ then the normalized output discharge from the exit link $\tilde{q}^{out}_{i,n}$ exponentially approaches $\tilde{q}_m$. For $\tilde{v}_{f_{i,n}}=\tilde{v}_{f_m}$ the output discharge from edge (i,n) can be written as:

$$\begin{aligned}
\tilde{q}^{out}_{i,n}(\tau) &= \tilde{\rho}_{i,n}(1-\tilde{\rho}_{i,n})\tilde{v}_{f_m} && (4.44)\\
&= \left(\frac{1}{2}+\left((\tilde{\rho}_{i,n})_0-\frac{1}{2}\right)\exp(-k_{\rho_{i,n}}\tau)\right)\left(\frac{1}{2}-\left((\tilde{\rho}_{i,n})_0-\frac{1}{2}\right)\exp(-k_{\rho_{i,n}}\tau)\right)\tilde{v}_{f_m}\\
&= \left(\frac{1}{4}-\left((\tilde{\rho}_{i,n})_0-\frac{1}{2}\right)^2\exp(-2k_{\rho_{i,n}}\tau)\right)\tilde{v}_{f_m}\\
&= \tilde{q}_m-\tilde{v}_{f_m}\left((\tilde{\rho}_{i,n})_0-\frac{1}{2}\right)^2\exp(-2k_{\rho_{i,n}}\tau). && (4.45)
\end{aligned}$$

This equation shows that the normalized output discharge from any exit edge (i, n) would exponentially approach the maximum normalized discharge corresponding to the Greenshields model $\tilde{q}_m = \frac{\tilde{v}_{f_m}}{4}$.

Total room discharge and total exit edge discharge: In this section we show that maximizing the payoff function f given by equation (4.41) indicating the total room discharge is equivalent to maximizing the total exit edge discharge. Also we will show that the total room discharge asymptotically approaches the total exit edge discharge in the controlled scenario. If the exit edge free flow velocity equals the maximum free flow velocity under the conditions stated above then the total room discharge and the total exit edge discharge together approach the total critical discharge possible from the exit edges. This total critical discharge is given by $n_e\tilde{q}_m$, where n_e is the total number of exit edges.

To show this, we form an equation by dividing equations (4.25) by $b_{t,h}$ and adding them up for all $(t, h) \in E$ as follows:

$$\sum_{(t,h)\in E} \frac{\dot{\tilde{\rho}}_{t,h}}{b_{t,h}} = \sum_{(t,h)\in E} \tilde{q}^r_{t,h} + \sum_{(t,h)\in E} \tilde{q}_{t,h} - \sum_{(t,h)\in E} \tilde{\rho}_{t,h}(1-\tilde{\rho}_{t,h})(1-\tilde{N}_h)\tilde{v}_{f_{t,h}} \tag{4.46}$$

Let us express the last two summation terms of equation (4.46) into four separate terms associated with the flow at the initial nodes ($t \in T_0$), the interior nodes ($t \in T$) and exit edges (t, n) as follows:

$$\begin{aligned}\sum_{(t,h)\in E} \tilde{q}_{t,h} - \sum_{(t,h)\in E} \tilde{\rho}_{t,h}(1-\tilde{\rho}_{t,h})(1-\tilde{N}_h)\tilde{v}_{f_{t,h}} &= \sum_{(t,h)\in E:t\in T_0} \tilde{q}_{t,h} \\ &+ \sum_{(t,h)\in E:t\in T} \tilde{q}_{t,h} - \sum_{(t,h)\in E:h\in T} \tilde{\rho}_{t,h}(1-\tilde{\rho}_{t,h})(1-\tilde{N}_h)\tilde{v}_{f_{t,h}} \\ &- \sum_{(t,n)\in E} \tilde{\rho}_{t,n}(1-\tilde{\rho}_{t,n})\tilde{v}_{f_{t,n}}.\end{aligned} \tag{4.47}$$

The first summation on the right hand side of the above equation for $t \in T_0$ is associated with the initial nodes that have no incoming edges and only the outgoing edges. The last summation term on the right hand side is associated with the discharge on the exit edges (t, n). The second and third summation terms are associated with the discharge on the interior nodes identifed by the tail node $t \in T$ and the head node $h \in T$. As mentioned earlier, T is the set of nodes that have at least one incoming edge and

at least one outgoing edge. From Figure 4.5 which shows a general node $i \in T$ these summation can be expressed as a summation of terms with node index $i \in T$ as follows:

$$\sum_{(t,h)\in E:t\in T} \tilde{q}_{t,h} - \sum_{(t,h)\in E:h\in T} \tilde{\rho}_{t,h}(1-\tilde{\rho}_{t,h})(1-\tilde{N}_h)\tilde{v}_{f_{t,h}} = \sum_{i\in T}(\sum_{h\in O_i} \tilde{q}_{i,h} - \sum_{t\in I_i} \tilde{\rho}_{t,i}(1-\tilde{\rho}_{t,i})(1-\tilde{N}_i)v_{f_{t,i}}) \tag{4.48}$$

Using equation (4.26), the inner summation in the above equation can be expressed as $\dot{\tilde{N}}_i$ as follows:

$$(\sum_{h\in O_i} \tilde{q}_{i,h} - \sum_{t\in I_i} \tilde{\rho}_{t,i}(1-\tilde{\rho}_{t,i})(1-\tilde{N}_i)v_{f_{t,i}}) = -\frac{\dot{\tilde{N}}_i}{\mu}. \tag{4.49}$$

Using equation (4.49) in equation (4.48) and then substituting it in equation (4.47), we obtain the following for the last two terms of equation (4.46):

$$\sum_{(t,h)\in E} \tilde{q}_{t,h} - \sum_{(t,h)\in E} \tilde{\rho}_{t,h}(1-\tilde{\rho}_{t,h})(1-\tilde{N}_h)\tilde{v}_{f_{t,h}} = \sum_{(t,h)\in E:t\in T_0} \tilde{q}_{t,h} - \sum_{i\in T} \frac{\dot{\tilde{N}}_i}{\mu} - \sum_{(t,n)\in E} \tilde{\rho}_{t,n}(1-\tilde{\rho}_{t,n})\tilde{v}_{f_{t,n}} \tag{4.50}$$

We note that the first summation in the above equation is 0 because it is the sum of input discharges into edges with initial nodes $t \in T_0$. Utilizing equation (4.34) which ensures the tracking of the nodal pedestrian mass to 0 for all nodes $i \in T$ in equation(4.50) and noting that the last summation in the above equation is that of the exit edge output discharges $\tilde{q}^{out}_{t,n}$ we can rewrite equation (4.50) as follows:

$$\sum_{(t,h)\in E} \tilde{q}_{t,h} - \sum_{(t,h)\in E} \tilde{\rho}_{t,h}(1-\tilde{\rho}_{t,h})(1-\tilde{N}_h)\tilde{v}_{f_{t,h}} = \sum_{i\in T} \frac{k_{N_i}}{\mu}(N_i) - \sum_{(t,n)\in E} \tilde{q}^{out}_{t,n} \tag{4.51}$$

Equations (4.33) ensure that normalized edge densities for edges $(t,h) \in E$ approach the critical density $\tilde{\rho}_{cr} = \frac{1}{2}$ exponentially on each edge. Dividing equations (4.33) by $b_{t,h}$ for all $(t,h) \in E$ and adding them up we get:

$$\sum_{(t,h)\in E} \frac{\dot{\tilde{\rho}}_{t,h}}{b_{t,h}} = -\sum_{(t,h)\in E} \frac{k_{\rho_{t,h}}}{b_{t,h}}(\rho_{t,h} - 1/2) \tag{4.52}$$

Substituting equations (4.52) and (4.51) in equation (4.46),we obtain:

$$\sum_{(t,h)\in E} \tilde{q}^{r}_{t,h} + \sum_{i\in T} \frac{k_{N_i}}{\mu}(N_i) - \sum_{(t,n)\in E} \tilde{q}^{out}_{t,n} = -\sum_{(t,h)\in E} \frac{k_{\rho_{t,h}}}{b_{t,h}}(\rho_{t,h} - 1/2), \tag{4.53}$$

We can re-arrange the above equation so that the total discharge from the rooms is given by:

$$\sum_{(t,h)\in E} \tilde{q}^r_{t,h} = \sum_{(t,n)\in E} \tilde{q}^{out}_{t,n} - \sum_{(t,h)\in E} \frac{k_{\rho_{t,h}}}{b_{t,h}}(\tilde{\rho}_{t,h} - 1/2) - \sum_{i\in T} \frac{k_{N_i}}{\mu}(\tilde{N}_i). \tag{4.54}$$

In equation (4.54) observe that the terms $\sum_{(t,h)\in E} \tilde{q}^r_{t,h}$ and $\sum_{(t,n)\in E} \tilde{q}^{out}_{t,n}$ are functions of the variables (the control variables $\tilde{v}_{f_{t,h}}$, $\tilde{q}^r_{t,h}$ and $\tilde{q}_{t,h}$) of the linear optimization problem (4.42). However as far as the optimization program is concerned the states $\tilde{\rho}_{t,h}$ for all $(t,h) \in E$ and $\tilde{N}_i$ for all $i \in T$ are constants. Hence the last 2 summation terms in equation (4.54) can be treated as constants in the optimization program (4.42). Thus the total room discharge $\sum_{(t,h)\in E} \tilde{q}^r_{t,h}$ and the total exit edge discharge $\sum_{(t,n)\in E} \tilde{q}^{out}_{t,n}$ only differ by a constant as far as the optimization program is concerned. Thus *maximizing the total instantaneous room discharge is equivalent to maximizing the total instantaneous exit edge discharge.*

We note that from equation (4.35) $\tilde{\rho}_{t,h} \to \frac{1}{2}$. Also from equation (4.36), we observe that $\tilde{N}_i \to 0$. The last 2 summation terms in equation (4.54) asymptotically converge to zero as time evolvs. Thus, we have the following asymptotic convergence relation:

$$\sum_{(t,h)\in E} \tilde{q}^r_{t,h} \to \sum_{(t,n)\in E} \tilde{q}^{out}_{t,n} \tag{4.55}$$

which states that, the total room discharge asymptotically approaches the total dischage from the exit edges. From equation (4.45) $\tilde{q}^{out}_{t,n} \to q_m$ if the exit edge free flow velocity $\tilde{v}_{f_{t,n}} = \tilde{v}_{f_m}$. If this conditions are met then we additionally have:

$$\sum_{(t,h)\in E} \tilde{q}^r_{t,h} \to n_e q_m \tag{4.56}$$

4.5 Gain scaling for infeasible constraints

In order for the linear programming problem to have a solution we need to ensure that the constraints (equalities:(4.37) and (4.38), Inequalities:(4.28), (4.27) and (4.29)) bound a feasible set. However if the gains $k_{\rho_{t,h}} > 0$ and $k_{N_i} > 0$ are too large then there is no guarantee that the constraints will bound a feasible set. Also it could happen that the initially chosen gains might not produce feasible constraints later as the system evolves. If we were to reach such a stage then gains would have to be changed such that

the constraints are feasible. Unfortunately there is no simple approach of selecting gains $k_{\rho_{t,h}}$ and k_{N_i} such that the constraints (equalities:(4.37) and (4.38),inequalities:(4.28), (4.27) and (4.29)) bound a feasible set. In this section we present a method of scaling the infeasible gains $k_{\rho_{t,h}}$ and k_{N_i} appropriately and optimally in some sense such that the constraints in the linear programming problem (4.42) with the scaled gains are feasible.

First we observe that due to the linearity of equalities (4.37) and (4.38), if $(\tilde{v}_f)^0_{i,j}$,$(\tilde{q})^0_{i,j}$,$(\tilde{q}^r)^0_{i,j}$ $\forall (i,j) \in E$ satisfy the linear equality constraints (4.37) and (4.38) with the gains $k_{\rho_{i,j}} = k^0_{\rho_{i,j}}$ and $k_{N_i} = k^0_{N_i}$ then $\frac{(\tilde{v}_f)^0_{i,j}}{\nu}$,$\frac{(\tilde{q})^0_{i,j}}{\nu}$,$\frac{(\tilde{q}^r)^0_{i,j}}{\nu}$ $\forall (i,j) \in E$ satisfy the linear equalities (4.37) and (4.38) with gains $k_{\rho_{i,j}} = \frac{k^0_{\rho_{i,j}}}{\nu}$ and $k_{N_i} = \frac{k^0_{N_i}}{\nu}$. This fact can be used to find a scaling factor $\nu > 0$ such that if the constraints (equalities:(4.37) and (4.38),inequalities:(4.28), (4.27) and (4.29)) are infeasible with gains $k_{\rho_{i,j}} = k^0_{\rho_{i,j}}$ and $k_{N_i} = k^0_{N_i}$ then replacing them with gains $k_{\rho_{i,j}} = \frac{k^0_{\rho_{i,j}}}{\nu}$ and $k_{N_i} = \frac{k^0_{N_i}}{\nu}$ would make them feasible. However the smaller this factor ν is the larger would the resulting gains $k_{\rho_{i,j}} = \frac{k^0_{\rho_{i,j}}}{\nu}$ and $k_{N_i} = \frac{k^0_{N_i}}{\nu}$ be implying faster exponential convergence to the tracking values. In order to get a low value for the factor ν we need to ensure that the solution to the equalities (4.37) and (4.38) with gains $k_{\rho_{i,j}} = k^0_{\rho_{i,j}}$ and $k_{N_i} = k^0_{N_i}$ that we seek, violates the bounds (4.27), (4.28) and (4.29) in a certain optimal way.

The optimality that we seek in the solution of the equalities (4.37) and (4.38) with gains $k_{\rho_{i,j}} = k^0_{\rho_{i,j}}$ and $k_{N_i} = k^0_{N_i}$ is that the bounds of the constraints (4.27), (4.28) and (4.29) are violated in a minimum cumulative sense by the infeasible solution. This implies that the sum of all the bound violations in the solution of the equalities (4.37) and (4.38) is minimum. In order to achieve this we formulate a new linear programming problem. This linear programming problem will retain the equalities (4.37) and (4.38) that need to be satisfied for some values of gains $k_{\rho_{t,h}}$ and k_{N_i}. The cost of this linear programming problem will equal the sum of all the bound violations of the constraints (4.27), (4.28) and (4.29). As the solution of the linear programming problem minimizes the cost hence the solution of this linear programming problem will minimize the cumulative constraint violations.

The procedure of formulating the new linear programming problem starts off with making the bound constraints (4.27), (4.28) and (4.29) more accommodative. To this effect we relax the upper bound of the constraints (4.27), (4.28) and (4.29) such that

all non-negative values of the control variables are admissible in the the solution of the equalities (4.37) and (4.38). Thus the new set of relaxed bounds can be written as:

$$0 \leq \quad \tilde{v}_{f_{t,h}} \quad \leq \infty \tag{4.57}$$

$$0 \leq \quad \tilde{q}_{t,h} \quad \leq \infty \tag{4.58}$$

$$0 \leq \quad \tilde{q}^r_{t,h} \quad \leq \infty \tag{4.59}$$

In order to quantify the violation of the original bound constraints (4.27), (4.28) and (4.29) in the solution of the equalities (4.37) and (4.38) we introduce a new set of variables namely the "'slack"' and the "'surplus"' variables. A pair of slack and surplus variables corresponds to a bound that was relaxed. For every variable $\tilde{v}_{f_{t,h}}$,$\tilde{q}_{t,h}$ and $\tilde{q}^r_{t,h}$ for all $(t,h) \in E$ of the linear programming problem (4.42) we have relaxed only the upper bound of the original bound constraint. Hence we have a pair of slack and surplus variables corresponding to every variable. The slack variable corresponding to a bound represents the amount by which the original bound were satisfied and the surplus variable corresponding to a bound represents the amount by which the original bound was violated. A given bound in the solution of the equalities (4.37) and (4.38) could be either satisfied or violated. Hence we need both these variables. The slack and the surplus variables are non-negative as they are representative of the amount by which a bound was either satisfied or violated respectively. Let the slack variables corresponding to the $\tilde{v}_{f_{t,h}}$, $\tilde{q}_{t,h}$ and $\tilde{q}^r_{t,h}$ be denoted by of $(\tilde{v}_{f_{t,h}})_{sl}$, $(\tilde{q}_{t,h})_{sl}$ and $(\tilde{q}^r_{t,h})_{sl}$. Let the surplus variables corresponding to the $\tilde{v}_{f_{t,h}}$, $\tilde{q}_{t,h}$ and $\tilde{q}^r_{t,h}$ be denoted by of $(\tilde{v}_{f_{t,h}})_{su}$, $(\tilde{q}_{t,h})_{su}$ and $(\tilde{q}^r_{t,h})_{su}$. As these variables are non-negative the bound constraints on them can be stated as:

$$0 \leq \quad (\tilde{v}_{f_{t,h}})_{sl} \quad \leq \infty \tag{4.60}$$

$$0 \leq \quad (\tilde{v}_{f_{t,h}})_{su} \quad \leq \infty \tag{4.61}$$

$$0 \leq \quad (\tilde{q}_{t,h})_{sl} \quad \leq \infty \tag{4.62}$$

$$0 \leq \quad (\tilde{q}_{t,h})_{su} \quad \leq \infty \tag{4.63}$$

$$0 \leq \quad (\tilde{q}^r_{t,h})_{sl} \quad \leq \infty \tag{4.64}$$

$$0 \leq \quad (\tilde{q}^r_{t,h})_{su} \quad \leq \infty \tag{4.65}$$

In the next step we define additional equality constraints that correspond to the original constraint bounds that were relaxed in terms of the surplus and slack variables.

As slack variables represent amount by which the original bounds were satisfied and the surplus variables represent the amount by which the original bounds were violated we have the following equations that relates the variable, the original bound and the corresponding slack and surplus variables: bounds:

$$\tilde{v}_{f_{t,h}} = \tilde{v}_{f_m} + (\tilde{v}_{f_{t,h}})_{su} - (\tilde{v}_{f_{t,h}})_{sl} \tag{4.66}$$

$$\tilde{q}_{t,h} = \tilde{q}_m + (\tilde{q}_{t,h})_{su} - (\tilde{q}_{t,h})_{sl} \tag{4.67}$$

$$\tilde{q}^r_{t,h} = \tilde{q}_m + (\tilde{q}^r_{t,h})_{su} - (\tilde{q}^r_{t,h})_{sl} \tag{4.68}$$

This completes the definition of the new surplus and slack variables, and the equality and bound constraints they need to satisfy. As each surplus variable denotes the amount by which an original bound corresponding to a relaxed bound is violated in the solution hence the sum of all the surplus variables will denote the cumulative amount by which all the original bounds constraints that were relaxed have been violated. Thus the cost that we intend to minimize in this optimization procedure can be defined as:

$$g = \sum_{(t,h)\in E} ((\tilde{v}_{f_{t,h}})_{su} + (\tilde{q}_{t,h})_{su} + (\tilde{q}^r_{t,h})_{su}). \tag{4.69}$$

Thus we have specified all the constraints and the cost function constituting the new linear programming problem. In its complete form, this new linear programming

problem can be stated as:

$$\text{Minimize } g = \sum_{(t,h)\in E} ((\tilde{v}_{f_{t,h}})_{su} + (\tilde{q}_{t,h})_{su} + (\tilde{q}^r_{t,h})_{su}).$$

subject to

$$(\tilde{q}_{t,h} + \tilde{q}^r_{t,h} - \tilde{\rho}_{t,h}(1-\tilde{\rho}_{t,h})(1-\tilde{N}_h)\tilde{v}_{f_{t,h}})b_{t,h} = -k_{\rho_{t,h}}(\tilde{\rho}_{t,h} - 1/2) \quad (4.37)$$

$$(\sum_{k\in I_i} \tilde{\rho}_{k,i}(1-\tilde{\rho}_{k,i})\tilde{v}_{f_{k,i}}(1-\tilde{N}_i) - \sum_{j\in O_i} \tilde{q}_{i,j})\mu = -k_{N_i}(\tilde{N}_i). \quad \forall i \in T \quad (4.38)$$

$$\tilde{v}_{f_{t,h}} = \tilde{v}_{f_m} + (\tilde{v}_{f_{t,h}})_{su} - (\tilde{v}_{f_{t,h}})_{sl} \quad (4.66)$$

$$\tilde{q}_{t,h} = \tilde{q}_m + (\tilde{q}_{t,h})_{su} - (\tilde{q}_{t,h})_{sl} \quad (4.67)$$

$$\tilde{q}^r_{t,h} = \tilde{q}_m + (\tilde{q}^r_{t,h})_{su} - (\tilde{q}^r_{t,h})_{sl} \quad (4.68)$$

$$0 \le \tilde{v}_{f_{t,h}} \le \infty \quad (4.57)$$

$$0 \le \tilde{q}_{t,h} \le \infty \quad (4.58)$$

$$0 \le \tilde{q}^r_{t,h} \le \infty \quad (4.59)$$

$$0 \le (\tilde{v}_{f_{t,h}})_{sl} \le \infty \quad (4.60)$$

$$0 \le (\tilde{v}_{f_{t,h}})_{su} \le \infty \quad (4.61)$$

$$0 \le (\tilde{q}_{t,h})_{sl} \le \infty \quad (4.62)$$

$$0 \le (\tilde{q}_{t,h})_{su} \le \infty \quad (4.63)$$

$$0 \le (\tilde{q}^r_{t,h})_{sl} \le \infty \quad (4.64)$$

$$0 \le (\tilde{q}^r_{t,h})_{su} \le \infty \quad (4.65)$$

(4.70)

As g is a sum of all the surplus variables that were introduced in the new linear programming problem and since each surplus variable ≥ 0, $g = 0$ would imply that each surplus variable has reached a value of 0. Thus the solution to this linear programming problem with $g = 0$ would indicate that the original constraints of the linear programming problem (4.42) are feasible with gains $k^0_{\rho_{t,h}} > 0$ and $k^0_{N_i} > 0$ as each variable representing the violation of the original relaxed constraint is zero. However if the gains are feasible this procedure will not be invoked. If $g > 0$ then atleast one of the constraints (4.28), (4.27) or (4.29) has been violated. We observe that due to the specific way in which the cost function has been formulated, only one of the corresponding slack or the surplus variable can be > 0 for a a given relaxed bound

constraint . This is so because as far as the constraints of the new linear programming problem (4.70) are concerned, the slack and the surplus variables appear only in the constraints (4.66), (4.67) and (4.68) and they appear together as a difference. Hence we can arbitrarily increase the value of the surplus variables by increasing the value of the slack variables and still have all the constraints satisfied. However in doing so we would arbitrarily increase the cost g of our new linear programming problem (4.70) which is contrary to our objective of minimizing the cost. Hence only one of slack or surplus variable corresponding to a bound can be > 0.

Let the solution the new linear programming problem (4.70) be $(\tilde{v}_{f_{t,h}})^0$, $(\tilde{q}^0_{t,h})^0$ and $(\tilde{q}^r_{t,h})^0$. For all $(t,h) \in E$ let the scaling factors $\nu^{v_f}_{t,h}$, $\nu^{q}_{t,h}$ and $\nu^{q^r}_{t,h}$ be such that:

$$\tilde{v}_{f_m} = \frac{(\tilde{v}_{f_{t,h}})^0}{\nu^{v_f}_{t,h}} \tag{4.71}$$

$$\tilde{q}_m = \frac{(\tilde{q}_{t,h})^0}{\nu^{q}_{t,h}} \tag{4.72}$$

$$\tilde{q}_m = \frac{(\tilde{q}^r_{t,h})^0}{\nu^{q^r}_{t,h}} \tag{4.73}$$

Thus the least scaling factor ν on the gains $k^0_{\rho_{t,h}}$ and $k^0_{N_i}$ that will make all constraints of the linear programming problem (4.42) (equalities:(4.37) and (4.38),inequalities:(4.28), (4.27) and (4.29)) feasible with gains $\frac{k^0_{\rho_{t,h}}}{\nu}$ and $\frac{k^0_{N_i}}{\nu}$ is given by:

$$\nu = min(\nu^{v_f}_{t,h}, \nu^{q}_{t,h}, \nu^{q^r}_{t,h}). \tag{4.74}$$

4.6 Local Corridor Control

We observe that our formulation assumes that the pedestrian density in a link is uniform. However, this may not be true for long corridors. Herein, we develop a control that is local to the corridor that strives to achieve uniform density in the corridor such that our proposed global model of the network represents more accurately the realistic situation.

In the development of our network control model, we assumed the cumulative discharge $q^r_{i,j}$ from all the rooms connected to a corridor (i,j) was one of the control variables. However, in a corridor (i,j) we would have multiple rooms aligned along its length each inputting its own discharge in to the corridor. These individual room

discharging in to the corridor provide additional flexibility for controlling the flow and density in the corridor. One of the objectives of this individual room control could be to achieve the uniformity of the density in the corridor which was assumed in the development of the network control in the previous section. This objective can be achieved by dividing the corridor into sections such that each section has at least one room adjacent to it. Thus we have at least one room discharge coming into every corridor section. This local control algorithm gives us a way to split the cumulative corridor room discharges into room discharges corresponding to each section. We can find each individual room discharge which reduces the spatial variability of the density by using the local control algorithm described below. Here, we propose that the discharge in to every section be manipulated in such a way that all the section densities approach each other exponentially, while maintaining the cumulative room discharge for the entire corridor equal to the one dictated by the network control. We again use feedback linearization as our control methodology to do this.

In the proposed local corridor control scheme, the section densities are used as the system states. The input discharge from the tail node, the free flow velocity in the link (which is the same for every section in the corridor) and the cumulative room discharge into the corridor are the inputs given by the network control, and thus they that cannot be manipulated or changed by the local control. Also the number of pedestrians at the head node is a given parameter, dictated by the network control. This ensures that the network control is completely preserved by the local control at the each link level. The local control, thus, only fine tunes the cumulative room discharge control parameter at the section level with the primary objective of minimizing the spatial variations in the density.

Consider a corridor or link consisting of n_c sections. The average density for the corridor be denoted by ρ. For each section i is associated a section density ρ^i. Let L^i be the length of the section i and let L denote the total corridor length. Thus we have the following relation between the average density and the section densities:

$$\rho = \frac{\sum_{i=1}^{n} \rho^i L^i}{L}. \tag{4.75}$$

It is noted that the network control uses the average density in each link where as the local control uses the section densities. The section densities constitute the state vector. Associated with each section i is a room discharge into that section $q^{r(i)}$. This discharge

comes from the rooms that are adjacent to that section. The individual section room discharges constitute the local control vector. We make sure that for every section there is at least one adjacent room for implementation of this control. This situation is schematically shown in Figure 4.6 for 3 sections. The free flow velocity for the link is

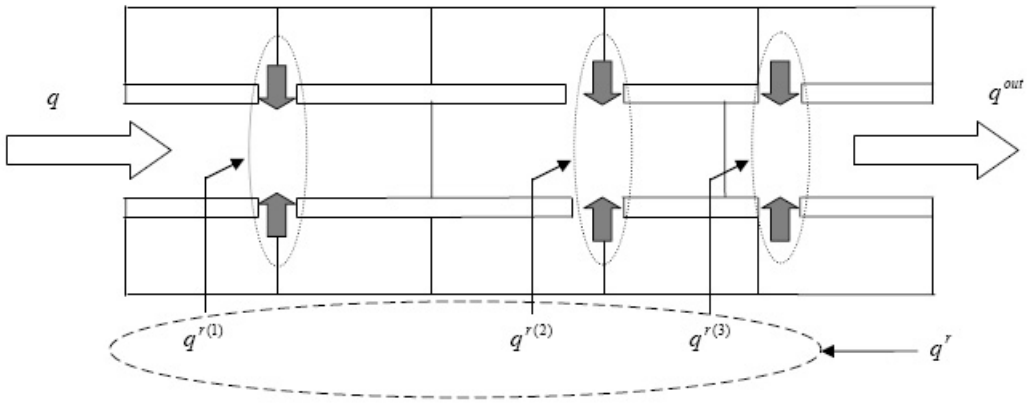

Figure 4.6: Local control in a corridor.

denoted by v_f, the nodal input discharge is denoted by q and the cumulative corridor room discharge is denoted by q^r. v_f, q and q^r are computed by the network control algorithm discussed earlier and are the given inputs to the local control algorithm. The nodal mass accumulated at the head node of the link is denoted by N. N is a state variable in the network control problem and is a given parameter for the local corridor control.

For each section we have a state equation that governs the evolution of the section density. Consider a section i. Applying conservation of mass to section i we get the following state equation:

$$\dot{\rho}^i = \frac{q^i_{in} - q^i_{out} + q^{r(i)}}{L^i}, \tag{4.76}$$

where q^i_{in} is the input discharge and q^i_{out} is the output discharge for the section. For the first section:

$$q^1_{in} = q, \tag{4.77}$$

where q is the nodal discharge into the link. For section $1 < i \leq n_c$ we have the input

discharge given by the greenshields formula as earlier:

$$q_{in}^{i} = \rho^{i-1}\left(1 - \frac{\rho^{i-1}}{\rho_m}\right) v_f. \tag{4.78}$$

The output discharge for sections $1 \leq i < n_c$ we have output discharge again given by the greenshields formula:

$$q_{out}^{i} = \rho^{i}\left(1 - \frac{\rho^{i}}{\rho_m}\right) v_f. \tag{4.79}$$

In order to maintain consistency with the network control algorithm for the last section n_c, the output discharge is assumed to be that used by the network control algorithm computed using the average link density ρ and the head node pedestrian mass N. If like the other sections the output discharge for the last section were to depend on the section density then the average link density used in the network control algorithm would end up being different from the average density computed using equation (4.75), thus creating an inconsistency in the network level and the link level control. Thus for the output discharge from the last section n_c we are assuming:

$$q_{out}^{n_c} = \rho\left(1 - \frac{\rho}{\rho_m}\right)\left(1 - \frac{N}{N_m}\right) v_f. \tag{4.80}$$

We have the following state equations corresponding to the n_c sections:

$$\dot{\rho}^1 = \frac{q - \rho^1\left(1 - \frac{\rho^1}{\rho_m}\right) v_f + q^{r(1)}}{L^1} \tag{4.81}$$

$$\dot{\rho}^2 = \frac{\rho^1\left(1 - \frac{\rho^1}{\rho_m}\right) v_f - \rho^2(1 - \frac{\rho^2}{\rho_m}\right) v_f + q^{r(2)}}{L^2} \tag{4.82}$$

$$\vdots$$

$$\dot{\rho}^k = \frac{\rho^{k-1}\left(1 - \frac{\rho^{k-1}}{\rho_m}\right) v_f - \rho^k\left(1 - \frac{\rho^k}{\rho_m}\right) v_f + q^{r(k)}}{L^k} \tag{4.83}$$

$$\vdots$$

$$\dot{\rho}^{n_c} = \frac{\rho^{n_c-1}\left(1 - \frac{\rho^{n_c-1}}{\rho_m}\right) v_f - \rho\left(1 - \frac{\rho}{\rho_m}\right)\left(1 - \frac{N}{N_m}\right) v_f + q^{r(n_c)}}{L^{n_c}}. \tag{4.84}$$

In order to preserve the network level control we need too ensure that the cumulative corridor room discharge computed by the network control equals the sum of the section room discharges. Thus we have the following equation representing this:

$$q^r = \sum_{i=1}^{n_c} q^{r(i)}. \tag{4.85}$$

Using the methodology similar to that in Sec. 4.2 we normalize the equations (4.81) to (4.84) and (4.85). Thus we get:

$$\dot{\tilde{\rho}}^1 = (q - \tilde{\rho}^1(1-\tilde{\rho}^1)\tilde{v}_f + \tilde{q}^{r(1)})b^1 \tag{4.86}$$

$$\dot{\tilde{\rho}}^2 = (\tilde{\rho}^1(1-\tilde{\rho}^1)\tilde{v}_f - \tilde{\rho}^2(1-\tilde{\rho}^2)\tilde{v}_f + \tilde{q}^{r(2)})b^2 \tag{4.87}$$

$$\vdots$$

$$\dot{\tilde{\rho}}^k = (\tilde{\rho}^{k-1}(1-\tilde{\rho}^{k-1})\tilde{v}_f - \tilde{\rho}^k(1-\tilde{\rho}^k)\tilde{v}_f + \tilde{q}^{r(k)})b^k \tag{4.88}$$

$$\vdots$$

$$\dot{\tilde{\rho}}^{n_c} = (\tilde{\rho}^{n_c-1}(1-\tilde{\rho}^{n_c-1})\tilde{v}_f - \tilde{\rho}(1-\tilde{\rho})(1-\tilde{N})\tilde{v}_f + \tilde{q}^{r(n_c)})b^{n_c}, \tag{4.89}$$

and

$$\tilde{q}^r = \sum_{i=1}^{n_c} \tilde{q}^{r(i)}. \tag{4.90}$$

As before in Sec. 4.2 we have:

$$\tilde{\rho}^i = \left(\frac{\rho^i}{\rho_m}\right) \tag{4.91}$$

$$\tilde{N} = \left(\frac{N}{N_m}\right) \tag{4.92}$$

$$\tilde{q} = \left(\frac{q}{\rho_m L_m}\right) \tag{4.93}$$

$$\tilde{q}^r = \left(\frac{q^r}{\rho_m L_m}\right) \tag{4.94}$$

$$\tilde{q}^r(i) = \left(\frac{q^r(i)}{\rho_m L_m}\right) \tag{4.95}$$

$$\tilde{v}_f = \left(\frac{v_f}{L_m}\right). \tag{4.96}$$

and

$$b^i = \frac{L_m}{L^i} = \left(\frac{L_m}{L}\right)\left(\frac{L}{L^i}\right). \tag{4.97}$$

Note that L_m here is the maximum length of a corridor in the entire network as in Sec. 4.2.

In order to attain our control objective of making the density in the corridor spatially uniform, we define the output quantities to be the difference between the adjacent section densities and use feedback linearization to achieve exponential convergence of

the output to zero. Thus we define the output vector $\mathbf{y}$ having components y_k for $1 \leq k < n_c$ given by:

$$y_k = \tilde{\rho}^{k+1} - \tilde{\rho}^k. \tag{4.98}$$

Taking the time derivative of y_k we get:

$$\dot{y}_k = \dot{\tilde{\rho}}^{k+1} - \dot{\tilde{\rho}}^k, \tag{4.99}$$

which results in:

$$\begin{aligned}
\dot{y}_1 &= (\tilde{\rho}^1(1-\tilde{\rho}^1)\tilde{v}_f - \tilde{\rho}^2(1-\tilde{\rho}^2)\tilde{v}_f + \tilde{q}^{r(2)})b^2 - (q - \tilde{\rho}^1(1-\tilde{\rho}^1)\tilde{v}_f + \tilde{q}^{r(1)})b^1 && (4.100)\\
\dot{y}_k &= (\tilde{\rho}^k(1-\tilde{\rho}^k)\tilde{v}_f - \tilde{\rho}^{k+1}(1-\tilde{\rho}^{k+1})\tilde{v}_f + \tilde{q}^{r(k+1)})b^{k+1} \\
&\quad -(\tilde{\rho}^{k-1}(1-\tilde{\rho}^{k-1})\tilde{v}_f - \tilde{\rho}^k(1-\tilde{\rho}^k)\tilde{v}_f + \tilde{q}^{r(k)})b^k && (4.101)\\
\dot{y}_{n_c-1} &= (\tilde{\rho}^{n_c-1}(1-\tilde{\rho}^{n_c-1})\tilde{v}_f - \tilde{\rho}(1-\tilde{\rho})(1-\tilde{N})\tilde{v}_f + \tilde{q}^{r(n_c)})b^{n_c} \\
&\quad -(\tilde{\rho}^{n_c-2}(1-\tilde{\rho}^{n_c-2})\tilde{v}_f - \tilde{\rho}^{n_c-1}(1-\tilde{\rho}^{n_c-1})\tilde{v}_f + \tilde{q}^{r(n_c-1)})b^{n_c-1}. && (4.102)
\end{aligned}$$

To attain exponential convergence, the time derivative y_k of must be of the following form:

$$\dot{y}_k = -K_{loc} y_k, \tag{4.103}$$

where K_{loc} is the gain at the local corridor level. Thus from equations (4.100), (4.101), (4.102) and (4.103) we get the following set of algebraic equations that need to be satisfied at every instant of time:

$$\begin{aligned}
(\tilde{\rho}^1(1-\tilde{\rho}^1)\tilde{v}_f - \tilde{\rho}^2(1-\tilde{\rho}^2)\tilde{v}_f + \tilde{q}^{r(2)})b^2 - (q - \tilde{\rho}^1(1-\tilde{\rho}^1)\tilde{v}_f + \tilde{q}^{r(1)})b^1 \\
= -K_{loc} y_1
\end{aligned} \tag{4.104}$$

$$\begin{aligned}
(\tilde{\rho}^k(1-\tilde{\rho}^k)\tilde{v}_f - \tilde{\rho}^{k+1}(1-\tilde{\rho}^{k+1})\tilde{v}_f + \tilde{q}^{r(k+1)}) - (\tilde{\rho}^{k-1}(1-\tilde{\rho}^{k-1})\tilde{v}_f \\
- \tilde{\rho}^k(1-\tilde{\rho}^k)\tilde{v}_f + \tilde{q}^{r(k)})b^k = -K_{loc} y_k
\end{aligned} \tag{4.105}$$

$$\begin{aligned}
(\tilde{\rho}^{n_c-1}(1-\tilde{\rho}^{n_c-1})\tilde{v}_f - \tilde{\rho}(1-\tilde{\rho})(1-\tilde{N})\tilde{v}_f + \tilde{q}^{r(n_c)})b^{n_c} - (\tilde{\rho}^{n_c-2}(1-\tilde{\rho}^{n_c-2})\tilde{v}_f \\
- \tilde{\rho}^{n_c-1}(1-\tilde{\rho}^{n_c-1})\tilde{v}_f + \tilde{q}^{r(n_c-1)})b^{n_c-1} = -K_{loc} y_{n_c}.
\end{aligned} \tag{4.106}$$

Note that in equations (4.104), (4.105) and (4.106) all the variables except $\tilde{q}^{r(i)}$ are known. Also note that the above equations are linear in $\tilde{q}^{r(i)}$. Thus we have n_c unknowns $\tilde{q}^{r(i)}$ and $n_c - 1$ equations. The additional equation needed to solve for the

unknowns $\tilde{q}^{r(i)}$ is provided by equation (4.90) which preserves the requirements of the network control $\tilde{q}^r$. Thus we have n_c linear equations given by (4.104), (4.105), (4.106) and (4.90) to solve for n_c unknowns $\tilde{q}^{r(i)}$. This system of linear equations can be easily solved to obtain the local control.

4.7 Example Problem

In this section we demonstrate the application of the control methodology presented in previous sections. The results for both controlled and uncontrolled flow scenarios are presented to numerically demonstrate the advantages of regulating the flow. For controlled scenarios the results are obtained according to the formulation developed in Sec. 4.4 and the results for the uncontrolled secenario are simulated according to approach outlined in Sec. 4.3. The proposed approach is applied to the shortest path evacuation problem of the Pentagon layout shown in Figure 4.2 which is described in more details in Chapter 2 . In particular, we apply the methodology to the red shortest path subgraph associated with one of the exists.

The complete flow control layout corresponding to the red shortest path subgraph is highlighted in Figure 4.7, with black arrows indicating the parts of the unresolved edges that point into the red shortest path subgraph. A local node numbering scheme shown in the Figure 4.7 is applied to the red subgraph, and it is different from that in Figure 4.2. In all we have 55 edges in this flow control layout. We assume that the longest corridor has the length of $L_m = 50m$ in this layout, and all other lengths have been scaled accordingly. We assign the initial pedestrian density $\rho^0_{t,h}$ to all the edges $(t,h) \in E$ randomly in $[0, 0.8\rho_m]$. Thus a wide range of initial densities are represented in the layout. No specific value for ρ_m is used as the results are presented in normalized form in terms of the normalized density $\tilde{\rho} = \frac{\rho}{\rho_m}$ and the normalized discharges $\tilde{q} = \frac{q}{\rho_m L_m}$ in performing the simulations and in plotting our results. The initial normalized average densities randomly assigned to different edges are shown in Table 4.1.

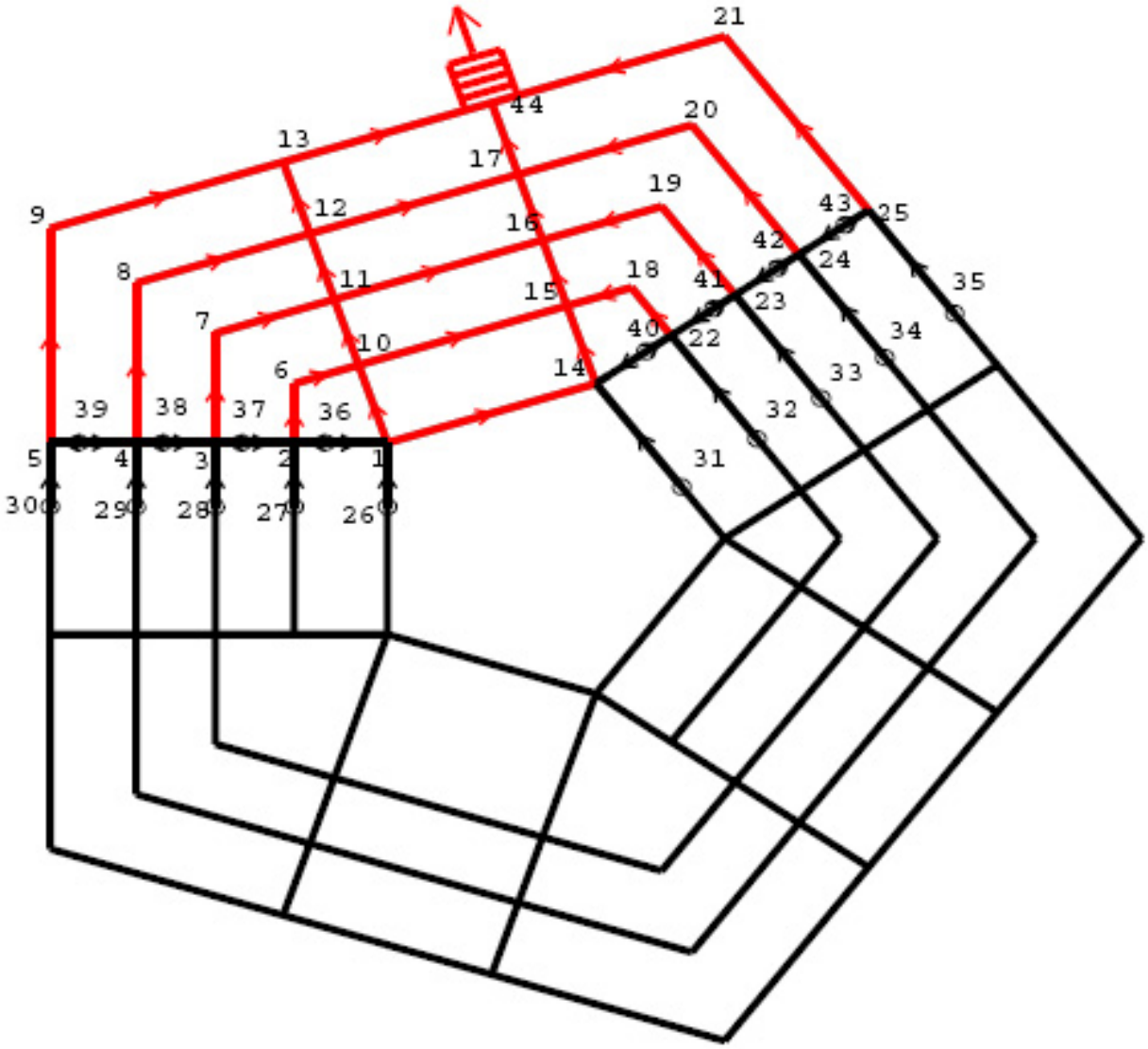

Figure 4.7: Red Tree of pentagon.

Likewise we assign the initial accumulated pedestrian mass N_i^0 randomly in $[0, 0.2N_m]$ at all nodes $i \in T$. Again we do not use any value for N_m as all results are presented in normalized form in terms of normalized pedestrian mass $\tilde{N} = \frac{N}{N_m}$ in the simulations. The normalized initial pedestrian masses on the nodes $i \in T$ in Figure 4.7 are presented in table 4.3. The maximum values of the nomalized edge densities and pedestrian nodal mass are related through the parameter μ in equation (4.24). For numerical simulation, herein a value $\mu = 50$ is assumed.This means that the maximum pedestrian mass that can accumulate along the longest edge is 50 times as much as the maximum pedestrian mass that can accumulate at a corner node. For the maximum value of the free flow velocity we assume a value of $v_{f_m} = 1.5m/s$. Using this we get the normalized maximum free flow velocity $\tilde{v}_{f_m} = \frac{v_{fm}}{L_m} = \frac{1.5}{50} = 0.03s^{-1}$. The gains used for the controlled scenario are $k_{\rho_{i,j}} = 4 \times 10^{-3}\ \forall (i,j) \in E$ and $k_{N_i} = 4 \times 10^{-3}\ \forall i \in T$. These numerical values have been used in the simulation for the uncontrolled and the controlled pedestrian flow scenarios.

In the following we present several sets of results. First, we present the results for the time evolution for the state variables of the normalized edge densities and normalized nodal masses to indicate how the congestion, if any, evolves in the entire system. This is followed by the results for the control variables of free flow velocities and the input and output discharges throughout the system. First these results are presented for all the edges and nodes shown collectively to see the trend in the entire system. In such presentations for 55 edges and 25 nodes, it becomes difficult to discern individual characteristics of different edges and nodes. Thus, to show more clearly these evolving response characteristics, here the results are also presented for the edges and nodes adjacent to the exit, called as the exit edges and nodes. The exit edges and nodes, perhaps, are also among the most critical locations of a layout. In Figure 4.8 we show the three exit edges in three different colors. This figure can be considered as a legend to subsequent figures in which the results for various state and control variables corresponding to the exit edges are presented. The results corresponding to a specific exit edge are plotted in the same color as the color of the edge shown in in Figure 4.8

Figure 4.9(a) and Figure 4.9(b) show the evolution of edge densities for all the 55 edges in the red flow control layout of Figure 4.7 for the controlled and the uncontrolled case. It can be seen in Figure 4.9(a) that in the uncontrolled scenario the 54 out of 55

Table 4.1: Assumed Average Normalized Initial Densities on the Edges

Edge No.	(t,h)	L(m)	$\tilde{\rho}_{t,h}$	Edge No.	(t,h)	L(m)	$\tilde{\rho}_{t,h}$
1	(1,10)	19.03	0.67	29	(25,21)	50	0.54
2	(1,14)	44.68	0.75	30	(26,1)	14.89	0.14
3	(2,6)	13.83	0.1	31	(27,2)	14.89	0.58
4	(3,7)	25.53	0.75	32	(28,3)	14.89	0.03
5	(4,8)	37.23	0.52	33	(29,4)	14.89	0.23
6	(5,9)	50	0.08	34	(30,5)	14.89	0.04
7	(6,10)	13.83	0.23	35	(31,14)	29.79	0.08
8	(7,11)	25.53	0.45	36	(32,22)	29.79	0.68
9	(8,12)	37.23	0.79	37	(33,23)	29.79	0.57
10	(9,13)	50	0.8	38	(34,24)	29.79	0.26
11	(10,11)	16.11	0.13	39	(35,25)	29.79	0.78
12	(10,15)	44.68	0.8	40	(36,1)	12.69	0.03
13	(11,12)	16.11	0.79	41	(36,2)	6.34	0.36
14	(11,16)	44.68	0.4	42	(37,2)	12.69	0.31
15	(12,13)	17.57	0.66	43	(37,3)	6.34	0.63
16	(12,17)	44.68	0.12	44	(38,3)	12.69	0.66
17	(13,44)	44.68	0.35	45	(38,4)	6.34	0.15
18	(14,15)	19.03	0.75	46	(39,4)	12.69	0.4
19	(15,16)	16.11	0.65	47	(39,5)	6.34	0.37
20	(16,17)	16.11	0.79	48	(40,14)	12.69	0.53
21	(17,44)	17.57	0.54	49	(40,22)	6.34	0.58
22	(18,15)	13.83	0.03	50	(41,22)	12.69	0.62
23	(19,16)	25.53	0.7	51	(41,23)	6.34	0.23
24	(20,17)	37.23	0.77	52	(42,23)	12.69	0.56
25	(21,44)	50	0.56	53	(42,24)	6.34	0.54
26	(22,18)	13.83	0.62	54	(43,24)	12.69	0.13
27	(23,19)	25.53	0.61	55	(43,25)	6.34	0.1
28	(24,20)	37.23	0.32				

.

Table 4.3: Assumed Normalized Initial Pedestrian mass at the nodes $i \in T$

Node No.	Assumed Normalized initial nodal mass
1	0.1039
2	0.2
3	0.0709
4	0.122
5	0.0466
6	0.1566
7	0.0532
8	0.1054
9	0.1457
10	0.1857
11	0.1999
12	0.114
13	0.0289
14	0.0311
15	0.0537
16	0.1752
17	0.053
18	0.1697
19	0.0507
20	0.1936
21	0.0729
22	0.041
23	0.0523
24	0.1284
25	0.0986

.

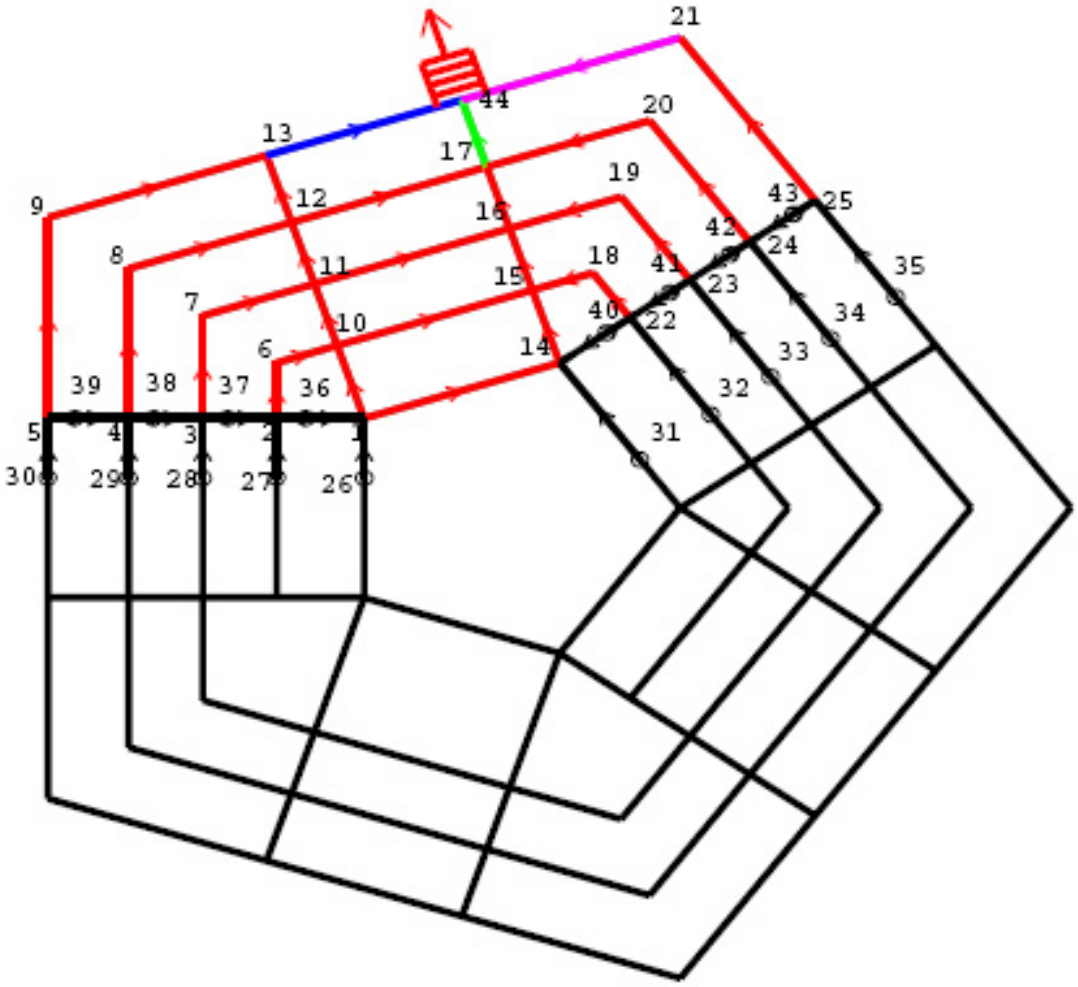

Figure 4.8: Red Subgraph on pentagon with highlighted exit edges in different colors

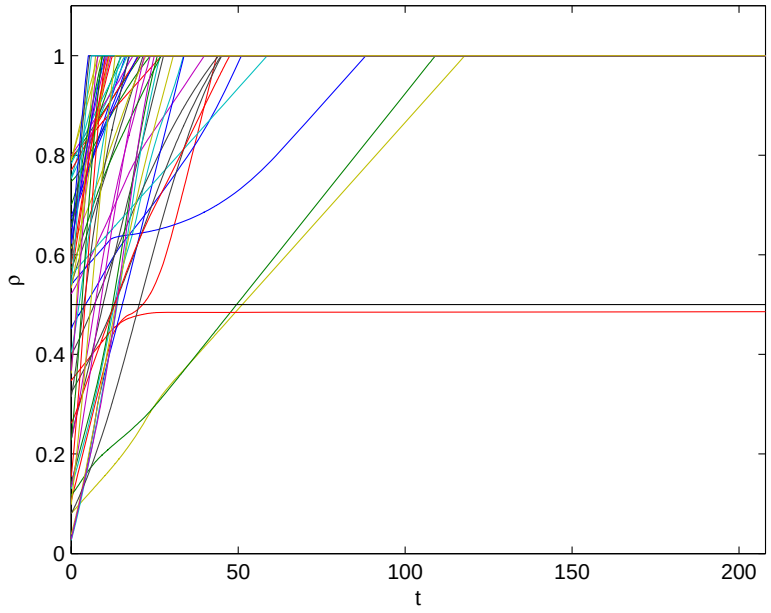

(a) Normalized average edge density $\tilde{\rho}_{t,h}$ in the uncontrolled case

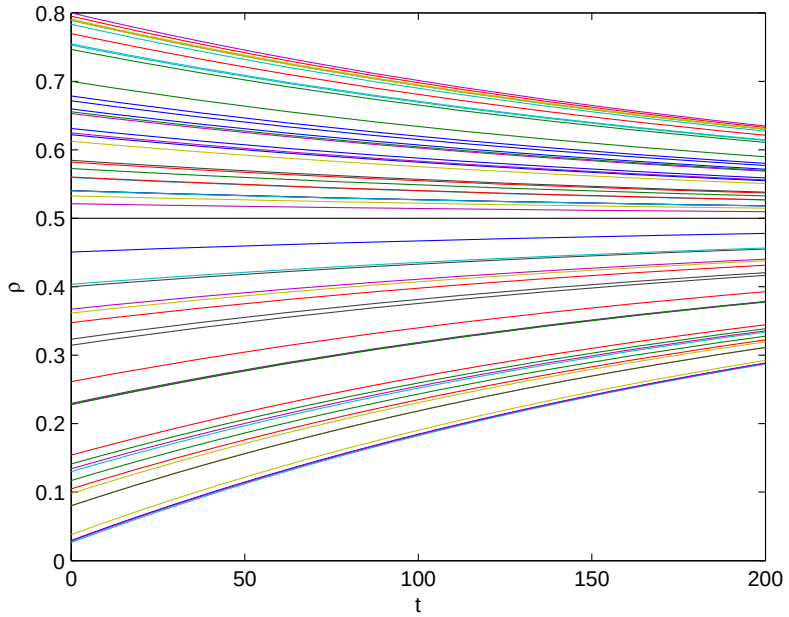

(b) Normalized average edge density $\tilde{\rho}_{t,h}$ in the controlled case

Figure 4.9: Normalized average edge densities $\tilde{\rho}_{t,h}$ for all edges $(t,h) \in E$ for the controlled and the uncontrolled case.

edge densities reach the jam density value in about 120 s from the start of evacuation. The precise timings for the edges reaching jam density are given in Table 4.5.

In Sec. 4.3 where the uncontrolled flow scenario is described we assume that the flow in a jammed link stops completely. Thus is 54 out of 55 edges the flow has completely stopped. Only one edge does not reach the jam density. This is the exit edge 17 with the tail node 13 and head node corresponding to the exit node 44. More will be said about the particular edge later in the discussion. In contrast to the uncontrolled case, the edge densities for the controlled case shown in Figure 4.9(b) are seen to track the critical normalized average density of 0.5 very well. As discussed earlier in this chapter that for a given free flow velocity the maximum discharge corresponds to this critical density. Thus a comparison of Figure 4.9(a) and Figure 4.9(b) shows the superiority of the controlled scenario in managing the pedestrian edge densities over the uncontrolled scenario.

In the above figure for all edges it is difficult to see the pattern of evolution for different edges. Thus in Figure 4.10(a) and Figure 4.10(b) we show separately the evolution of the average normalized densities for the exit edges in the uncontrolled and the controlled scenarios. From Table 4.5 it can be seen that the green exit edge (edge 21) reaches jam density in 21.53 s from the start of the evacuation and the magenta exit edge (edge 25) reaches jam density in 58.74 s from the start of evacuation for the uncontrolled case. Thus within 60 s of the start of evacuation 2 out of the 3 exit edges reach jam density and hence become unusable for evacuation by decreasing the exit capacity drastically at the very beginning of the evacuation process. The exit edges 17 is, however, noted to remain below the jam density through out the evacuation process. In fact quite surprisingly it is seen to be very close to the critical density of 0.5. However this occurrence is entirely coincidental. It may have to do with the way the initial densities were distributed in various edges which leads to congestion in the other two edges and not in this one. In fact, from the evolution of input discharge associated with this edge, we note that as this edge comes close to the critical density, the nodal input discharge at its tail node falls to zero as shown in Figure 4.16(a) later. This input discharge becomes zero as the paths preceding this node get jammed to block the flow of pedestrians. However, as the density in this edge at this point in time happens to be close to the critical density, the cumulative discharge from the rooms

Table 4.5: Times to jamming for various edges.

Edge No.	(t,h)	jam time (sec)	Edge No.	(t,h)	jam time (sec)
43	(37,3)	5.1222	24	(20,17)	20.3619
49	(40,22)	5.4945	9	(8,12)	20.8463
53	(42,24)	6.0468	21	(17,44)	21.5302
41	(36,2)	7.3459	54	(43,24)	21.8956
47	(39,5)	7.9508	27	(23,19)	22.3583
20	(16,17)	8.1305	33	(29,4)	23.679
13	(11,12)	8.9862	2	(1,14)	23.7537
51	(41,23)	9.2339	40	(36,1)	24.8738
44	(38,3)	9.4501	30	(26,1)	25.7999
50	(41,22)	9.9826	32	(28,3)	26.6688
45	(38,4)	10.1811	37	(33,23)	26.9793
18	(14,15)	10.6538	10	(9,13)	27.101
19	(15,16)	10.8978	7	(6,10)	27.6757
52	(42,23)	11.2092	34	(30,5)	30.6075
48	(40,14)	11.481	11	(10,11)	33.6538
26	(22,18)	11.8601	22	(18,15)	33.7937
31	(27,2)	12.3225	5	(4,8)	39.906
55	(43,25)	13.1684	3	(2,6)	43.6262
46	(39,4)	14.7577	14	(11,16)	44.1728
23	(19,16)	15.0866	28	(24,20)	44.9619
39	(35,25)	16.0894	35	(31,14)	45.1015
1	(1,10)	16.3148	38	(34,24)	47.5161
4	(3,7)	16.8185	8	(7,11)	50.991
42	(37,2)	17.2713	25	(21,44)	58.7414
15	(12,13)	17.4952	29	(25,21)	88.2799
12	(10,15)	18.5229	16	(12,17)	109.103
36	(32,22)	20.0085	6	(5,9)	117.9167

.

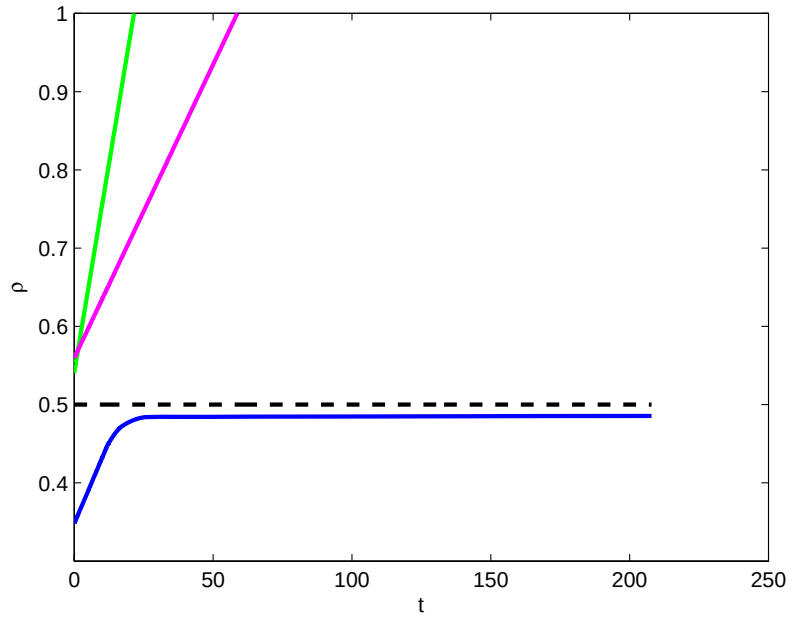

(a) Normalized average edge density $\tilde{\rho}_{t,n}$ in the uncontrolled case for exit edges

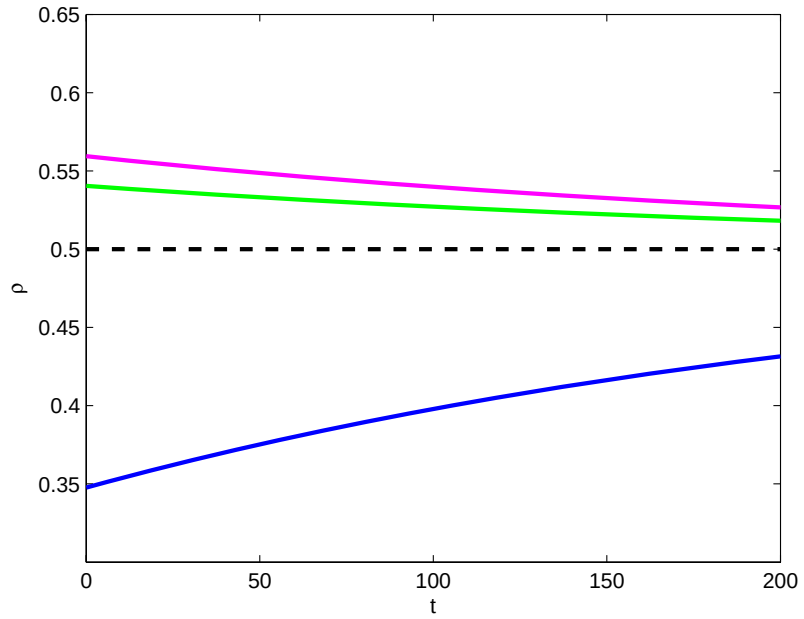

(b) Normalized average edge density $\tilde{\rho}_{t,n}$ in the controlled case for exit edges

Figure 4.10: Normalized average edge densities $\tilde{\rho}_{t,n}$ for all exit edges $(t, n) \in E$ for the controlled and the uncontrolled case. The lines in this plot have the same color as the exit edges in Figure 4.8

connected to this edge which equals the critical discharge maintains the edge density close to the critical density of 0.5. Thus the only pedestrians benefiting from this high level of exit edge discharge are the pedestrians in the rooms aligned along this edge.

In Figure 4.11(a) and Figure 4.11(b), respectively, we show the evolutions of the nodal pedestrian masses for all the nodes $i \in T$ for the uncontrolled and the controlled scenarios. From the uncontrolled scenario results in Figure 4.11(a), we observe two different types of evolution profiles for the nodal masses. In the first profile, the nodal pedestrian masses at certain nodes hit a value of zero at some point and stay there and in the other profile they reach a constant value sometime after the start of the simulation. The first type of profile is desirable as it prevents the pedestrian slowdown in the links near the node. On the other hand the second profile is undesirable as it implies a high level of congestion at the nodes which results in the reduction of the exit velocity from edges that have these nodes as their head node. The situation is, however, different for the controlled case for which the results are shown in Figure 4.11(b). In this case the nodal pedestrian masses at all nodes steadily decay to 0 exponentially, implying that nodes are not congested to hinder the pedestrian flow which results in fast and efficient flow at the nodes.

In the next set of Figure 4.12(a) and Figure 4.12(b), we show the evolution of the pedestrian mass only at the tail nodes of the exit links, that is at nodes 13, 17 and 21. Being next to the exit node, they are important as a jam at these nodes will prevent the entry of the pedestrians to the exit links and then to the exit. It can be seen from the results for the uncontrolled case in Figure 4.12(a) that for node 17 on the green exit edge and the node 25 on the magenta exit edge the normalized nodal mass reaches the jam value of 1 within 100 s of the start of the simulation. Thus the entrance to the exit edge connected to these two nodes gets blocked early on in the evacuation process. On the other hand in the controlled case the normalized mass at these nodes as shown in Figure 4.12(b) decays to 0 exponentially thus avoiding congestion to enter the exit links. The Pedestrian mass at node 13 in uncontrolled case approaches zero in a little more than 10 sec. However this is due to the fact that the edges having this node as the head node get jammed and not due to any efficient flow situation.

The from the Figure 4.9(b), Figure 4.9(a), Figure 4.10(b) and Figure 4.10(a) displaying the evolution of the edge density and the nodal pedestrian mass in the con-

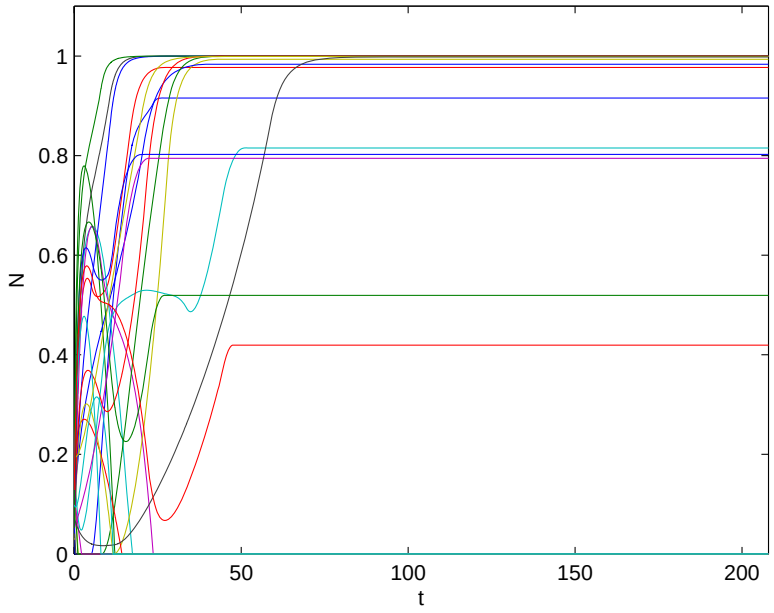

(a) Normalized nodal pedestrian mass $\tilde{N}_i$ in the uncontrolled case

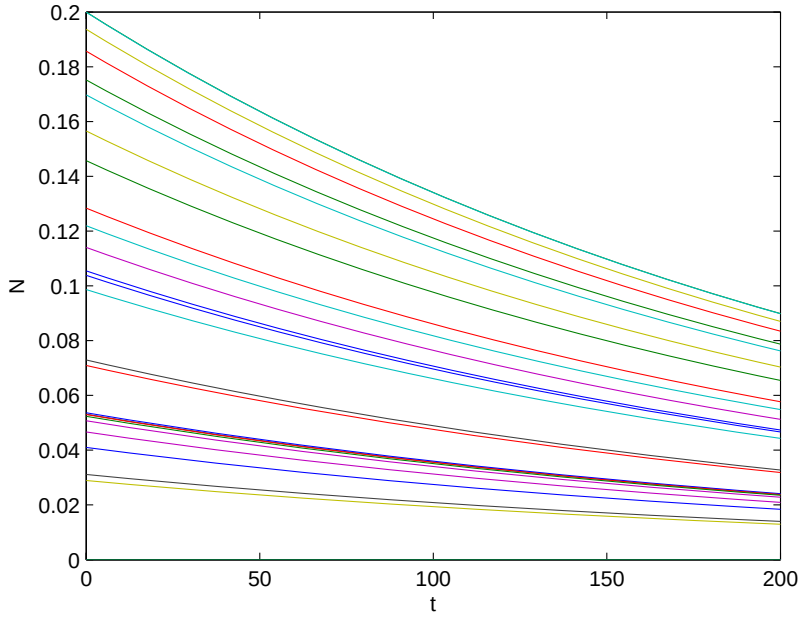

(b) Normalized nodal pedestrian mass $\tilde{N}_i$ in the controlled case

Figure 4.11: Normalized nodal pedestrian mass $\tilde{N}_i$ for all nodes $i \in T$ for the controlled and the uncontrolled case.

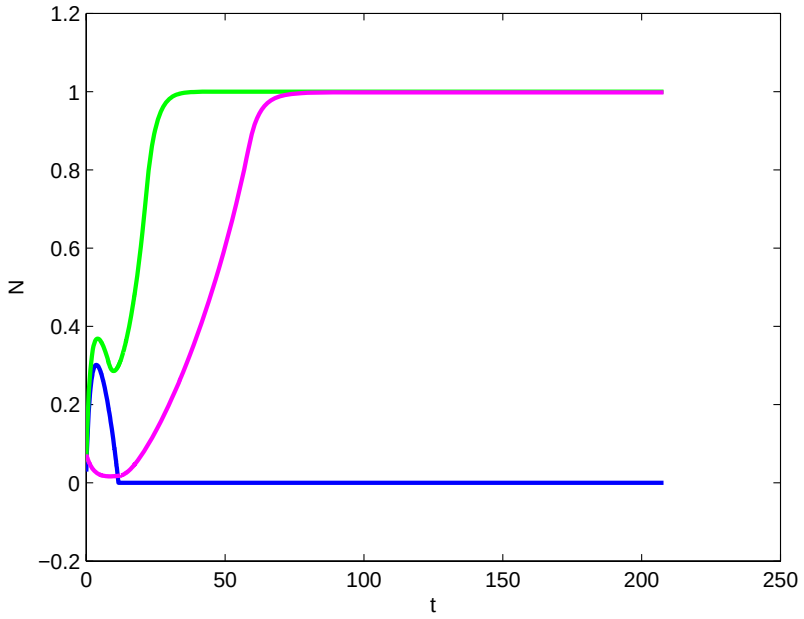

(a) Normalized tail node pedestrian mass $\tilde{N}_i$ in the uncontrolled case for the exit edges

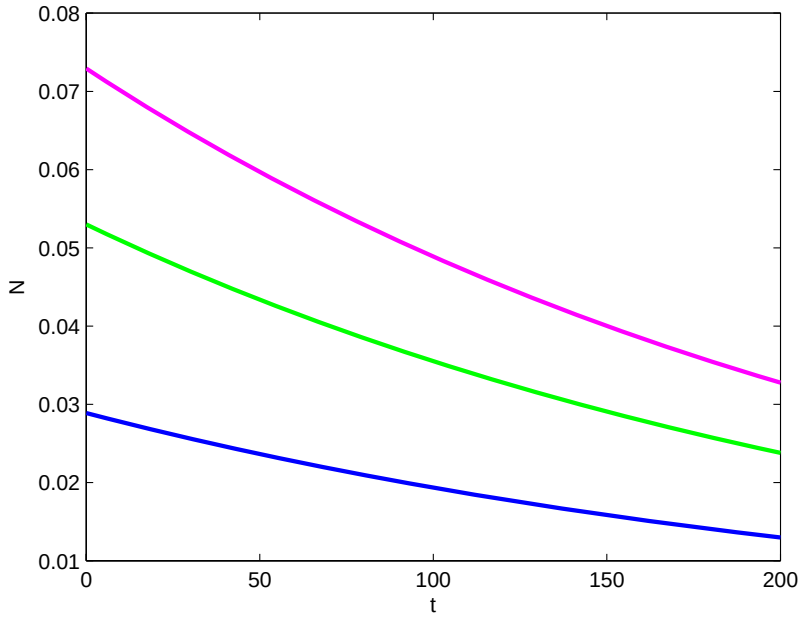

(b) Normalized tail node pedestrian mass $\tilde{N}_i$ in the controlled case for the exit edges

Figure 4.12: Normalized tail node pedestrian mass $\tilde{N}_i$ for all exit edges $(i, n) \in E$ for the controlled and the uncontrolled case. The lines in this plot have the same color as the exit edges in Figure 4.8

trolled and the uncontrolled scenario we clearly see that in terms of congestion in both the edges and the nodes, the pedestrian traffic evolves much more efficiently in the controlled scenario as compared to the uncontrolled scenario. The flow gets blocked at several locations either in the corridors or at the nodes in uncontrolled case where the movement is primarily driven by haste and panic.

The previous set of figures showed the evolution of the state variables of the pedestrian densities and nodal masses. Next set of results show the evolution of the control variables of the free flow velocity, cumulative edge room disharges on various edges, and the input discharge into the edges and output discharges from the nodes. In the uncontrolled case, since no control is enforced, these variable are primarily determined by the reaction of the pedestrians in a panic situation as discussed in Sec. 4.3. Thus the control values shown for the uncontrolled case start off at the maximum values with which the pedestrian can move. The values shown for the controlled case, on the other hand, are obtained by the control algorithm developed in Sec. 4.4.

Figure 4.13(a) and Figure 4.13(b) show the evolution of the free flow velocity in the unconrolled and the controlled scenario for all the edges. From the Figure 4.13(a) for the uncontrolled scenario, we observe that the free flow velocity starts at the maximum allowable value indicated by the black dashed line and then drops to 0 suddenly as the edge gets jammed thus indicating a stoppage of flow in that link. Whereas the results for the controlled case shown in Figure 4.13(b), we note that the free flow velocities not only remain within the implementable bounds indicated by the dashed lines but they also stay consistently non-zero indicating that the flow never stops in any of the links. We also note that the time variation of the free flow velocity in all links is very gradual. This gradual change is also easy to implement in a real situation. Since in the previous figure it was difficult to see the evolution in individual edges, in Figure 4.14(a) and Figure 4.14(b) we show the evolution of the free flow velocities only for the exit edges. It can be seen in Figure 4.14(a) that while for the blue exit edge (edge 17) the free flow velocity remains at the maximum value for the green (edge 21) and magenta (edge 25) edges the free flow velocities start at their maximum values but then suddenly drop to 0 indicating the jamming and stoppage of flow in the links. In the controlled case, Figure 4.14(b), on the other hand we observe that the free flow velocities in these links consistently remains at its maximum value. It was proven in

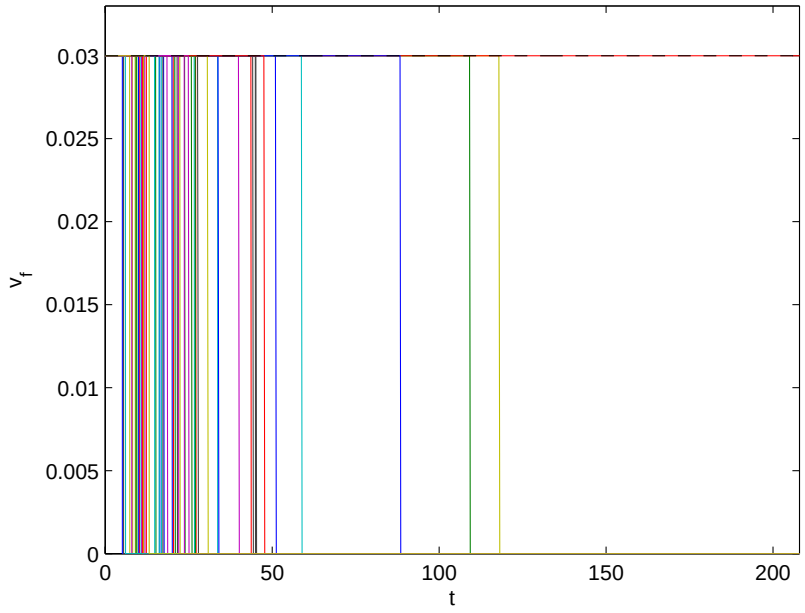

(a) Normalized free flow velocity $\tilde{v}_{f_{t,h}}$ in the uncontrolled case

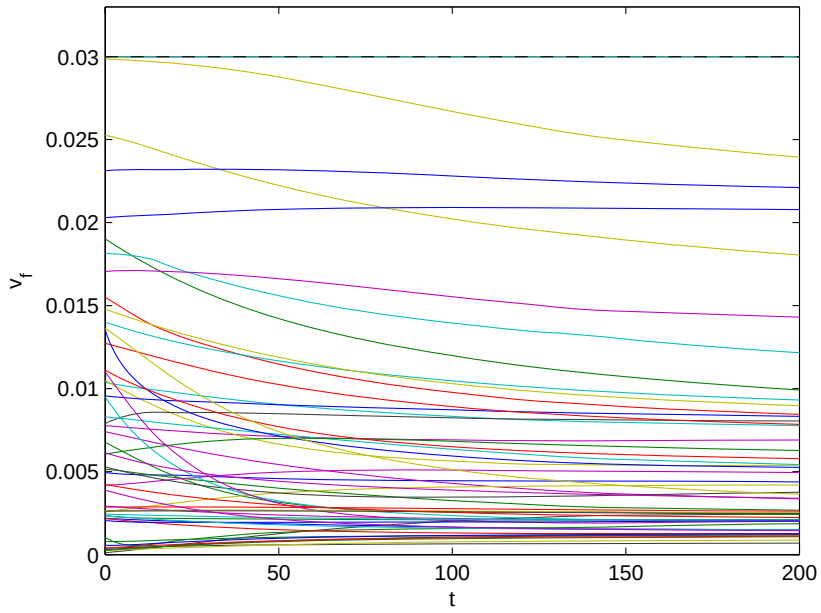

(b) Normalized free flow velocity $\tilde{v}_{f_{t,h}}$ in the controlled case

Figure 4.13: Normalized free flow velocity $\tilde{v}_{f_{t,h}}$ for all edges $(t,h) \in E$ for the controlled and the uncontrolled case.

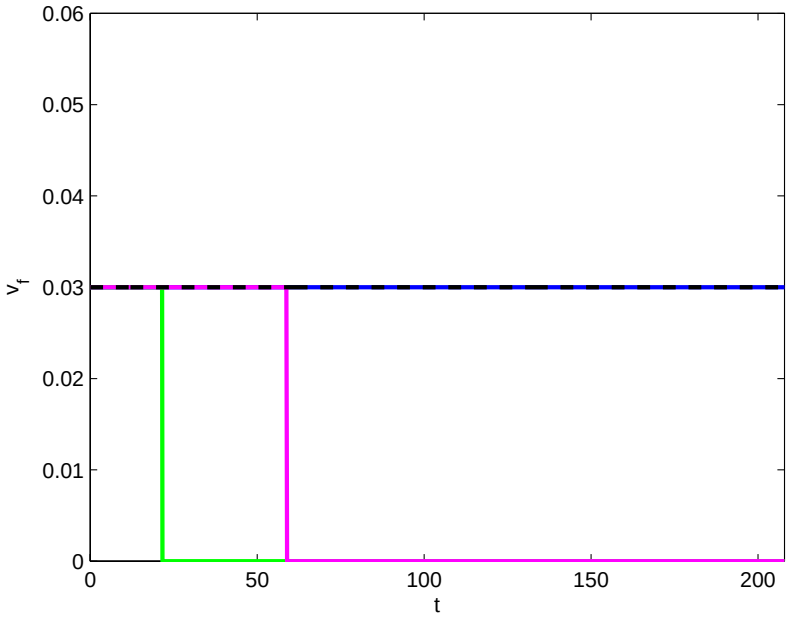

(a) Normalized free flow velocity $\tilde{v}_{f_{t,n}}$ in the uncontrolled case for the exit edges

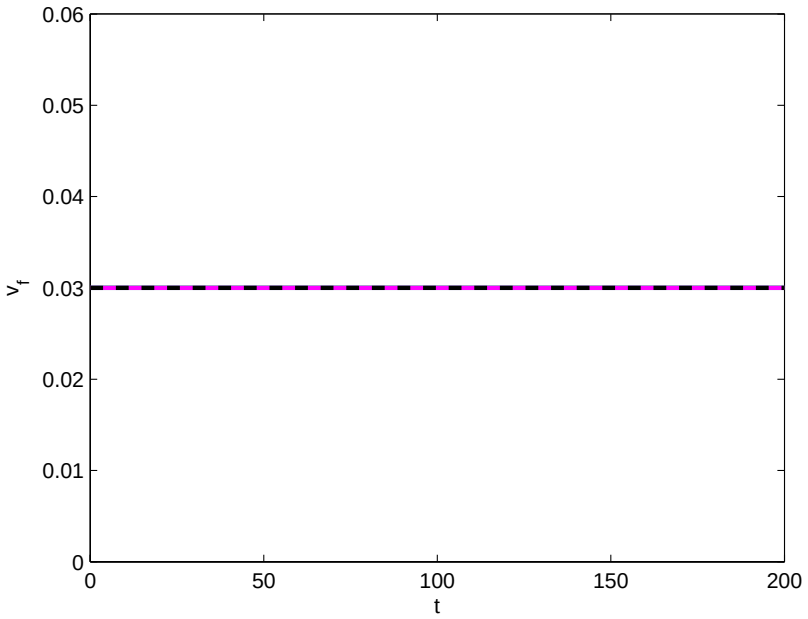

(b) Normalized free flow velocity $\tilde{v}_{f_{t,n}}$ in the controlled case for the exit edges

Figure 4.14: Normalized free flow velocity $\tilde{v}_{f_{t,n}}$ for all exit edges $(t, n) \in E$ for the controlled and the uncontrolled case. The lines in this plot have the same color as the exit edges in Figure 4.8

Sec. 4.4 that this would happen under certain conditions. These conditions are met in our simulation.

In Figure 4.15(a) and Figure 4.15(b) are shown the normalized nodal input discharges for all the edges. It can be seen in Figure 4.15(a) for the uncontrolled case that the normalized nodal input discharge falls off to 0 in many links once the edges get jammed. The zero value of this nodal input discharge implies that no pedestrians enter the links from the previous links of the layout. Thus, it essentially prunes the edges in which this occurs from the rest of the layout resulting in the under utilization of the available routes for the evacuation process. In contrast to this case, the normalized nodal input discharge in controlled scenario shown in Figure 4.15(b) not only satisfies the control bounds it also consistently remains at a non-zero value for all edges $(t, h) \in E$ with $t \in T$ indicating complete usage of the layout for regulating the pedestrian flow.

In Figure 4.16(a) and Figure 4.16(b) we show the evolution of the nodal input discharge only for the exit edges. From the results for the uncontrolled case shown in Figure 4.16(a), we observe that the nodal input discharge in all the three exit edges falls off to zero indicating that no pedestrians outside these links can get into these links. This creates a critical situation as it indicates a complete blockage of pedestrian flow from the rest of the layout. This does not happen in controlled scenario, Figure 4.16(b), where the nodal input discharge to all three exit edges not only satisfies the bounds as per the control design but also consistently remains at a non-zero value indicating a availability of the exit links at all times. It can also be seen that the time variation of the discharge is not appreciable indicating ease of implementation.

In the next Figure 4.17(a) and Figure 4.17(b), respectively, we show the results for the cumulative room discharges for all the links in the layout for the uncontrolled and the controlled situations. The results for the uncontrolled case, Figure 4.17(a), show that the cumulative room discharges start off at a maximum value and then suddenly drop off to zero as the edges get jammed. This results in a virtual entrapment of the pedestrians in the rooms adjoining the corridor. In contrast with this, the room discharges are within bounds and are positive at all times in the controlled scenario as indicated in Figure 4.17(b).

In Figure 4.18(a) and Figure 4.18(b) we show the time evolutions of the cumulative

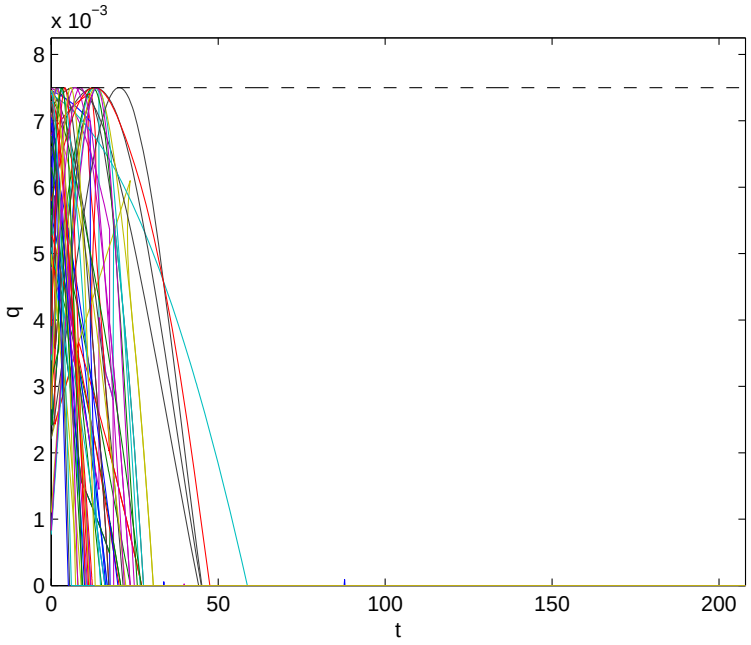

(a) Normalized nodal input discharge $\tilde{q}_{t,h}$ in the uncontrolled case

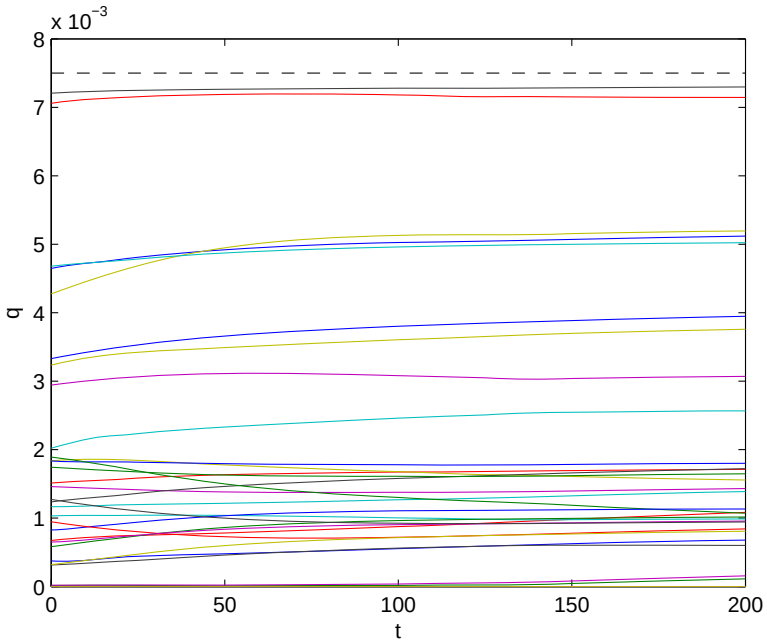

(b) Normalized nodal input discharge $\tilde{q}_{t,h}$ in the controlled case

Figure 4.15: Normalized nodal input discharge $\tilde{q}_{t,h}$ for all edges $(t,h) \in E$ for the controlled and the uncontrolled case.

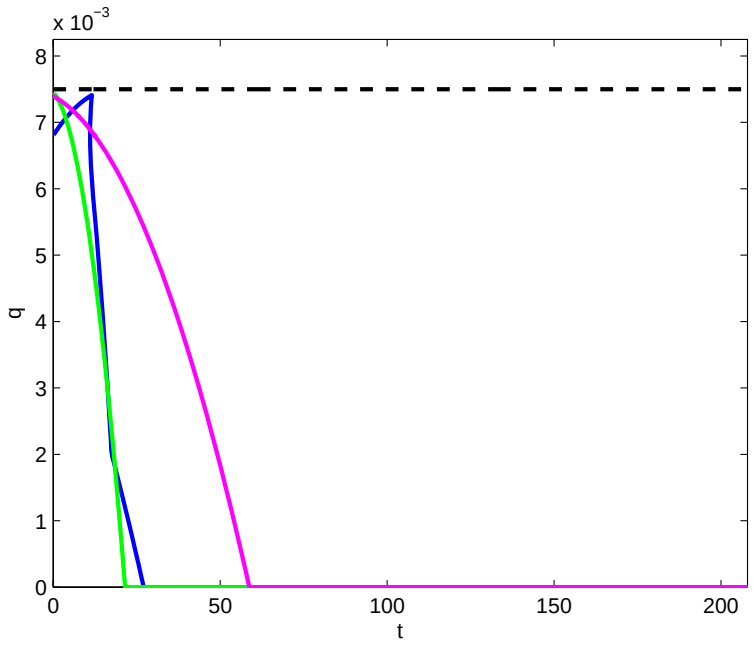

(a) Normalized nodal input discharge $\tilde{q}_{t,n}$ in the uncontrolled case for exit edges

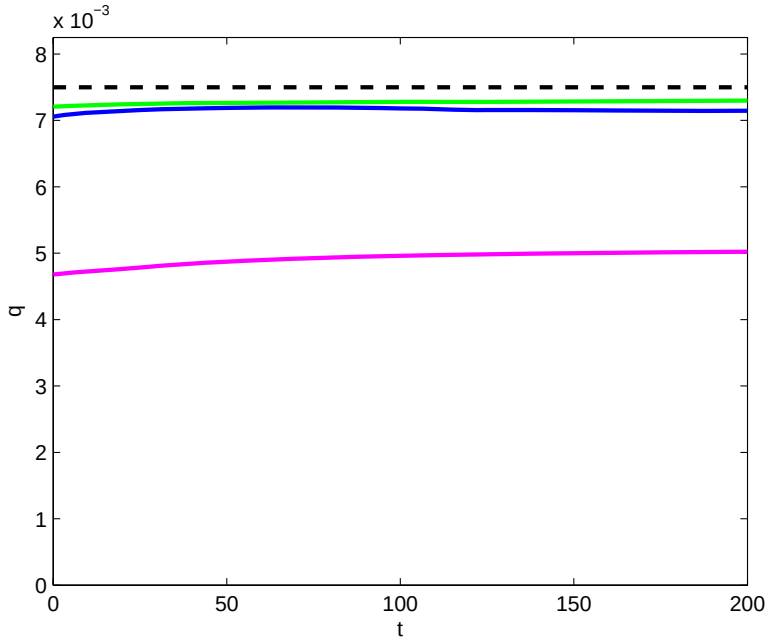

(b) Normalized nodal input discharge $\tilde{q}_{t,n}$ in the controlled case for the exit edges

Figure 4.16: Normalized nodal input discharge $\tilde{q}_{t,n}$ for all exit edges $(t, n) \in E$ for the controlled and the uncontrolled case.The lines in this plot have the same color as the exit edges in Figure 4.8

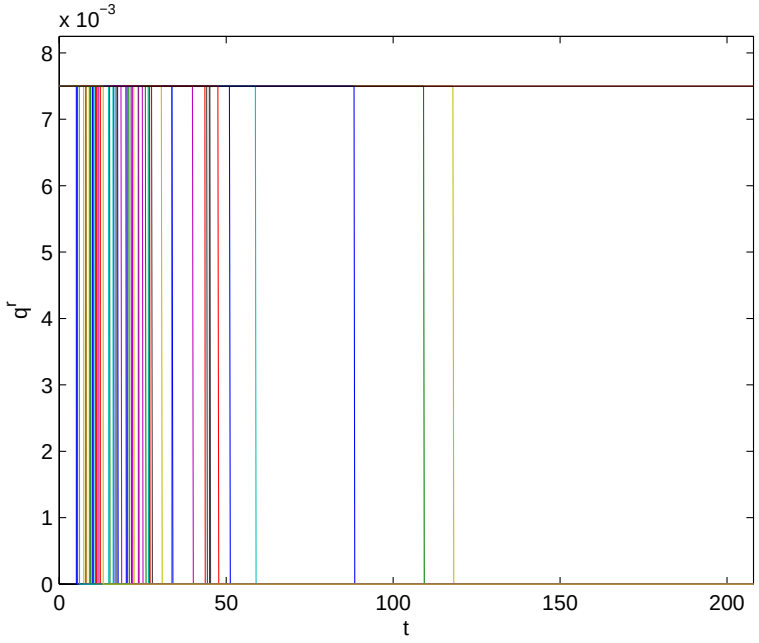

(a) Normalized cumulative room discharge $\tilde{q}^r_{t,h}$ in the uncontrolled case

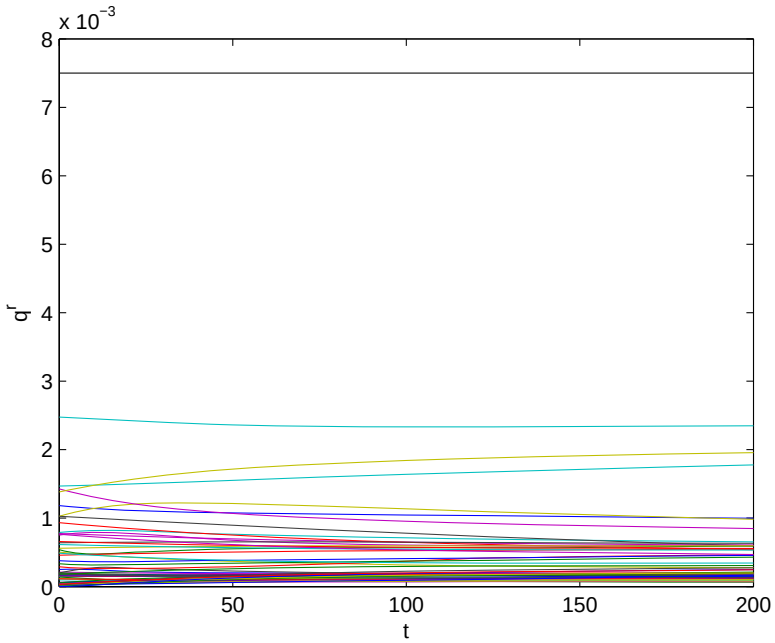

(b) Normalized cumulative room discharge $\tilde{q}^r_{t,h}$ in the controlled case

Figure 4.17: Normalized cumulative room discharge $\tilde{q}^r_{t,h}$ for all edges $(t,h) \in E$ for the controlled and the uncontrolled case.

room discharges on the exit links. It can be seen in Figure 4.18(a) the cumulative room discharges in the green exit edge (edge 21) and the magenta exit edge (edge 25) start off at a maximum value and then suddenly drop down to 0 indicating jamming in the edge. This indicates a virtual entrapment of the pedestrians in the rooms adjacent to the exit links. However for the blue exit edge the discharge remains at its maximum value all through. This happens because the discharge from the blue exit link matches this cumulative room discharge which is at its maximum value. However this is a completely unsatisfactory situation as the nodal input discharge into this link as indicated in Figure 4.16(a) settles to zero and the only pedestrians evacuating from this links after that point are the ones present in the rooms adjacent to this link. In contrast to this the results for the controlled scenario in Figure 4.18(b) show that the cumulative edge room discharges are consistently evolving while satisfying the control bounds as per the design requirement.

Next in Figure 4.19(a) and Figure 4.19(b) we show the evolution of the output discharges from the exit links in the uncontrolled and the controlled scenario. From the results in Figure 4.19(a) for the uncontrolled case we note that the output discharge in the green exit edge (edge 21) and magenta exit edge (edge 25) hit a value of zero and stay there during the simulation. This indicates that no pedestrians exit using these exit edges. The blue exit edge (edge 17) has an output discharge close to the critical discharge only coming from the rooms feeding into this edge as discussed earlier. The results for the controlled case in Figure 4.19(b), on the other hand, show that the output discharge approaches the critical discharge in all the exit edges. This is important as it emphasizes an important design aspect of the proposed control that the exit edge output discharge asymptotically approaches the critical discharge so long as the free flow velocity at the exit edge remains at its maximum value. This observation was also analytically proved in Sec. 4.4 .

In Figure 4.20(a) and Figure 4.20(b) we compare the total room discharges and the total exit discharges in the uncontrolled and the controlled scenarios. The blue lines in the Figure 4.20(a) and Figure 4.20(b) correspond to the $3q_m$ level indicating the maximum total exit discharge possible from the layout. From the results for the uncontrolled case shown in Figure 4.20(a), we note that the total room discharge indicated by black solid line starts off at a very high value as would be expected of

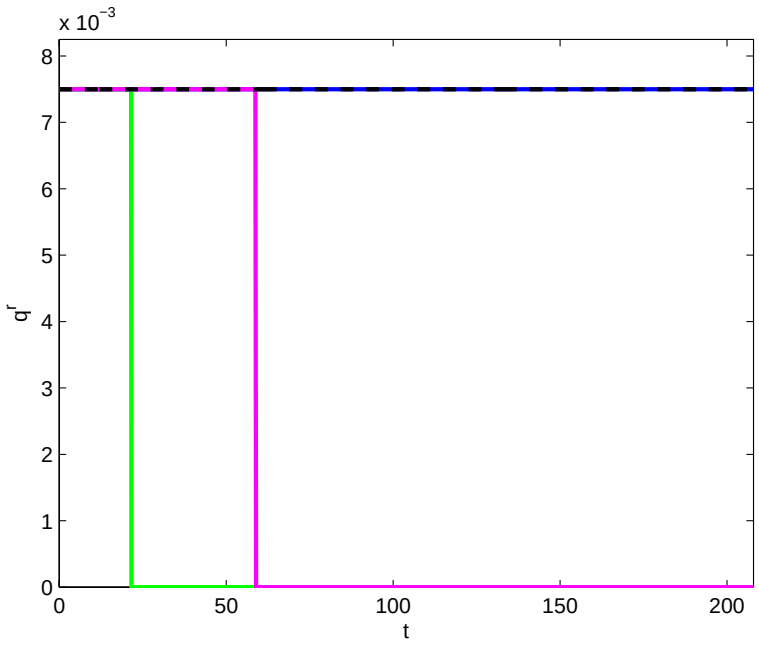

(a) Normalized cumulative room discharge $\tilde{q}^r_{t,n}$ in the uncontrolled case for the exit edges

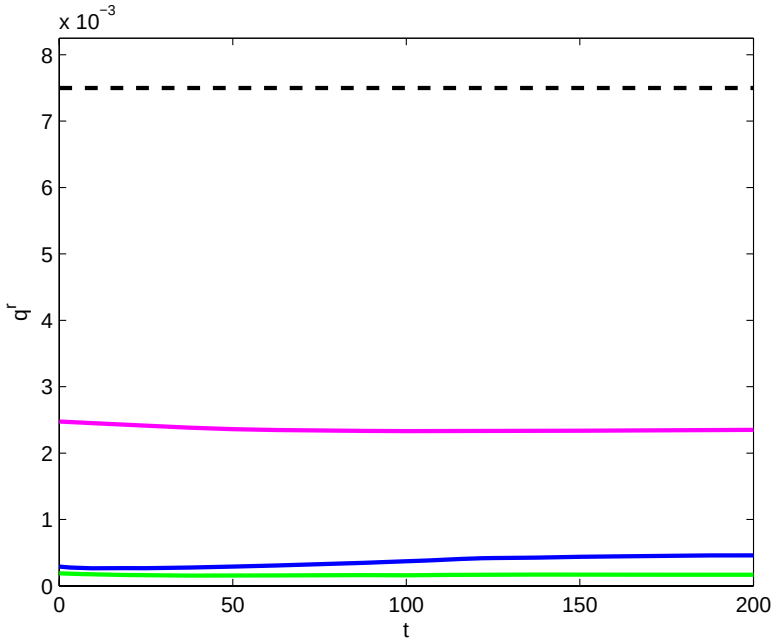

(b) Normalized cumulative room discharge $\tilde{q}^r_{t,n}$ in the controlled case for the exit edges

Figure 4.18: Normalized cumulative room discharge $\tilde{q}^r_{t,n}$ for all exit edges $(t, n) \in E$ for the controlled and the uncontrolled case.The lines in this plot have the same color as the exit edges in Figure 4.8

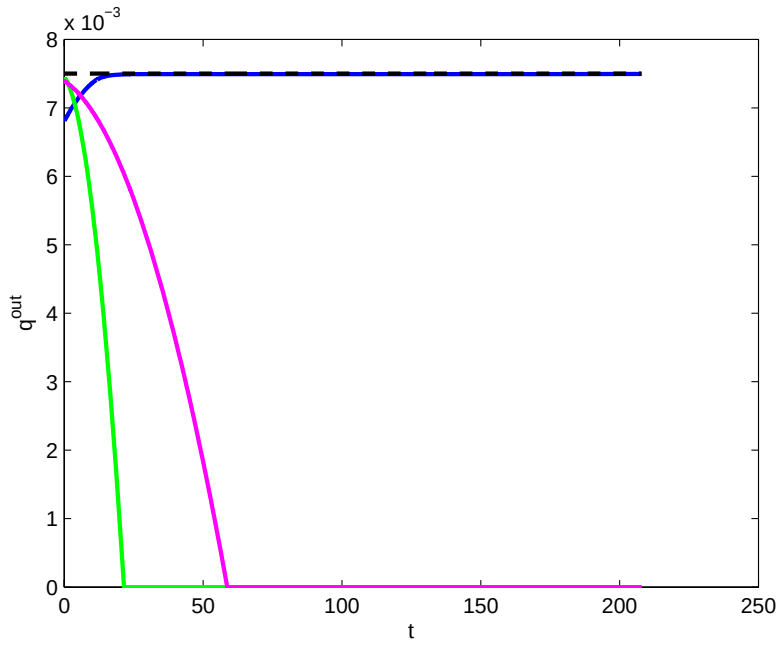

(a) Normalized output discharge $\tilde{q}_{t,n}^{out}$ in the uncontrolled case for the exit edges

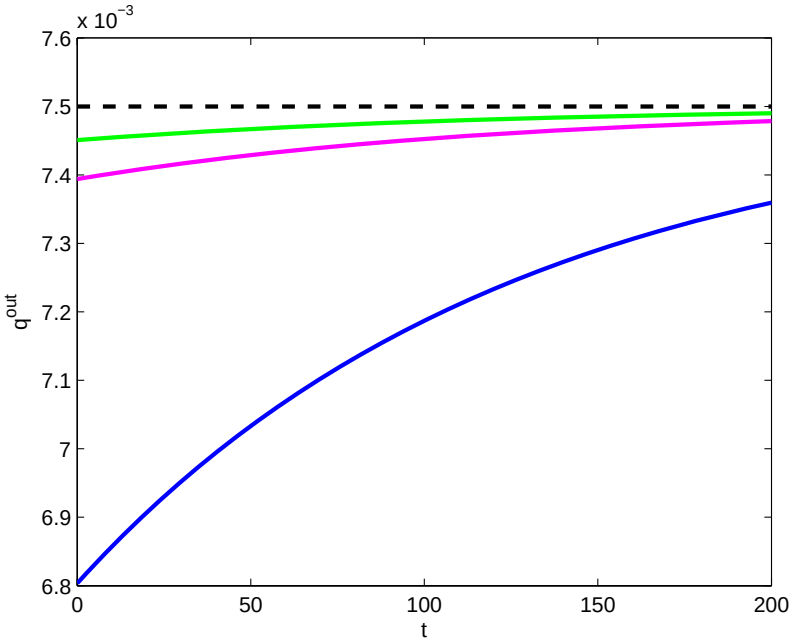

(b) Normalized output discharge $\tilde{q}_{t,n}^{out}$ in the controlled case for the exit edges

Figure 4.19: Normalized output discharge $\tilde{q}_{t,n}^{out}$ for all exit edges $(t,n) \in E$ for the controlled and the uncontrolled case.The lines in this plot have the same color as the exit edges in Figure 4.8

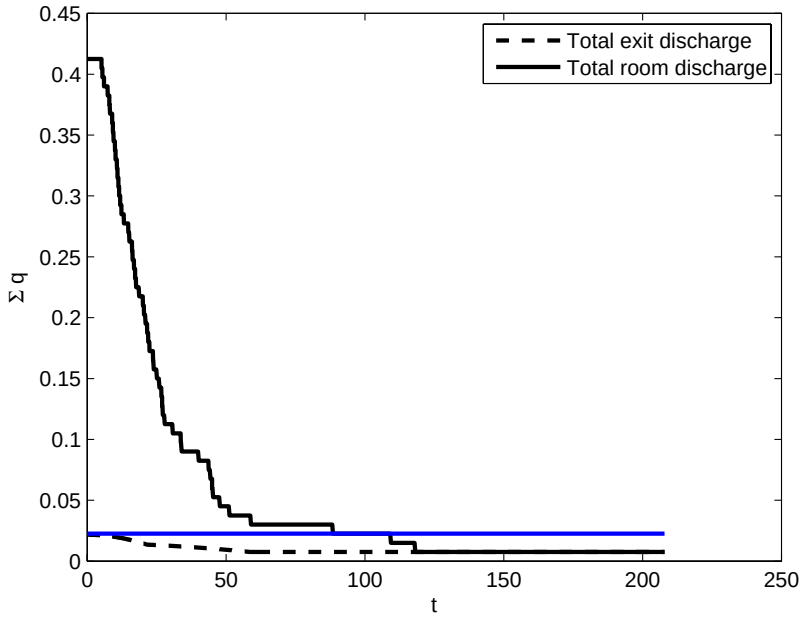

(a) Normalized Total exit discharge and total room discharge in the corridors for the pentagon red subgraph for the un-controlled scenario.

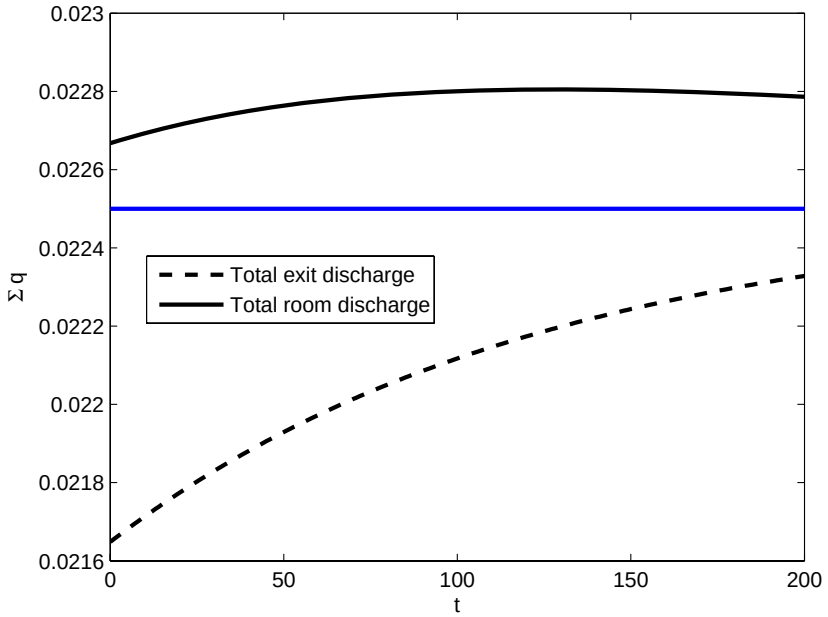

(b) Normalized Total exit discharge and total room discharge in the corridors for the pentagon red subgraph for the controlled scenario.

Figure 4.20: Normalized Total exit discharge and total room discharge in the corridors for the pentagon red subgraph for the un-controlled scenario.

a panic driven rush to the exits. But then the edges get jammed, preventing the room discharges causing a virtual entrapment of the pedestrians. The only edge where this does not happen is the exit edge 17, which is the only edge that does not get jammed. For this edge the critical value of edge density resulting in the critical value for the output discharge is sustained by the cumulative edge room discharge which keeps operating at its critical value without dropping to 0. As was discussed earlier this occurrence is purely coincidental and of little consequence to the cause of evacuating most pedestrians. Also it can be seen that the total exit discharge starts dropping down as the exit edges keep getting progressively jammed and then finally settling down to the value corresponding to the critical discharge value for an edge. Thus the total exit dishcarge and the total room discharge settle down to a value of critical output discharge for a single edge. As stated earlier this is due to the critical output discharge in edge 17 being sustained by the cumulative edge room discharge in this edge operating at a critical value and all other exit and room discharge falling to a value of 0. The situation is however, quite different in the controlled case as seen from the results in Figure 4.20(b) where both the total room discharge and the total exit discharge evolve in a smooth manner without any drastic variations. Eventually both the total discharges exponentially approach the $3q_m$ level indicated by the blue line. This aspect of both the total exit discharge and the total room discharge approaching the level of maximum possible exit discharge in the controlled scenario was analytically shown in Sec. 4.4.

As a simulation experiment we examined the scenario by considering rooms as both sources and absorbers of pedestrians in the evacuation flow. In that case we allow as much discharge into the rooms from the evacuating flow as we allow out of it. Thus the bound constraints in our problem become more accommodative. Due to this we can use higher gains to accomplish a controlled evacuation using the control algorithm above. We found that we can set the gains as high as $k_{\rho_{t,h}} = k_{N_i} = 2 \times 10^{-2}$ which is 5 times more than when we have a zero lower bound in the case above. The resulting speed up in approaching the tracking values of the state variables of ρ and N is evident in the Figure 4.21(a) and Figure 4.21(b). In that case the control corresponding to the cumulative edge room discharges are plotted in Figure 4.22. It is evident here that for quite a few corridors the cumulative edge room discharge is always negative throughout

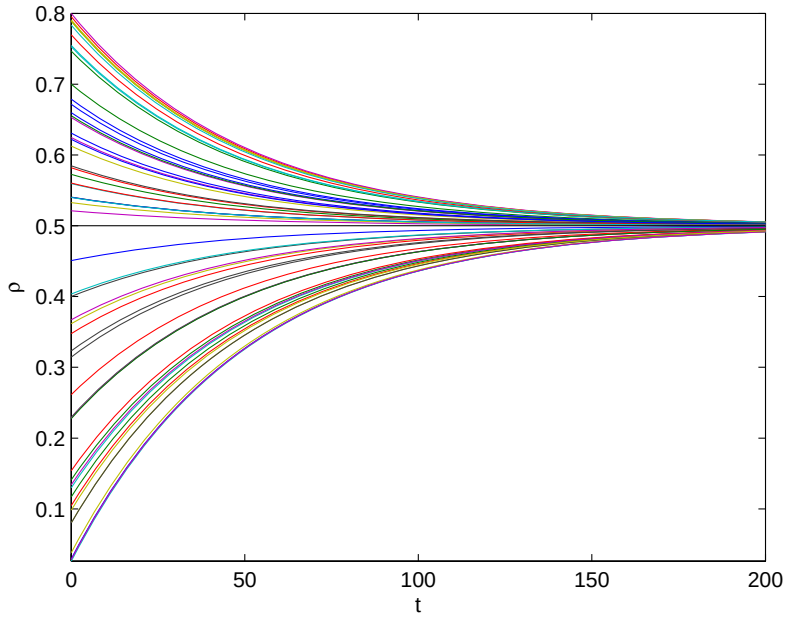

(a) Normalized average edge density $\tilde{\rho}_{t,h}$ in the high gain controlled case.

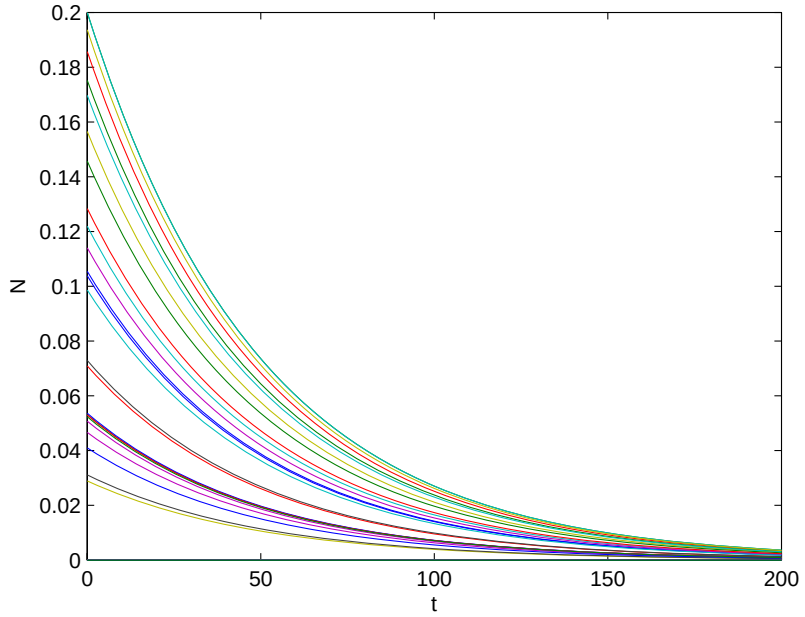

(b) Normalized nodal pedestrian mass $\tilde{N}_i$ in the high gain controlled case.

Figure 4.21: Normalized average edge densities $\tilde{\rho}_{t,h}$ for all edges $(t,h) \in E$ and normalized nodal pedestrian mass $\tilde{N}_i$ for all nodes $i \in T$ for the high gain controlled case with negative lower bound permitted on edge room discharges.

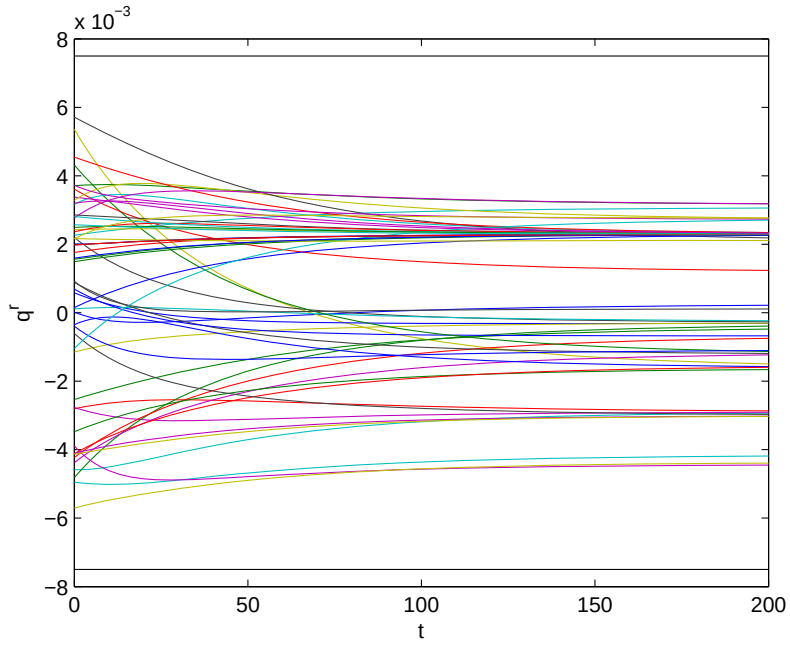

Figure 4.22: Normalized cumulative edge room discharge $\tilde{q}^r_{t,h}$ for all edges $(t,h) \in E$ for the high gain controlled case with negative lower bound permitted on edge room discharges.

the simulation. Hence we do not adopt this strategy of allowing rooms to be absorbers as well as sources as it will result in the entrapment of pedestrians in some rooms even though the approach towards the tracked states is much faster.

Now we show a comparison of the normalized pedestrian mass getting out of the flow control layout for the 3 cases of the controlled flow with low gain where rooms only act as sources, the uncontrolled flow and the controlled flow with high gain where rooms can act both as sources and absorbers. This is shown in Figure 4.23. From the figure it

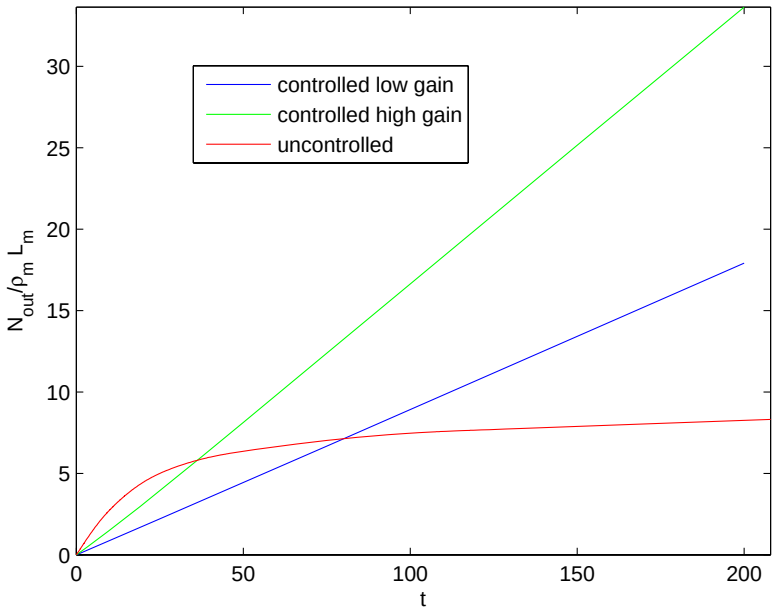

Figure 4.23: Total pedestrian mass getting out of the building for the 3 cases of low gain control, high gain control and the uncontrolled flow. Pedestrian mass normalized with $\rho_m L_m$.

can be seen that while there is good increase in the number of pedestrians evacuating in the low gain case over the uncontrolled case, there is a substantial increase in the high gain case over the low gain case.

In the next set of figures we show the results obtained by local control algorithm developed in Sec. 1.6 for the low gain case for an edge where we fine tune the network control results further to achieve uniform density in the edge. For this we choose edge 17 connecting nodes 13 and 44. The edge is divided in to three sections. For the local

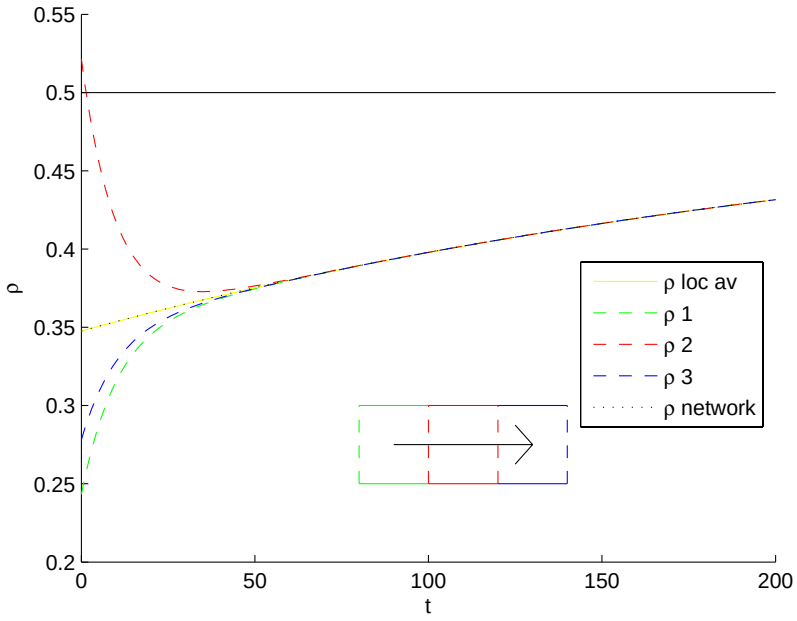

(a) Section densities.

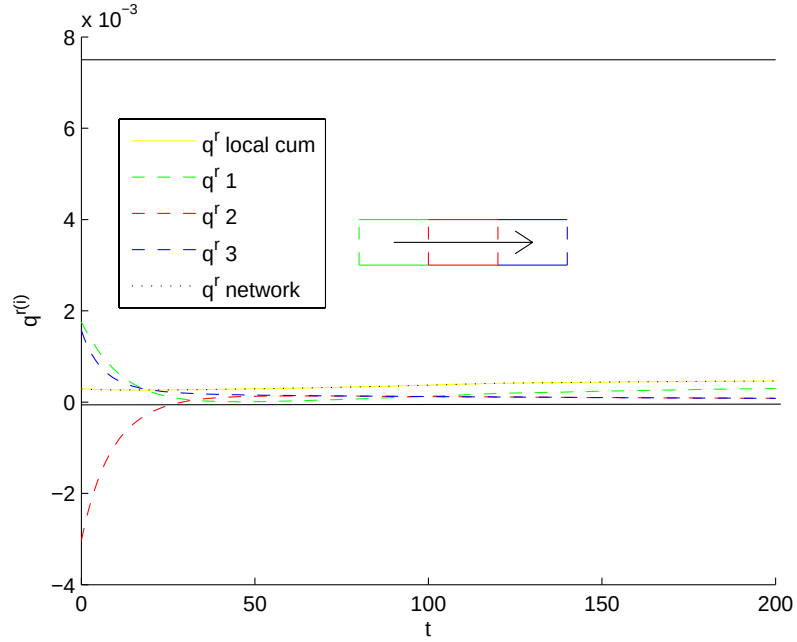

(b) Section room discharges.

Figure 4.24: Section densities and section room discharges under local control for edge 17 (exit edge) divided into 3 sections.

gain parameter, we use a value of $K_{loc} = 0.1$ and the flow parameters determined the global control. The global network control defines the time evolution of the input and output to the edge as well as the the cumulative discharge from all the rooms connected to the edge. The local control keeps these values unchanged but adjusts the individual room discharges in different section of the edge such that different densities in the section approach each other and to the average density used in the network control. The results for the three section of the edge are shown in Figure 4.24 . In the top part of the Figure 4.24(a) are shown the densities in the three sections. The density curve for each section is shown in color of the section with the first section being the green section, the second the red section and the third as the blue section. It is seen that all section densities approach each other and in the process approach the average density of the section indicated by the yellow line which coincides with the average density used in the network control algorithm indicated by the black dashed line. Thus the objective of using such a local control namely of making the density uniform and making the average density a good representative of the edge conditions is achieved. Also since the network control ensures that the average density approaches the critical value of 0.5,the same value is approached by each section densities exponentially. In the bottom subfigure, Figure 4.24(b), are shown plots of the individual section room discharges used as control variables in the local control. The lines are in the same colors as used to indicate the section colors. It is noted that the network control parameters of $\tilde{q}_{t,h}$ and $\tilde{v}_{f_{t,h}}$ are taken as prescribed values for the local corridor control and are not manipulated by it. The only control that is fine tuned is the cumulative edge room discharge parameter $q^r_{t,h}$ from the corridor level to the section level. In this fine tuning, the sum of the individual section room discharges is kept equals the cumulative corridor room discharge by the local control, thus preserving the network control conditions. In Figure 4.24(b) this can be seen by the overlap of black dotted line which is the cumulative room discharge parameter prescribed by the network control and the yellow line which is the total of the section room discharged computed by the local control. This confirms that the local control can effectively fine tunes the network level control.

4.8 Chapter Summary

In this chapter we present an optimization based control methodology for pedestrian evacuation on a network of corridors. We develop a system of ordinary differential equations to model the pedestrian flow on a network of corridors at the macroscopic level. These equations were developed using the conservation of mass principle applied to the corridors and their intersections (nodes). The state variables corresponding to these equations were the edge density (for the corridors) and the nodal pedestrian mass (for the nodes). We propose a scenario corresponding to the uncontrolled state of flow that one could expect in the haste resulting from panic in the evacuation situation. For accomplishing flow control we use the approach of state feedback linearization to obtain equations to meet the tracking objectives for densities and nodal pedestrian mass. These equations are linear in the control variables. We then formulate an optimization problem using these equations as equality constraints on the control variables. In order to do this we formulate a payoff or utility function that we maximize in the optimization routine. This payoff function is the total room discharge on the entire network which is specified as the sum of room discharges on individual corridors, which are the control variables in our problem. Along with this we also impose the bound constraints on the control variables in the optimization problem. As both the constraints and the payoff function are linear in the control variables which are now the variables of the optimization problem the optimization problem is a linear programming problem. This linear programming problem is solved at every instant of time to obtain the control vector at every instant of time.

A methodology is developed to address the issue of infeasibility of constraints of the proposed linear programming problem. The constraints could be infeasible in case of high gains. This methodology scales the control gains in such a way that the constraints are feasible. In order to do this it first formulates a new linear programming problem to obtain the solution of the equality constraints that violates the original bound constraints in the a minimum cumulative sense. This means that the total of bound violations is minimized for infeasible constraints. Then it finds the least factor that scales the solution to satisfy the original bound constraints. When the original infeasible gains are scaled by this factor the resulting constraints become feasible. Thus a computational procedure is proposed to adjust the gains in case of infeasible gains.

In addition to this a methodology is developed to fine tune the network control at the local link level in all the links. The motivation to develop such a local control lies in the fact that the accuracy of our network pedestrian flow model increases with uniformity of link densities. We divide the corridor into sections and fine tune the cumulative edge room discharge parameter which is a network control parameter at the section level. In doing this we make sure to preserve all the network control parameters so that the network control is unaffected. The objective of the local link level control is to make the densities all section progressively uniform as time progresses. The procedure proposed here is computational and involves solving a system of linear equations.

We apply the above developed control methodologies and the uncontrolled flow scenario to the red shortest path tree for the pentagon layout that was obtained in Chapter 2. We plot the results corresponding to the state variables of edge densities and the nodal pedestrian mass. We also plot the results corresponding to the control parameters of edge free flow velocities, nodal input discharge and the cumulative edge room discharge. These results conclusively indicate that the pedestrian flow situation in the evacuation scenario is considerably improved in the case of controlled evacuation.

Chapter 5

Dissertation summary and future work

5.1 Dissertation summary

In this study the problem of pedestrian evacuation form a network of corridors is divided into two basic problems of (1) the efficient flow routing and, (2) the flow control on selected evacuation paths. The solutions to the both problems are needed to provide a comprehensive workable solution for uninterrupted and smooth evacuation of pedestrians from a network or corridors.

It was emphasized in the introduction that different occupants in a building have different perceptions about the nearness of the exits in the building from their current location. When an evacuation alarm is sounded this can given rise to confusion amongst different occupants, which to a certain extent can be expected to be managed by the evacuation maps and the tendency of the pedestrians to follow the crowd. However avoiding such confusion and routing the pedestrians to the nearest exits is of paramount importance in the evacuation process. This is addressed by the flow routing aspect of our work. In addition to the confusion arising from variation in the knowledge and the choice of the exits we also need to tackle the problem of congestion in the links in the evacuation scenario. Very high levels of congestion are possible in the corridors and the stairwells due to the urgency of the situation and possible haste of the occupants to egress quickly. This can be dealt with by regulation of the pedestrian velocities and

discharges in various parts of the network. This is addressed by the flow control aspect of our work. The flow routing aspect of our work is presented in Chapter 2 and the flow control aspects are presented in Chapters 3 and 4.

In Chapter 2 we address the flow routing aspect of the problem using the shortest path methodology. This involves treating the building layout as a graph consisting of nodes and edges. For the building floor layout the nodes are the corridor intersections or exits and the edges are the corridors that span between these intersections. The methodology of dynamic programming is utilized to obtain the shortest paths from each node of the graph (corridor intersection) to the exit node (exit of the layout). The shortest path from a node is a sequence of directed edges from a node to the exit node such that the sum of the lengths of these edges is a minimum of all such directed paths that connect the node to the exit. In order to deal with the multi-exit case shortest path corresponding to each exit from every node is identified and the node is assigned to the exit that has the least shortest path from that node. However if we replace the lengths of the edges by the congestion based time estimates then we get the shortest-time-to-exit paths from all the nodes. These traverse time estimates can be obtained using simple models like the Greenshields model of traffic flow. If such time estimates are used in the routing problem then we can affect a real time routing by re-computing the shortest paths based on these time estimates.

In computing these shortest paths however it is possible that some of the edges in the layout do not fall on any of the shortest paths. These are the un-resolved edges as no flow direction is assigned to them. The pedestrians flow on these edges is guided to either of the end nodes of the edge by splitting the edge in the middle. The procedure of dividing this edge in the middle is elaborated in Sec. 2.5 was developed as a part of this chapter. The procedure of computing the shortest paths for multi-floor buildings is addressed by treating each floor separately and coupling it to the rest of the layout by assigning the stair exits an exit weight which corresponds to the onward time estimate from the stair exit to the building exit. In Sec. 2.7 we describe the implementation aspects of this entire flow routing model. In Sec. 2.8 we present the results of the flow routing in relation to the Pentagon layout. We compute and present the results for both the possibly damaged and the undamaged layouts. For the damaged layout we present a comparison of how much excess distance would have to be covered in case the

pedestrians are not guided by the above developed routing procedure. Thus Chapter 2 comprehensively deals with the flow routing problem.

In Chapter 3 we begin to address the flow control aspect of our problem. Here specifically we deal with the pedestrian flow control in a corridor. Flow control in a corridor is especially critical in the exit corridor due to high rush. We propose a macroscopic model of the corridor. This model divides the corridor into sections and uses the section density of each section as a state variable. Conservation of mass is used to derive a system ordinary differential equations that governs the evolution of these section densities. These are the state equations of our model. The control variables in the state equations are the section free flow velocities, the section room discharges and the rear input discharge. Based on the proposed model we categorize the flow in a corridor into three cases. These three cases correspond to the end, middle and the beginning phase of the pedestrian evacuation process. The end phase is categorized by the absence of any input discharge in the corridor. As we are dealing with the exit corridors in this chapter hence this would be the case as we wont have pedestrians entering the corridor either from behind or from the adjoining rooms. The middle phase is categorized by the absence of the room input discharges and the presence of the rear input discharges. This makes physical sense as pedestrians from all over the layout enter from the rear end and they can typically be expected to far exceed the pedestrians in the adjoining rooms. In the beginning phase we can expect both room input and the rear input discharges.

For each of these three cases we first present the uncontrolled scenario. The uncontrolled scenario proposes typically what can be expected in a panic driven haste situation. Then we proceed to develop control strategies to manage the pedestrian flow. The controlled situation manipulates the flow variables of discharges and velocities to attain appropriate levels of congestions. Further we indicate the superiority of the controlled flow over uncontrolled flow by presenting the numerical simulation results. The control developed for the end phase is a feedback control that achieves asymptotic convergence of the section densities to 0. It does so ensuring that there are no jams and no control saturations. The control developed for the beginning and the middle phases is an optimization based control. This control ensures the tracking of the section pedestrian densities to their critical values corresponding to maximum

discharge for a given free flow velocity. Along with this it ensures that at every instant of time the net input discharge into the system is a maximum. Equivalently it was shown that the net output discharge from the corridor is also a maximum. However the most appealing feature from the implementability point of view is that it attain tracking and maximization objectives while maintaining the bound constraints. This is a crucial advantage of optimization based control methodology.

In Chapter 4 we extend the flow control aspect of our problem to address the case of a network of corridors. This is a more comprehensive case and it deals with flow regulation on an entire single exit corridor network, again at a macroscopic level. This model treats the average corridor pedestrian densities and the corridor intersection (node) pedestrian mass as the state variables. It then uses the conservation of mass approach to derive the state equations corresponding to these. The control variables are the link free flow velocities, the link room input discharges and the link tail node input discharges.

We first propose the uncontrolled case assigning values to the control variables that would correspond to the panic driven haste situation. Then we proceed to design the control to ensure appropriate levels of congestion at the corridors and the nodes. This is an optimization based control. The control design ensures the tracking of all the corridor densities to the critical density and that of the nodal pedestrian mass to 0. Along with this it ensures that the input discharge from all the rooms to the corridor network is at its maximum possible value. This is shown to equivalently ensure that the exit discharge from the network gets maximized at the given state. Again as before it is ensured that the control bounds are satisfied if appropriate gains are chosen. In case the gains are too high then it might not be possible to satisfy the control bounds. In that case a methodology of gain scaling is proposed that scales down the gains optimally such that the control bounds are satisfied. It is noted that the accuracy of the macroscopic model is contingent on the uniformity of the link density. In case of a long corridor this might not be always possible. In order to deal with this situation in addition to the network control a local link level control is also developed that fine tunes the room discharge parameter of the network control while preserving the network control. Simulation results on the red shortest path layout of the Pentagon corridor network consistently point to the fact that the controlled evacuation is significantly

better than the uncontrolled evacuation in terms of flow efficiency.

5.2 Future Work

Due to the multi-faceted nature of the problem research concerning pedestrian evacuation can be done in multiple areas. Due to the human aspect involved in the process this is not entirely an engineering or a mathematics problem. Various calibrations and validations of the models and control methodologies need to be addressed by the fields of psychology, sociology, ergonomics etc. However in this section we would only mention the areas to be explored that could directly impact our work.

The control methodology that we proposed is a feedback control methodology that uses the the pedestrian congestion in corridors and intersections of corridors to determine determine the control inputs of discharges and velocities. Thus in order to implement it we need to probe into the sensing and the actuation aspects of it. In order to sense the congestion optical sensors or pressure sensors need to be developed. In developing such sensors it is mandatory that speed of reporting the data is of paramount importance. In addition to this estimators need to be developed that can give a good estimate of the state of congestion using the data gathered from the sensors. This estimated state can them be used to compute the control input variables using the algorithm proposed.

In order to affect the control actuation various methodologies need to be probed into. As the actuation involves human motion it is critical that ideas and inputs from the field of psychology and sociology be borrowed. This is especially true as the actual control that gets implemented is a human interpretation of the instructions that are issued. Thus devices like the matrix displays, speaker phones etc. need to be looked into to issue the instructions that would affect the flow velocities and flow discharges. Also experimentation need to be done to find what values should be assigned to the explicit bounds that we specify on the control variables of free flow velocity and discharges. It is also important to know to what degree of accuracy can a specific control be implemented. As uncertainties are inherent in the sensing and actuation processes a study dealing with uncertainty quantification using probabilistic methods would be a interesting sequel to our current study.

As pedestrian flow model is control oriented hence it does not capture all the details of the pedestrian flow. The details especially at the local level are ignored to a certain extent to facilitate control design. The kind of local effects that seem interesting at this stage from an evacuation perspective are the temporary stoppages that might occur due to local obstructions that might be an effect of a damaged layout. A study that finds the global effects due to these local obstructions would be an interesting companion study.

The effects like shock waves, rarefactions waves are not accounted for in this model. Thus a study that formulates the whole corridor network pedestrian flow problem as a system of pde's instead of ode's would be an interesting step forward. However it should be noted that control design for a networked pde system of equations is quite complicated.

As is obviously true the problem of pedestrian evacuation is multi-disciplinary. Also it is quite evident that the success of the pedestrian evacuation largely relies on the scale and nature of the emergency being dealt with. Thus this dissertation should be viewed as an attempt to develop a formal methodology to aid pedestrian evacuation in network of corridors. By no means should this be looked at as a complete solution to the problem of pedestrian evacuation control from building structures.

Bibliography

[Bertsekas, a] Bertsekas, D. P. *Dynamic Programming and Optimal Control*, volume ‘1. Athena Scientific.

[Bertsekas, b] Bertsekas, D. P. *Dynamic Programming and Optimal Control*, volume ‘2. Athena Scientific.

[Bovy and Stern, 1990] Bovy, P. H. L. and Stern, E. (1990). *Route Choice: Wayfinding in Transport Networks*. Kulwer Academic Publishers, Dordrecht.

[Burstedde et al., 2001] Burstedde, C., Klauck, A., and Zittartz, J. (2001). Simulation of pedestrian dynamics using a two-dimensional cellular automaton. *Physica A: Statistical Mechanics and its Applications*, 295(3-4):507–525.

[Cote and Harrington, 1987] Cote, R. and Harrington, G. E. (1987). Life safety code handbook. Technical report, NFPA, Avon,MA.

[Gipps, 1986] Gipps, P. G. (1986). Simulation of pedestrian traffic in buildings. Technical report, University of Karlsruhe.

[Greenshields, 1935] Greenshields, B. D. (1935). A study in highway capacity. *Highway Research Board*, 14:458.

[Helbing et al., 2000] Helbing, D., Farkas, I., and Viscek, T. (2000). Simulating dynamic features of escape panic. *Nature*, 407:487–490.

[Hill, 1982] Hill, M. R. (1982). *Spatial Structure and Decision-Making of Pedestrian Route Selection through an Urban Environment*. PhD thesis, University Microfilms International.

[Hoogendoorn, 2001] Hoogendoorn, S. P. (2001). Pedestrian flow behavior: Theory and applications. Technical report, Transportation and Traffic Engineering Section, Delft University of Technology.

[Hoogendoorn and Bovy, 2004] Hoogendoorn, S. P. and Bovy, P. H. L. (2004). Pedestrian route-choice and activity scheduling theory and models. *Transpn. Res. B.*, 38:169–190.

[Hughes, 2002] Hughes, R. L. (2002). A continuum theory for the flow of pedestrians. *Tranportation Research Part B*, 36:507–535.

[Khalil, 1996] Khalil, H. K. (1996). *Nonlinear Systems*. Prentice Hall.

[Kirchner et al., 2004] Kirchner, A., Kulpfel, H., Nishinari, K., Schadschneider, A., and Schreckenberg, M. (2004). Discretization effects and the influence of walking speed in cellular automata models for pedestrian dynamics. *Journal of Statistical Mechanics-Theory and Experiment: Art. No. P10011.*

[Kirchner et al., 2003] Kirchner, A., Nishinari, K., and Schadschneider, A. (2003). Friction effects and clogging in a cellular automaton model for pedestrian dynamics. *Phys. Rev. E*, 67:056122.

[Kirchner and Schadschneider, 2002] Kirchner, A. and Schadschneider, A. (2002). Simulation of evacuation process using a bionics inspired cellular automaton model for pedestrian dynamics. *Physica A: Statistical Mechanics and its Applications*, 312(1-2):260–276.

[Nijmeijer and van der Schaft, 1990] Nijmeijer, H. and van der Schaft, A. (1990). *Nonlinear Dynamical Control Systems*. Springer-Verlag, New York, NY.

[Rugh, 1996] Rugh, W. J. (1996). *Linear Systems Theory*. Prentice Hall.

[Schadschneider, 2002] Schadschneider, A. (2002). Cellular automata approach to pedestrian dynamics-theory. In Schreckenberg, M. and Sharma, S., editors, *Pedestrian and Evacuation Dynamics*, pages 75–86. Springer.

[Slotine and Li, 1991] Slotine, J.-J. and Li, W. (1991). *Applied Nonlinear Control*. Prentice Hall, New Jersey.